Chlamydia trachomatis overcomes human cell-autonomous immunity through secretion of a novel inclusion membrane protein IncU

Mark Christopher Fernandez

A dissertation

submitted in partial fulfillment of the

requirements for the degree of

Doctor of Philosophy

University of Washington

2021

Reading Committee:
Kevin Hybiske, Chair
Lee Ann Campbell
Sheila Lukehart

Program Authorized to Offer Degree:
Pathobiology

University of Washington

Abstract

Chlamydia trachomatis overcomes human cell-autonomous immunity through secretion of a novel inclusion membrane protein IncU

Mark Christopher Fernandez

Chair of the Supervisory Committee:
Kevin Hybiske, Associate Professor,
Department of Medicine

Chlamydia is the most common sexually transmitted bacterial infection in the world. In the United States, over 100 million people are infected each year, and from 2015 to 2019 incidence of chlamydia rose by 19%. Of extreme concern, this increase has occurred despite readily available effective antibiotics and national screening recommendations for young women at highest risk of contracting chlamydia. A chlamydia vaccine is needed, however our near-complete lack of knowledge of protective immune responses that could prevent infection is a major barrier for vaccine development. Research to unveil correlates of protection is a significant challenge—studies in humans carry major ethical considerations, and there is no animal model that faithfully recapitulates the natural history of infection as it occurs in humans. Careful design of *in vitro* research using human cells and tissues and work to identify the utility and limitations of various animal models are critical research priorities. To date, interferon gamma (IFNγ) secreting T-cells represent the strongest plausible correlate of protection against

chlamydia. Because the etiological agent of chlamydia, the bacterium *Chlamydia trachomatis*, is an obligate intracellular pathogen that primarily infects human epithelial cells, an important aspect to the protective capacity of IFNγ lies in the ability of this cytokine to stimulate innate immunological responses in the cells that harbor and support chlamydial growth. The ability of these classically non-immune cells to mount innate immune responses to protect themselves against intracellular pathogens is often termed cell-autonomous immunity. IFNγ-stimulated cell-autonomous immunity against intracellular pathogens is a topic of ongoing investigation in the *Chlamydia* field and other systems, and its importance as a potent anti-*Chlamydia* response is only recently appreciated. While murine cell-autonomous immunity renders epithelial cells able to mark *C. trachomatis*-containing vacuoles for destruction, this pathogen readily evades detection and growth restriction in its native human host cells.

I have dedicated my dissertation work to understanding the relationship between human cell-autonomous immunity and *Chlamydia trachomatis* and, importantly, identifying how this pathogen resists this potent immune pathway. By screening a novel library of chimeric interspecies *Chlamydia* mutant strains, I identified a genetic locus required for resistance. Follow up analysis of mutant *C. trachomatis* strains aided my identification of a single virulence gene, *incU*. Human cells infected with *incU*-mutants can recognize chlamydial vacuoles, termed inclusions, leading to the recruitment of downstream cell-autonomous immunity proteins. Ultimately, this leads to severe growth restriction of these *C. trachomatis* mutants. With contributions from collaborators at the University of Washington and Oregon State University, I found that *incU* mutants failed to replicate *in vivo* in the nonhuman primate model. *In vitro* infection of primary NHP

fibroblasts revealed that NHP cells exhibit an IFNγ-inducible cell-autonomous immune response that is mechanistically similar to the human pathway, providing supporting evidence that *in vivo* growth defects were due to *incU* mutants' susceptibility to IFNγ-stimulated cell-autonomous immunity. Taken together, these data shed new light on the relationship between IFNγ-stimulated immunity and *C. trachomatis*, while identifying a relevant animal model in which to further explore the protective capacity of IFNγ in humans.

Table of Contents

List of Figures

List of Tables

Acknowledgements

I must first thank my parents, Jeff and Erin, and my wife, Jenna. Their endless encouragement and support throughout all aspects of my life have been invaluable to my success, and I dedicate this work to them.

The work described in this dissertation would not have been possible without major contributions from our outstanding collaborators. Dr. Dorothy Patton and Yvonne Cosgrove-Sweeney performed key nonhuman primate studies and graciously provided us with *Chlamydia* strains that were essential to this work. I am also grateful to Dr. Daniel Rockey and Steven Carrell who performed the whole genome sequencing experiments described.

I am extremely fortunate to be surrounded by faculty and scientists at the University of Washington whom I consider my mentors and friends. I thank Dr. Kevin Hybiske for giving me the freedom to pursue my ideas in the laboratory, and for helping me to become a better scientist. Bob Suchland has been instrumental in my various projects—his enthusiasm for science and intuition at the bench are second to none. I thank Dr. Yibing Wang for sharing her expertise with me throughout my time in the Hybiske lab. I am immensely grateful for the continual mentorship I have received from Dr. Sheila Lukehart over the past decade. No one has been a stronger advocate for me in my professional life, and I am honored to be one of her many trainees.

Chapter 1. Introduction

Chlamydia

Chlamydia trachomatis causes the most common notifiable infection in the United States. Despite the availability of highly effective antibiotics and national screening recommendations[1], cases of urogenital chlamydia continue to increase year-after-year[2]. Infection is typically asymptomatic, and untreated or repeated infection with *C. trachomatis* can lead to severe sequelae in women, including pelvic inflammatory disease, ectopic pregnancy, and tubal infertility[3,4]. The natural history of chlamydia is poorly understood. There are 19 serovars of the human pathogen *Chlamydia trachomatis*, which are subtypes classified according to sequences of variable regions of the major outer membrane protein (MOMP)[5]. While there is a high level of genomic conservation across these serovars, the pathogenesis and tissue tropism of *C. trachomatis* strains are distinct. Serovars A, B, Ba, and C preferentially infect ocular tissues and cause trachoma, a globally important disease that is transmitted through ocular secretions of infected to naïve individuals. Trachoma can lead to conjunctival scarring and blindness in severe cases[6]. The work described in this dissertation is most relevant to urogenital and lymphogranuloma venereum (LGV) serovars of *C. trachomatis* that are transmitted through vaginal, oral, or anal sex[7,8].

Urogenital infections are caused by *C. trachomatis* serovars D/Da, E, F, G/Ga, H, I/Ia, J, and K[5]. These serovars preferentially infect columnar epithelial cells in penile and cervical mucosal tissues. Through poorly defined mechanisms, urogenital serovars can

ascend to the upper genital tract of infected women, triggering inflammation that can lead to severe sequelae[3,7]. Serovars L1, L2, L2a and L3 are more invasive strains and are capable of causing LGV. Infection by LGV serovars leads to unique clinical manifestations, where primary infection is marked by a small, typically painless ulcer on genital or anal epithelial tissues[9]. Anorectal infection with LGV serovars is an emerging interest in the field given the recent finding that infection among men who have sex with men is widespread, and can cause proctitis and proctocolitis in addition to traditional inguinal lymphadenopathy[10]. LGV is characterized by invasion of the lymphatic system, whereby *C. trachomatis* invades regional lymph nodes through a poorly defined mechanism. LGV serovars survive within macrophages better than the urogenital serovars[11], and a model wherein *C. trachomatis*-infected macrophages trafficking to lymphatic tissues deliver the pathogen to these sites is the leading 'Trojan horse' theory of chlamydial delivery to lymphatic tissue[12].

Chlamydia **biology**

Chlamydia trachomatis is a Gram-negative obligate intracellular bacterium that undergoes a unique, biphasic developmental cycle: it transitions between an infectious, predominantly extracellular elementary body (EB) and a noninfectious reticulate body (RB). EBs bind to the surface of host epithelial cells and are subsequently internalized into a vacuole, termed the inclusion, which they extensively modify and inhabit throughout their intracellular phase[13]. After establishment of the inclusion, EBs differentiate into RBs and actively divide in the inclusion microenvironment, eventually transitioning asynchronously back into EBs that go on to infect new cells following either lysis of their

host cells or via extrusion of the chlamydial inclusion[14]. This developmental cycle lasts approximately 48 hours.

C. trachomatis encodes a type-III secretion system (T3SS). T3SSs are found in many pathogenic gram-negative bacteria, and effector proteins secreted by these T3SSs facilitate pathogenic processes, ranging from tissue colonization to evasion of host immunity[15]. The chlamydial T3SS is no exception to this paradigm[16]. EBs contain presynthesized T3SS machinery and effector proteins that are secreted into the host cytosol and are essential for invasion and establishment of the inclusion microenvironment[17,18].

Chlamydia species encode a novel family of type-III secreted inclusion membrane proteins (Incs) that are embedded in inclusion membranes after their secretion into the host cell. *C. trachomatis* is predicted to encode 59 Incs, accounting for over 6% of its entire genome[19,20]. These proteins were originally defined by the presence of a common bilobal hydrophobic region of approximately 60 amino acids with at least two hydrophobic alpha helices separated by a small hairpin loop that facilitates their anchoring to the inclusion membrane[21,22]. The predominantly hydrophilic domains of Incs can directly interface with the host cytosol, suggesting that they are capable of mediating protein-protein interactions with host or chlamydial protein targets. The molecular bases of interactions between Incs and host proteins are not well characterized. Incs have limited sequence similarities to each other outside of the hallmark topology described above, and they have no known homologues in any other species, hindering any prediction of their functions[19]. A lack of direct studies to determine individual Incs functions is in part due to the historic lack of tools to genetically manipulate this organism[23]. More recently,

however, the field is beginning to understand the diverse host-pathogen interactions these proteins orchestrate during *C. trachomatis* infection[24–28]. The work described in this dissertation details the discovery of an Inc that is required for resistance of host cell-autonomous immunity.

Mouse and nonhuman primate models of chlamydia

Barriers to understanding protective immunity include the ethical barriers to studying untreated chlamydia in humans and the lack of an animal model that reliably reproduces human disease[29]. While mice can be acutely infected with *C. trachomatis*, the duration of the infection is much shorter than for humans, and *C. trachomatis* does not naturally ascend into the upper genital tracts of female mice[29]. Many important immunological studies have, however, been performed in mice infected with a native rodent pathogen *Chlamydia muridarum*, which encodes a genome highly syntenous to *C. trachomatis*[30]. *C. muridarum* can naturally ascend the murine genital tract and trigger intense inflammation and can lead to similar pathological outcomes observed in human chlamydial disease[31,32]. Mice spontaneously resolve infection with *C. muridarum*, and acquire long-lasting immunity that protects against reinfection[33]. Additionally, a recently published subunit vaccination strategy confers sterilizing immunity against *C. muridarum* and *C. trachomatis* in this model organism[34].

Despite the insights gained from studies in the mouse model, there are several limitations that urge caution for their translatability to human disease. First, studies of chlamydia have been performed in a wide variety of mouse strains—many of which are more permissible to *C. trachomatis* because of their genetic background that makes them

partially or completely immunocompromised. Second, the murine estrous cycle is distinct from the menstrual equivalent in humans, and the timing of infection with various stages of the estrous cycle results in extreme variability in pathological outcomes[35]. Third, and most important to this dissertation, mice encode distinct proteins not found in the human genome that are required for innate, cell-autonomous immune clearance of intracellular pathogens, including *Chlamydia*.[36]. Finally, *C. muridarum* was originally isolated from mouse lungs[37], and it is possible that its natural niche is not within the female genital tract.

Perhaps the most translatable studies of *Chlamydia* infection are those performed in nonhuman primate models (NHP), most notably in the pigtailed macaque (*Macaca nemestrina*)[29]. Pigtailed macaque studies carry significant benefits that are not observed in the mouse model. Infection of macaques with *C. trachomatis* results in a productive infection that better matches the duration of human infections. Moreover, untreated monkeys that spontaneously resolve their primary infections exhibit immunological protection against reinfection, which agrees with similar correlations from human studies[38]. Additionally, the menstrual cycle of these NHPs is similar to that of humans, and its manipulation is not required for experimental infection with *C. trachomatis*. Finally, the common evolutionary history of NHP and humans has led to a shared loss of innate immunity genes that are important for controlling infection by intracellular pathogens in the mouse model[36]. The lack of efficient and realistic tools to manipulate NHP genomes limits certain studies, however the reasons precluding pigtailed macaques from being the primary animal model for chlamydia are largely non-biological. The ethics of performing studies in NHP are controversial, and sophisticated laboratory, surgical, and personnel costs are significant, especially when compared to relatively inexpensive mouse

studies[39]. These limitations must always be considered before embarking on studies in the NHP model. However, because the mouse model of chlamydia has significant limitations, NHPs will undoubtedly play a critical role in furthering our understanding of *Chlamydia* immunology and in designing a protective vaccine.

Chlamydia immunology

Some infected individuals naturally resolve infection by *C. trachomatis* without antibiotic treatment[40,41], and natural immunity following spontaneous resolution of chlamydia has been associated with a decreased rate of reinfection in humans[40]. However, immunological factors conferring protection versus those that promote inflammation and exacerbate severe sequelae have not been determined[42].

A highly debated topic in the field is the role B-cells play in protective immunity against *Chlamydia*. Knockout mice lacking mature B-cells were originally shown to effectively control primary infection by *C. muridarum* similar to wildtype mice, suggesting only a minor role for humoral immunity in the host response to *Chlamydia*[43]. In a separate study disputing this finding, mice that naturally resolved a primary infection by *C. trachomatis* were depleted of CD4+ and CD8+ T-cells and were subsequently shown to be protected from secondary challenge. The authors attributed this outcome to maintenance of an intact memory B-cell response in these mice[44]. These competing findings were published over 2 decades ago, and even with the advent of modern immunological methods the importance of B-cell-mediated immunity in controlling infection by *Chlamydia* remains unclear[45]. Future research should consider a protective role from the wide variety of antibody-independent B-cell functions that have been

discovered to be protective against infection by other pathogens[46]. For example, B-cell antigen presentation by class II major histocompatibility complex molecule (MHC-II) is required for mice to control infection with the parasite *Heligomosomoides polygyrus*[47]. Another study in the mouse model suggested that cytokine production by B-cells following *Salmonella enterica* infection may influence T-cell differentiation[48].

In contrast to the controversial relationship between B-cells and *Chlamydia* immunity, it is evident that T-cells are required for controlling and preventing *Chlamydia* infection in the mouse model[34,49]. MHC-II-restricted CD4+ T-cells are required for controlling *Chlamydia* infection, whereas MHC-I-restricted CD8+ T-cells have a less well-defined role in the mouse model of protective immunity[50]. There has been some evidence that MHC-I may be downregulated in *C. trachomatis* infected cells[51], suggesting that *Chlamydia* has evolved mechanisms to evade detection by CD8+ T-cells by inhibiting presentation of chlamydial antigens by host cell MHC-I. The most definitive association with sterilizing immunity in mice is the secretion of IFNγ by either type 1 CD4+ T helper (Th1) cells[52–55] or innate immune cells[56]. A similar finding has been observed in humans, as women with circulating IFNγ-secreting Th1 cells following *C. trachomatis* infection are less susceptible to subsequent reinfection, although the observed protection does not appear to be long-lasting[57]. A dogma in the field has emerged from these studies: IFNγ secretion is the most critical aspect of protective immunity against *Chlamydia* infection. However, it is vital to remember that *C. trachomatis* evades IFNγ-stimulated immune responses elicited within its native human host cells[58,59]. Additionally, in the NHP model of *Chlamydia*, IFNγ and interleukin 2 (IL2) cytokine secretion has been shown to promote severe inflammation in the upper genital tract following repeated infection of this site,

suggesting that *C. trachomatis*-specific Th1 cells may contribute to immunopathology associated with severe sequelae[60]. Such host responses that contribute to disease rather than or in addition to protecting against infection are important to define. A previous vaccine trial against ocular *C. trachomatis* infection revealed that stronger immune responses (determined by antibody titer) to the vaccine were associated with more severe disease following challenge[61].

The direct studies supporting the IFNγ dogma were done in the non-native mouse model, in which *C. trachomatis* is completely susceptible to IFNγ-stimulated immunity[62]. Previous studies have revealed that the potency of IFNγ-mediated control of *Chlamydia* in the mouse model is due to infected epithelial cells eradicating *C. trachomatis* by IFNγ-induced cell-autonomous immune pathways[49,62,63].

IFNγ-inducible cell-autonomous immunity against intracellular pathogens

Cell-autonomous immunity is emerging as an important and highly conserved immune response across all forms of eukaryotic life[64]. This arm of innate immunity contains the capacity of non-immune cells, such as the epithelial cells that are the primary targets of infection by *Chlamydia*, to defend themselves from infection by intracellular pathogens. While often considered to be an arm of innate immunity, this pathway likely represents a crossroad between innate and adaptive immunity, as cytokine secretion from the latter can activate specific pathways in classically non-immune cells to kill invading pathogens. Additionally, cell-autonomous immunity has been shown to increase antigen processing and presentation in infected cells, which leads to *in vivo* education of adaptive lymphocytes[65]. Many of the critical molecular mechanisms that govern pathogen

clearance by cell-autonomous immunity remain uncharacterized. This is especially true in human cells, which employ a distinct yet unknown mechanism to initiate this immune response compared to the better studied mouse pathway[36]. Cell-autonomous immunity can refer to a variety of effector mechanisms that are induced by various stimuli, ranging from pathogen- or damage-associated molecular patterns to stimulation of infected cells with cytokines[64,66].

When cytosolic pathogens like *Listeria* and *Shigella* spp. invade nonimmune cells such as epithelial cells, they are contained within a vacuole from which they quickly escape via virulence mechanisms that rupture the membrane-bound compartment[67,68]. The exposed luminal faces of these damaged vacuoles contain host glycans that are recognized as damage-associated molecular patterns (DAMPs) in the cytosol[69]. The galectin family of lectin proteins, conserved amongst a wide variety of animal species, recognize these DAMPs and trigger degradation of damaged membranes[69,70]. The recruitment of autophagy machinery to recently ruptured pathogen-containing vacuoles can lead to pathogen degradation by autophagy, a process termed 'xenophagy'[70]. Recently, galectins were shown to coordinate with cytokine-stimulated effector proteins to further mediate clearance of various pathogens that cause damage to vacuoles to escape into the cytosol[71]. This galectin-mediated interaction between classical autophagy and cytokine-stimulated genes implicates galectins as early pathogen-recognition receptors that initiate microbial clearance by cell-autonomous immunity.

The work described in this dissertation focuses on a distinct arm of cell-autonomous immunity induced by IFNγ stimulation of cells infected with vacuolar pathogens. While poorly understood, the general mechanism of pathogen clearance is

mediated by IFNγ-stimulated genes in concert with canonical autophagy factors[72]. Many pathogens like *Chlamydia* have evolved to carry out their intracellular developmental cycle within pathogen-containing vacuoles (PCVs), rendering galectins ineffective at detecting their intact vacuoles. The mechanism of marking PCVs for eradication by cell-autonomous immunity is unknown in human cells, and the downstream events leading to cell-autonomous immune clearance are not fully characterized. The initiating events of PCV clearance by cell-autonomous immunity is best understood in the murine model. IFNγ-stimulation of infected mouse cells promotes the expression of a family of p47 immunity related GTPases (IRGs) that are critical for marking PCVs as foreign. The majority of these IRGs encode a canonical GXXXXGKS motif in their GTP-binding domain, hereafter referred to as GKS-IRGs[66]. These GTPases hydrolyze GTP into GDP to promote their oligomerization on lipid membranes. Most GKS-IRGs in the cytosol of IFNγ-stimulated cells exist as inactive, GDP-bound monomers and do not localize to host organellar membranes[73]. A subset of IRGs are called IRGMs due to a K→M mutation within their GTPase domain (GXXXXGMS) that renders them enzymatically inactive[73]. IRGMs selectively anchor to 'self' organelle membranes (e.g. endoplasmic reticulum, golgi apparatus, and lipid droplets) and not to PCVs[74]. The GKS-IRGs and IRGMs orchestrate the early marking of PCVs via a 'missing self' phenomenon: IRGMs transiently interact with GKS-IRGs and maintain them in their inactive, GDP-bound state thereby preventing their oligomerization-dependent deposition onto self-organelles[73]. In contrast, GKS-IRGs readily oligomerize and assemble on the lipid membranes of chlamydial inclusions and other PCVs that are devoid of IRGMs[74].

GKS-IRG assembly on membranes recruits E3 ubiquitin ligases, including TRIM21 and TRAF6 that deposit abundant amounts of the small protein modifier ubiquitin onto PCVs[66]. This ubiquitin coat acts as a scaffold to which downstream effectors are recruited, including canonical autophagy proteins—possibly through their ubiquitin binding domains—and IFNγ-stimulated effector proteins. Deposition of this complete suite of host factors onto PCVs facilitates pathogen clearance by disrupting this protective niche[62].

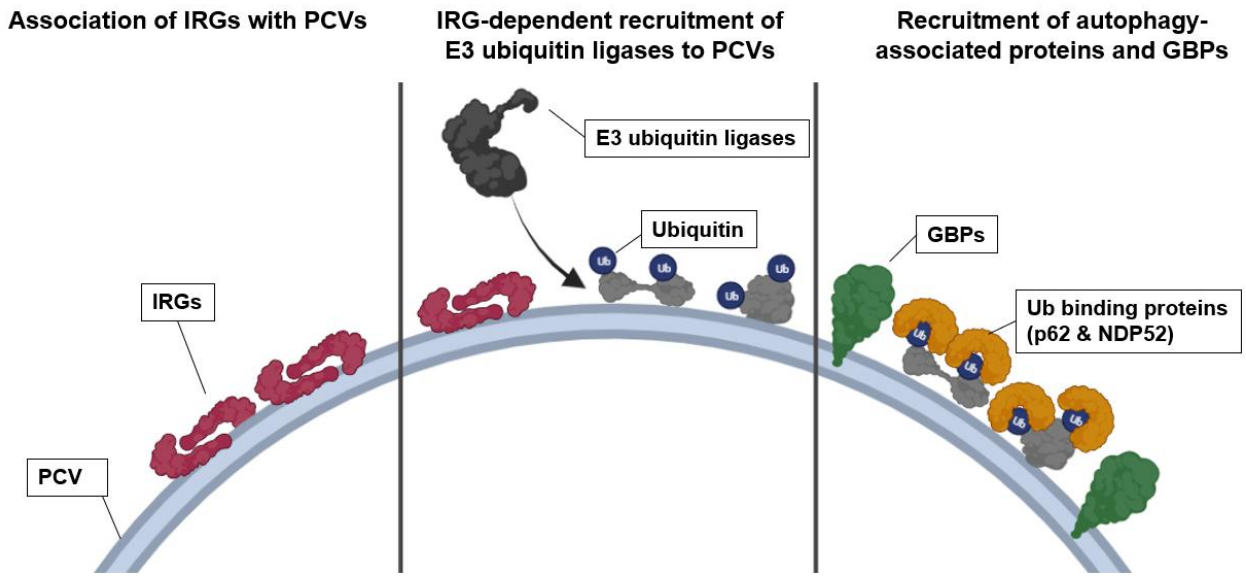

Figure 1.1 Stages of murine cell-autonomous immunity against vacuolar pathogens. Pathogen containing vacuoles (PCVs) are recognized as foreign by IFNγ-stimulated immunity-related GTPases (IRGs) that oligomerize on the PCV surface (left panel). IRGs recruit E3 ubiquitin (Ub) ligases that promote ubiquitination of proteins on the PCV surface—for organisms like *Chlamydia* species that extensively modify this compartment, ubiquitinated targets likely represent a mixture of pathogen and host proteins (middle panel). Autophagy-associated proteins with ubiquitin binding domains (e.g., p62 and NDP52) are recruited to ubiquitinated PCVs, as are IFNγ-stimulated guanylate binding proteins (GBPs, right panel). PCV membranes are directly disrupted, releasing pathogens into the cytosol of infected cells.

There are major caveats to studying cell-autonomous immunity in the mouse model. Over evolutionary history, humans and other primates have lost functional copies of all GKS-IRGs[36]. A single *irgm* remains the only conserved member of the IRG family in humans and other great apes—however it is not IFNγ-inducible. An evolutionary event led to the insertion of a retroviral element within the promoter region of the *irgm* pseudogene that restored its transcription, and it is constitutively expressed in humans and great apes[36]. In contrast to the mouse model, human IRGM does not appear to have any role in the cell-autonomous immune recognition and clearance of *Chlamydia*[59].

Despite these major differences, the events that follow IRG marking of PCVs (Fig. 1.1, center and right panels) in mouse cells are partly conserved in humans. An important family of IFNγ-induced GTPases involved in the cell-autonomous clearance of intracellular pathogens are guanylate binding proteins (GBPs). GBPs are dynamin-like GTPases that can consecutively hydrolyze GTP to GDP and then to GMP[75,76]. This family is partially conserved in human and mouse genomes, encoding 7 and 11 members, respectively. Human and mouse GBP1, GBP2, and GBP5 encode prenylation motifs (CaaX) in their carboxyl termini, which have been shown to promote their direct association with intracellular bacteria or their vacuoles[75]. GTP hydrolysis by GBPs facilitates the formation of GBP homodimers and heterodimers, a feature that is also critical for their association with PCVs[77]. While GBPs have been clearly shown to be important to cell-autonomous immune clearance of intracellular pathogens[75,78], their specific functions are poorly understood.

Chlamydial inclusions and PCVs containing other pathogens are decorated with ubiquitin following IFNγ stimulation of host cells. This leads to the recruitment of GBPs

and autophagy proteins that potently restrict pathogen growth. *C. trachomatis* is highly susceptible to IFNγ-induced cell-autonomous immunity in mouse cells, whereas the rodent pathogen *C. muridarum* is entirely resistant[62]. When evaluating cell-autonomous immunity in human cells, a reciprocal outcome is observed. *C. trachomatis* is resistant in its native host, whereas *C. muridarum* inhabits inclusions that are readily targeted by this pathway and is severely growth-restricted in IFNγ-stimulated human cells[59]. Interestingly, when these human cells were coinfected with both *Chlamydia* species, inclusions that were coinhabited by *C. trachomatis* and *C. muridarum* were found to be devoid of ubiquitin and downstream cell-autonomous immunity effectors[59]. These findings support a major hypothesis underlying this dissertation: *C. trachomatis* secretes a virulence factor(s) that actively facilitates resistance to IFNγ-induced cell-autonomous immunity in its native human host. *C. trachomatis* completely prevents inclusion ubiquitination in IFNγ-stimulated human cells, suggesting that the mechanism of immune evasion occurs at or upstream of this event. At present, there are no candidate host factors that could potentially be inhibited/inactivated by such a virulence factor—the IRG-mediated events preceding ubiquitination in the mouse model by necessity must be completely unique in the human system given the absence of functional IRGs in the human genome[36]. The events preceding ubiquitination in human cell-autonomous immunity should be a major research priority, and the findings from this dissertation may be pivotal in furthering our understanding of this important human pathway against intracellular vacuolar pathogens.

Chapter 2. Genetic screen for candidate *C. trachomatis* virulence factors

Introduction

There has been a historic paucity of genetic tools available for performing studies to identify *C. trachomatis* virulence factors and critical mechanisms of chlamydial pathogenesis[23]. Most *Chlamydia* species carry a native ~7.5kb plasmid, and in 2011 a transformation protocol was developed to deliver foreign genetic material encoded on the native plasmid backbone into *Chlamydia trachomatis*[79]. In the time since, a growing number of genetic tools have been developed that have been instrumental in advancing our understanding of *Chlamydia* biology[23]. Most notably, technology to stably insert transposons randomly throughout chlamydial genomes has facilitated the generation of transposon mutant libraries[80]. This represents a promising step forward for the field; however, the current sizes of these libraries are small and transposon insertion into *Chlamydia* genomes remains a low-efficiency event. Our group's collection of *C. trachomatis* transposon mutants is the largest of these libraries, currently containing 220 mutants. Although the lab is continually generating new transposon mutants in *C. muridarum* and *C. trachomatis* backgrounds, we are a long way from a library allowing us to screen the ~900 genes in these organisms on a genome-wide scale. The sobering reality is that we may never develop transposon libraries nearing genome-wide coverage of these species. *Chlamydia* have streamlined genomes of approximately ~1 Mb, a direct result of their coevolution with, and parasitic adaptation to, their animal hosts, and it is

likely that many of their genes are essential[81]. These small genomes are highly conserved amongst *Chlamydia* species. Interestingly, their syntenous genomes can undergo homologous recombination with one another[82]. This phenomenon has been artificially induced *in vitro* by coinfecting cells with two distinct parent species and has been observed through whole genome sequencing of *Chlamydia trachomatis* clinical samples[82,83].

In an effort to generate a mutant library that can facilitate genome-wide screens of species-level phenomena, we previously generated a large library of *C. trachomatis* x *C. muridarum* interspecies chimeras through *in vitro* recombination[84]. We have generated >1000 chimeras that encode a predominantly *C. trachomatis* serovar L2 genome with unique regions of *C*. *muridarum* genes recombined into them. To date, 134 clones with unique recombination events have been fully genome sequenced. Given their high synteny, we predict many homologous gene pairs have redundant functions between *C. trachomatis* and *C. muridarum*. This mutant library is especially useful for screening for genes that are responsible for disparate infection and growth phenotypes between these species—for example, their distinct resistance to IFNγ-induced cell-autonomous immunity in their native host species[59,62]. We hypothesize that a subset of chimeras has lost the gene(s) required for resistance to cell-autonomous immunity in human cells, and instead carry the ineffective *C. muridarum* homologue(s).

Because ubiquitination is the earliest known step in the human cell-autonomous immune response against *Chlamydia*, we designed a screen based on published methods to assess whether any chimera-containing inclusions were targeted by ubiquitin in IFNγ-primed human cells[59]. In this chapter, we detail the discovery of 3 such chimeras.

These 3 chimeras possess recombined *C. muridarum* loci that overlap with one another, sharing 11 genes that are not recombined in any chimeras that retain resistance to inclusion ubiquitination. Two of these genes are consistent with our hypothesis that the virulence factor(s) are type-III secreted effectors; they encode inclusion membrane proteins, and within our 11-gene candidate locus they are the most highly divergent targets between *C. trachomatis* and *C muridarum*. The identification of a focused number of genes underlying this specific phenotype is a major triumph that emphasizes the utility of our novel chimera library in studying *Chlamydia* pathogenesis and virulence.

Results

Selection of recombinant chimeras for screening.

Recombinant chimeras were previously generated by coinfecting McCoy cells with members of our chloramphenicol-resistant *C. muridarum* transposon library and a single tetracycline-resistant *C. trachomatis* serovar L2 parent (Fig.2.1A)[82]. While all 134 genome-sequenced chimeras in our library would in theory maximize our ability to screen the entire *C. trachomatis* genome, we sought to select a more manageable number that would still allow us to screen a majority of *C. trachomatis* genes. We selected 13 chimeras whose recombined loci collectively replaced 66% of *C. trachomatis* genes (RC1-13, Fig. 2.1B). On average, these chimeras encoded 52 recombined *C. muridarum* genes (range = 12-113 *C. muridarum* genes, orange bars in Fig. 2.1B). The gap between RC3 and RC4 represents the genomic region of the *C. trachomatis* parent encoding the tet^R allele[85]. Chimeras in a *C. trachomatis* background with recombination events within this genetic

locus would have lost the tet^R allele and would not have survived the dual antibiotic selection we used to select for recombinants. The gaps between RC-11, RC-12, and RC13 were originally covered by additional chimeras, but we were unable to cultivate these strains *in vitro* following freeze-thaw. Future screens may include selecting other chimeras from the larger library to complement these gaps.

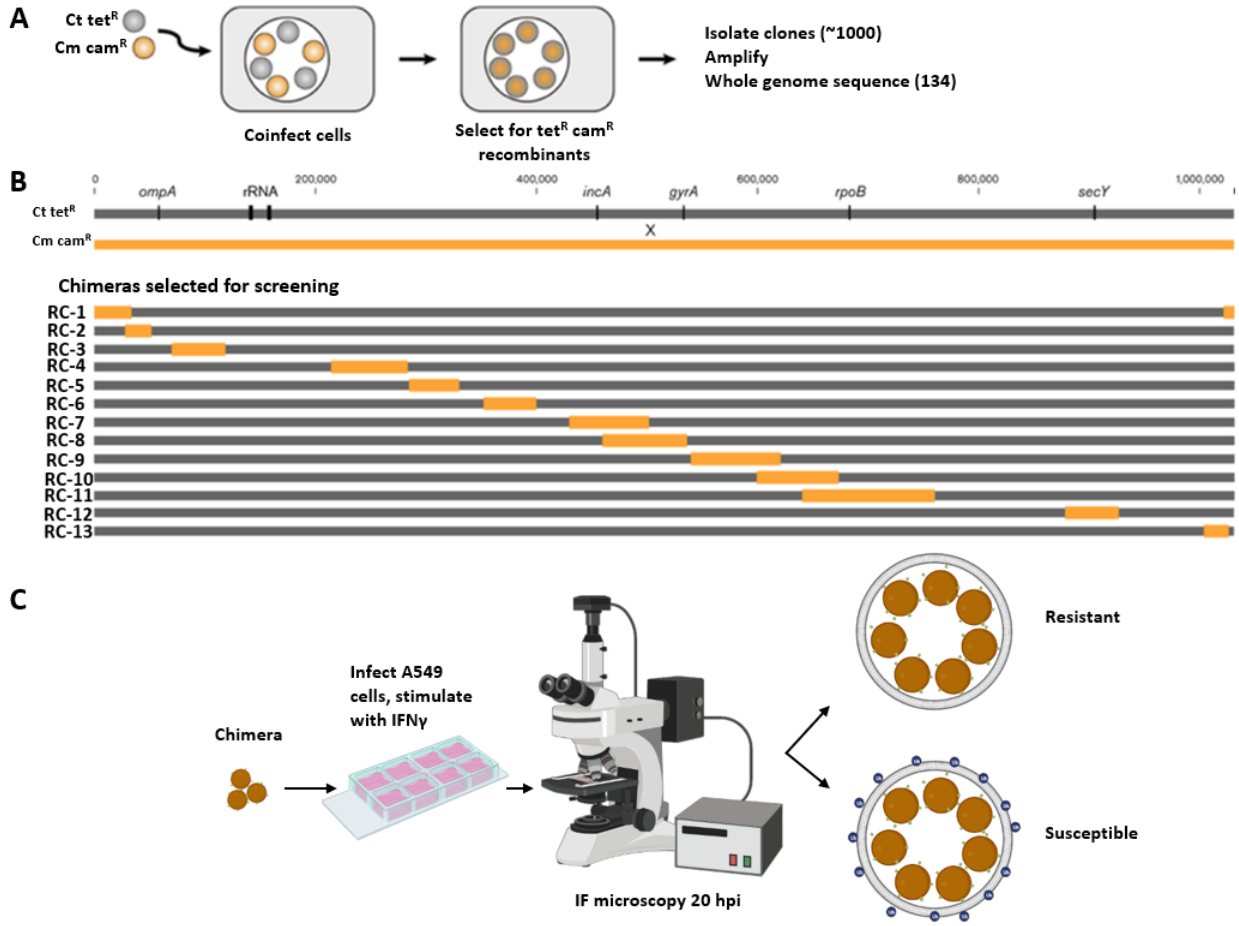

Figure 2.1 Overview of chimeras and screening approach. (A) Interspecies chimeras were previously generated by crossing a tetracycline resistant *C. trachomatis* parent (gray) with a series of chloramphenicol resistant *C. muridarum* transposon mutants (orange)[84]. (B) 13 chimeras were selected with recombined *C. muridarum* loci (orange bars) that collectively replace 66% of the *C. trachomatis* genome (gray bars). (C) Chimeras were phenotypically screened for susceptibility to IFNγ-stimulated inclusion ubiquitination (blue circles on susceptible inclusion membrane) in human A549 epithelial cells.

Identification of chimeras susceptible to IFNγ-stimulated cell-autonomous immunity.

Given the disparate susceptibility of *C. trachomatis* and *C. muridarum* to IFNγ-stimulated defense mechanisms in human epithelial cells[59], we hypothesized that one or more of the 13 selected chimeras had lost the *C. trachomatis* virulence factor(s) required for resistance to human cell-autonomous immunity and instead express non-complementary *C. muridarum* homologues[86]. Because ubiquitin deposition onto inclusions is the first known event of this IFNγ-induced pathway in human cells, we designed a visual screen to identify chimeras exhibiting a ubiquitin susceptibility phenotype in human epithelial cells. Human A549 epithelial cells were infected with *C. trachomatis*, *C. muridarum*, or our chimeras in 8-well chamber slides. Infected cells were stained for ubiquitin and *C. trachomatis* MOMP at 20 hours post infection (hpi). The *C. muridarum* strain used in this study encodes a green fluorescent protein (GFP) on a transposon inserted into an intergenic region of its genome. The percentage of inclusions with a clearly visible ring of ubiquitin surrounding them (arrows in right panel of Fig. 2.2A) were quantified and representative images were captured. We determined that 40.9% of *C. muridarum* inclusions were targeted by ubiquitin in IFNγ-treated A549 cells, whereas *C. trachomatis* inclusions were devoid of ubiquitin. These species-specific differences are in agreement with previously published data[59]. That we and others[59] do not observe complete ubiquitination of *C. muridarum* inclusions could suggest that there are multiple *C. trachomatis* factors involved in resistance to cell-autonomous immunity, and that *C. muridarum* encodes functional copies of some but not all of them. Alternatively, there may be heterogenous expression of the IFNγ-receptor in the A549 cell line we use, which

could result in some cells being sub-optimally stimulated in our *in vitro* assay. Chimeras RC1-6 and RC9-13 resisted inclusion ubiquitination in IFNγ-stimulated cells (Fig. 2.2A). We identified 2 chimeras, RC7 and RC8, whose inclusions were coated with ubiquitin at a rate similar to that observed for *C. muridarum*: 28% and 37% of their inclusions were targeted by ubiquitin in IFNγ-stimulated cells, respectively (Fig. 2.2A).

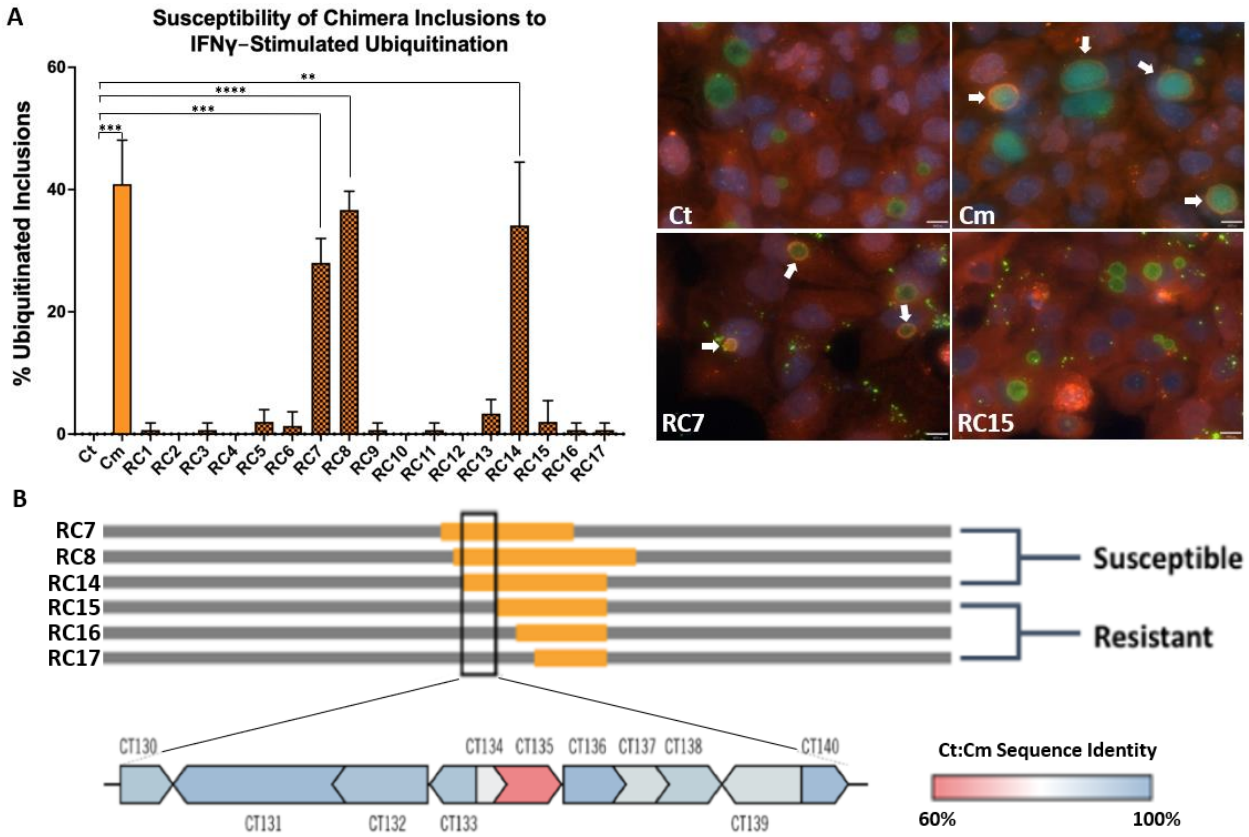

Figure 2.2 Chimera screen. (A) Human A549 epithelial cells were infected with parent species or chimeras and stimulated with IFNγ at 3 hours post infection (hpi). Cells were fixed at 20 hpi and stained for ubiquitin (red), Ct MOMP (green), and DNA (DAPI, blue). IF panels depict parental strains *C. trachomatis* (Ct), *C. muridarum* (Cm), a representative susceptible chimera (RC7) and a resistant chimera (RC15). Percentages of *Chlamydia* inclusions targeted by ubiquitin (arrows in IF images) were calculated. (B) Susceptible chimeras share an 11-gene locus of *C. muridarum* genes that are not recombined in any resistant chimeras. Data are representative of three technical replicates per *Chlamydia* strain. Data were analyzed for statistical significance using unpaired two-tailed *t* tests. Significant values are marked as follows: **, P < .005, ***, P < .001; ****, P < .0001.

RC7 and RC8 encode 75 and 71 recombined genes, respectively, and have an overlapping locus of 37 *C. muridarum* genes. To determine a more targeted locus of candidate virulence factors, we selected four additional chimeras, RC14-17, from our parent library with recombined loci that overlap with RC7-8 (Fig. 2.2B). 34% of a third chimera's (RC14) inclusions were targeted by ubiquitin, whereas the other three (RC15-17) were resistant, each with less than 3% ubiquitinated inclusions (Fig. 2.2A). Analysis of *C. trachomatis* genes missing in susceptible chimeras but present in resistant organisms led to our identification of an 11-gene candidate locus involved in immune evasion (Fig. 2.2B and Table 2.1). These results emphasize the utility of interspecies *Chlamydia* chimera libraries to efficiently perform genome-wide screens to identify discrete genetic loci that underlie phenotypes disparate between two species or strains of *Chlamydia*.

Table 2.1 Genes within candidate virulence locus

Gene	Ct:Cm Identity	Function
ct130	81.50%	Glutamine ABC transporter
ct131	85.40%	Hypothetical
ct132	83.10%	Inner membrane protein
ct133	82.70%	Hypothetical
ct134	70.20%	Inclusion membrane protein
ct135	65.10%	Inclusion membrane protein
ct136	85.70%	Putative serine esterase
ct137	74.40%	Threonylcarbamoyl-AMP synthase
ct138	78.70%	Putative dipeptidase
ct139	74.10%	ABC transporter, substrate-binding protein
ct140	84.90%	Putative preQ0 transporter YhhQ

Genes are given with *C. trachomatis* serovar D nomenclature for consistency with other tables and figures. Percent identity was calculated by comparing the coded amino acid sequence of *C. trachomatis* serovar L2 and *C. muridarum* homologues for each gene.

Analysis of candidate genes.

The identification of a conserved locus of 11 *C. trachomatis* genes replaced in susceptible chimeras (summarized in Table 2.1) suggested that one or more of those genes are required for *C. trachomatis* resistance to cell-autonomous immunity. We prioritized individual genes for follow up analysis based upon the following parameters: 1) given the high synteny of *C. trachomatis* and *C. muridarum* genomes, we hypothesize that the virulence gene has experienced divergent evolution between these two species. 2) The virulence factor is likely secreted by the chlamydial T3SS. As discussed in the introduction section, the T3SS is responsible for secreting factors outside of bacterial cells—either to be inserted in the inclusion membrane (Inc proteins) or freely soluble in the host cytosol, such that they are properly localized to interfere with host cytosolic machinery and cell-autonomous immune-mediated recognition of the inclusion membrane. We ranked two genes, *ct134* and *ct135*, as the highest priority based upon these parameters, as they are validated inclusion membrane proteins (Incs)[87] and possess the highest divergence among the candidate genes between *C. trachomatis* and *C. muridarum* (Table 2.1). While *ct134* has not been characterized, *ct135* has been implicated as a potential virulence factor[88,89], therefore it was selected as the top candidate for follow up experiments.

Conclusion

The paucity of identified *C. trachomatis* virulence factors is largely due the historic lack of genetic tools to manipulate the chlamydial genome, and recent advances in genetic engineering of *Chlamydia* species have revolutionized the field[23]. While small-

scale genetic engineering of *Chlamydia* strains is invaluable for investigating focused questions at the single-gene level, the field needs large-scale mutant libraries amenable to genome-wide screens to elucidate genes underlying various phenotypes. Despite advances in genetic manipulation, the only such mutant libraries have been generated through chemical mutagenesis of *Chlamydia*[90]. However, the random nature of chemical mutagenesis can make genotype-phenotype linkages difficult to interpret, as there are often mixtures of nonsense, missense, and frameshift mutations in multiple genes for any given mutant clone.

Our group has generated a methodology to cross two *Chlamydia* species to create large interspecies chimera libraries amenable to genome-wide screens for genes underlying disparate phenotypes between parent species. Our current library consists of >1000 *C. trachomatis* x *C. muridarum* chimeras. These strains were uniquely suited to screen for genes underlying *C. trachomatis*-restricted resistance to human cell-autonomous immunity, although other known phenotypes can readily be investigated with our library—examples include genes important to *C. muridarum* colonization and ascension of the murine genital tract and those contributing to the shorter developmental cycle of *C. muridarum*. The application of our chimera library to probe for genes affecting chlamydial virulence is unprecedented. Our identification of 11 candidate virulence genes out of ~900 in the *C. trachomatis* genome is a major success of this screen and strongly supports this approach to identify genes related to species-specific phenomena among *Chlamydia* species.

Materials and Methods

Antibodies and reagents

Information for all primary antibodies: anti-Ubiquitin (Enzo Life Sciences, Farmingdale, NY; BML-PW8810-0500, 1:500), anti-MOMP (Virostat, Westbrook, ME; 1621, 1:1000). Secondary antibodies were all obtained from Thermo Fisher Scientific (Rockford, IL) and diluted 1:400 for immunofluorescence staining: Donkey anti-Goat Alexa Fluor 488 (A11055) and Rabbit anti-Mouse Alexa Fluor 594 (A11062). 4',6-diamidino-2-phenylindole (DAPI, Fisher Scientific, 1:2000) was used to visualize host nuclei and *Chlamydia* DNA.

Cell lines and bacterial strains

A549 (obtained from Dr. Michael Gale) and McCoy (obtained from Dr. Walt Stamm) cell lines were cultured at 37°C, 5% CO_2 in Dulbecco's modified Eagle medium (DMEM) supplemented with 1x GlutaMax (Gibco) and 10% fetal bovine serum (FBS, HyClone). Fully supplemented medium is referred to as DMEM-complete (DMEMc). *Chlamydia trachomatis* serovar L2 (434/Bu), and a *Chlamydia muridarum* strain that encodes green fluorescent protein (GFP) on a transposon inserted in an intergenic region were used in these experiments. *Chlamydia* strains were propagated by infecting McCoy cells for 48 hours. Infected cells were scraped into growth medium and centrifuged at 3500 x *g* for 5 minutes. Pellets were resuspended in 10% PBS and lysed by bead bashing. An equivalent volume of 2x sucrose phosphate buffer was added to lysates (final concentration: 0.2M sucrose, 8mM sodium phosphate pH 7.1). Lysates were centrifuged at 250 x *g* for 5 minutes and supernatants with *Chlamydia* elementary bodies (EBs) were

aliquoted and frozen at -80°C. Infection of host cells was performed by diluting *Chlamydia* EBs in DMEMc and adding to adherent host cells, then centrifuging at 700 x *g* for 30 minutes. Wherever indicated, human interferon gamma (IFNγ, R&D Systems, Minneapolis, MN; 285-IF-100) was added to the media at a final concentration of 100U/mL.

Generation of interspecies recombinant chimeras

Generation of our chimera library was previously described in detail[82]. Briefly, recombination experiments were performed in shell vials ($12mm^2$) seeded with 4.0×10^5 McCoy cells. These monolayers were coinfected with a single tetracycline-resistant (tet^R) *C. trachomatis* serovar L2 strain (CtL2tet9) and individual members of a previously generated chloramphenicol-resistant (cam^R) *C. muridarum* transposon mutant library. The CtL2tet9 parent encodes a 16kb genomic region acquired from *Chlamydia suis* containing a *tet*(C) gene[82,91]. Monolayers of McCoy cells were infected with approximate multiplicity of infection of 2.0 of both CtL2Tet9 and selected *C. muridarum* transposon mutants. Cultures were incubated for 30 hours at 37°C and 5% CO_2 in DMEM supplemented with 0.5 µg/mL tetracycline, 0.5 µg/mL chloramphenicol, and 1mg/mL cycloheximide to prevent overgrowth of McCoy cells. EBs were released at 30 hpi by freeze-thaw and were used to infect fresh McCoy monolayers in shell vials. This process was repeated until inclusions with dual resistant (cam^R and tet^R) *Chlamydia* were detected by immunofluorescence microscopy using an anti-*Chlamydia* lipopolysaccharide (LPS) monoclonal antibody. Recovered dual-resistant strains were cloned by limiting two-fold dilution and recombinants with a predominantly *C. trachomatis* serovar L2 genome were

determined by serological typing of MOMP via immunofluorescence microscopy and were subjected to whole genome sequencing.

Whole genome sequencing.

Chimera EBs were centrifuged at 16,000 x *g* for 10 minutes and supernatants were discarded. EB pellets were resuspended in water and treated with RQ1 DNase (Promega) at 37°C for 30 minutes. Reactions were terminated by adding RQ1 stop solution and incubating at 65°C for 10 minutes. EBs were supplemented with 5mM dithiothreitol and incubated at 56°C for 1 hour, and genomic DNA (gDNA) was extracted using a DNeasy blood and tissue kit (Qiagen). gDNA was prepared for sequencing with a Nextera XT DNA library preparation kit (Illumina), and whole genome sequencing was performed on an Illumina HiSeq 3000 at the Oregon State University Center for Genome Research and Biocomputing Core. Raw sequence reads were trimmed using Trimmomatic[92] and processed sequences were mapped to *C. muridarum* (NC_002620.2) and L2tet9 (CP035484.1) reference genomes using Bowtie2[93] and Trinity[94] programs. Final assemblies were analyzed with the sequence analysis software Geneious. Replication and termination sites of the chlamydial chromosome were determined through analyzing GCskew plots[95] (window size = 2,000, step size = 1,000).

Ubiquitination assay

8-well Nunc Lab-Tek II chambered cover glass slides (Thermo Fisher Scientific, Rockford, IL) were seeded with A549 cells. Cells were infected with *Chlamydia* strains such that three technical replicates are represented in the final data. Wells were either left untreated or stimulated with 100U/mL human IFNγ 3 hpi. Infected cells were fixed at 20 hpi with 3.7% paraformaldehyde for 20 minutes, washed 3 times with PBS, and

permeabilized with 0.5% Triton X-100 for 15 minutes. Wells were washed 3 times and blocked with 3% bovine serum albumin (BSA) in phosphate buffered saline (PBS) for one hour. Primary antibodies against ubiquitin and L2-MOMP were diluted (dilution factors listed under 'Antibodies and Reagents') in 1% BSA-PBS and incubated at room temperature for 1 hour, after which we performed three five-minute washes before adding secondary antibodies. Secondary antibodies and DAPI were diluted (dilution factors listed under 'Antibodies and Reagents') in 1% BSA-PBS and incubated for 45 minutes at room temperature in the dark. We performed 3 5-minute washes with PBS and slides were imaged in PBS and stored at 4°C. A Nikon Ti-E inverted microscope was used to image stained chamber slides. A Hamamatsu camera controller C10600 was used to capture images that were visualized using the software Volocity (PerkinElmer, Waltham, MA). For inclusion-recruitment assays, 50 inclusions were counted in each well, and each inclusion was defined as positive for ubiquitin recruitment if there was a complete ring clearly visible around the inclusion. The data in our recruitment assay represent the number of ubiquitin-positive inclusions divided by 50 (the total number of inclusions counted in each well). Data are representative of 3 technical replicates. Immunofluorescence images in figures are representative of the annotated strains/conditions. The microscopist was not blinded to conditions.

Chapter 3. *incU* (*ct135)* encodes an inclusion membrane protein that protects *Chlamydia trachomatis* inclusion membranes from ubiquitination in IFNγ-stimulated human cells

Introduction

The virulence factor(s) underlying *C. trachomatis* resistance to human cell-autonomous immunity is unknown. Our data in chapter 2 reveal striking differences between *C. trachomatis* and *C. muridarum* susceptibilities to IFNγ-stimulated immunity in human cells[59]. Nearly half of *C. muridarum* inclusions were decorated with ubiquitin in IFNγ-treated A549 cells in contrast to *C. trachomatis* inclusions that were completely devoid of ubiquitin in these same conditions (Fig. 2.2A). Two competing hypotheses could explain the complete nature of resistance observed for *C. trachomatis*. Evasion may be actively mediated through a virulence factor that directly interferes with or inhibits a key component of human cell-autonomous immunity. This interference would likely occur upstream of ubiquitination. An alternative hypothesis is that virulence is mediated through molecular mimicry of a host protein to disguise the inclusion membrane as 'self'. Detection of pathogen-containing vacuoles (PCVs) by murine cell-autonomous immunity is mediated by a missing-self mechanism allowing cells to differentiate endogenous organelles from PCV membranes[66]. This process is driven by immunity-related GTPases (IRGs) that are not encoded in the human genome[36]. It is conceivable that the general missing-self mechanism of detection is conserved in humans, and that a unique set of undefined factors evolved to replace IRGs in this process. Identification of a single *C.*

trachomatis gene from the genetic locus identified in chapter 2 may aid in generating a clearer hypothesis regarding the molecular mechanism of cell-autonomous immune resistance.

Of the 11 candidate genes identified in our initial chimera screen, *ct135* emerged as a priority for follow up based upon predetermined criteria. It is the most divergent candidate gene between *C. trachomatis* and *C. muridarum* (Table 2.1) and it encodes an inclusion membrane protein (Inc), placing it at the interface between the chlamydial inclusion and the host cytosol. Previous publications implicated *ct135* as a potential virulence factor with unknown function[88,96]. There is also evidence to suggest that *ct135* may be important in human infection, as this gene accumulates deleterious mutations during serial passage *in vitro*[89] but is intact in sequence data from clinical isolates[88]. To test whether *ct135* functions to inhibit cell-autonomous immunity, we obtained two previously isolated *C. trachomatis* strains encoding unique frameshift mutations within the *ct135* open reading frame, D-EC and D-LC. D-EC encodes a frameshift induced early stop codon towards the central region of *ct135*, whereas the premature stop codon within D-LC occurs much further upstream. D-EC also lacks the native *C. trachomatis* plasmid[96]. We predict that these mutant ORFs encode truncated versions of CT135 missing carboxyl-terminus amino acids following their early stop codons.

Results

Reinterpretation of D-LC and D-EC *ct135* open reading frames

D-EC and D-LC strains were derived by Dr. Harlan Caldwell's group in 2010 using a complex serial passage of the *C. trachomatis* D/UW-3/CX laboratory reference strain. D-EC encodes a frameshift-induced early stop codon in the middle of the *ct135* ORF whereas the second, D-LC, encodes a frameshift much earlier in the ORF (Fig 3.1). Full genome sequencing of these isolates revealed that they each encode 18 genomic mutations (Table 3.1). These strains are isogenic with one another except for their unique frameshift mutations in *ct135* (Fig. 3.1). The mutation in the D-LC strain was originally interpreted as non-deleterious to the mature protein, and previous studies have used D-LC as a 'wildtype' control to compare against D-EC to elucidate the role of *ct135* in virulence[88,96,97].

The original interpretation of the D-EC and D-LC frameshift mutations was that they would lead to two unique proteins translated from each of their *ct135* cistrons, corresponding to partial ORFs on the 5' and 3' sides of their premature stop codons (Fig. 3.1). According to this scheme, D-LC would translate a near full-length protein product missing 56 amino acids in its amino terminus[88]. There are several issues with this model. First, there is no start codon in the proposed location from which a ribosome could begin translation after the frameshift-induced premature stop[88]. Second, if alternative start codons initiate translation of the downstream from these premature stop codons, they would in theory require internal ribosome binding sites. Such a mechanism of internal ribosome entry has not been documented for *Chlamydia*. Finally, if the original

interpretation is correct, the main IncU fragment for D-LC would lack the first 56 amino acids in its primary sequence. The first 20 amino acids of CT135 were previously shown to encode a type-III signal sequence[98], and deletion of these residues in the mature CT135 of D-LC would likely impede its secretion by the *Chlamydia* T3SS, prohibiting its translocation into the inclusion membrane. Because of these issues, we believe that the mutations within D-EC and D-LC are both deleterious and that they likely encode truncated versions of IncU.

Table 3.1. Mutations within D-EC and D-LC genomes

Gene	D-EC	D-LC
ct025	C→G‡	C→G‡
ct049	G→C‡, A→G	G→C‡, A→G
ct135	::T°	ΔT°
ct352	A→C‡	A→C‡
ct394	A→G‡	A→G‡
*ct446-ct447**	G→T	G→T
ct511	G→T	G→T
ct551	::G°	::G°
*ct556-ct557**	C→T	C→T
ct621	T→C‡	T→C‡
ct630	T→C‡	T→C‡
*ct632-ct633**	A→T	A→T
ct638	::G°	::G°
ct640	T→C‡	T→C‡
*ct655-656**	::C	::C
23S rRNA	G→A	G→A
23S rRNA	G→A	G→A
23S rRNA	ΔC	ΔC

Summary of nucleotide (nt) mutations in open reading frames or intergenic regions (*) and whether they lead to synonymous or nonsynonymous (‡) changes to encoded amino acids, or frameshifts (°) caused by nt insertion (::) or deletion (Δ).

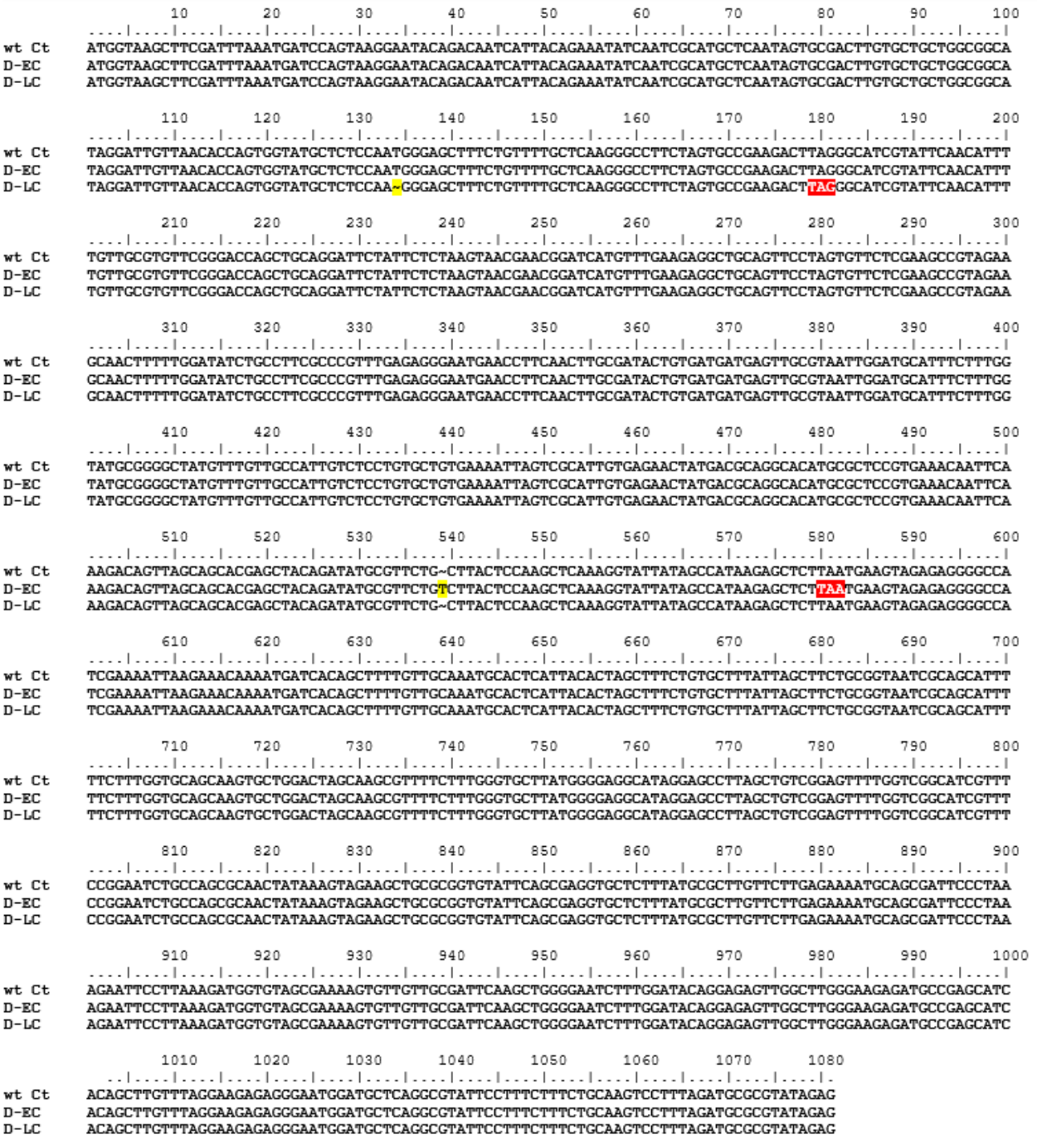

Figure 3.1 Comparison of *ct135* open reading frames. *ct135* open reading frames are shown for wildtype *C. trachomatis* (wt Ct), D-EC, and D-LC. Single nt deletions/insertions are highlighted in yellow for D-LC and D-EC. The early stop codons induced by these frameshifts are highlighted in red.

Susceptibility of D-EC and D-LC mutants to ubiquitination and decreased progeny production in IFNγ-primed human cells.

In chapter 1 we identified a subset of interspecies chimeras that were susceptible to inclusion ubiquitination in IFNγ stimulated human cells. Eleven genes were uniquely shared in their recombined loci and were not recombined in any resistant chimera. Analysis of these candidate genes led us to prioritize *ct135* for follow up experiments. To test whether this gene facilitates resistance to cell-autonomous immunity, we obtained the published D-EC and D-LC strains of *C. trachomatis,* which possess frameshift mutations in *ct135* (Fig. 3.1), from Dr. Harlan Caldwell. We infected A549 human epithelial cells with D-EC, D-LC, a wildtype strain of *C. trachomatis* serovar D, and *C. muridarum*. Infected cells were stimulated with IFNγ (100U/mL) at 3 hours post infection (hpi) and fixed at 20 hpi and we stained them for ubiquitin and *C. trachomatis* MOMP. Our *C. muridarum* strain expresses GFP from a transposon inserted into an intergenic region of its genome. Immunofluorescence microscopy revealed *C. muridarum,* D-EC, and D-LC all inhabited inclusions that were targeted by ubiquitin (Fig. 3.2).

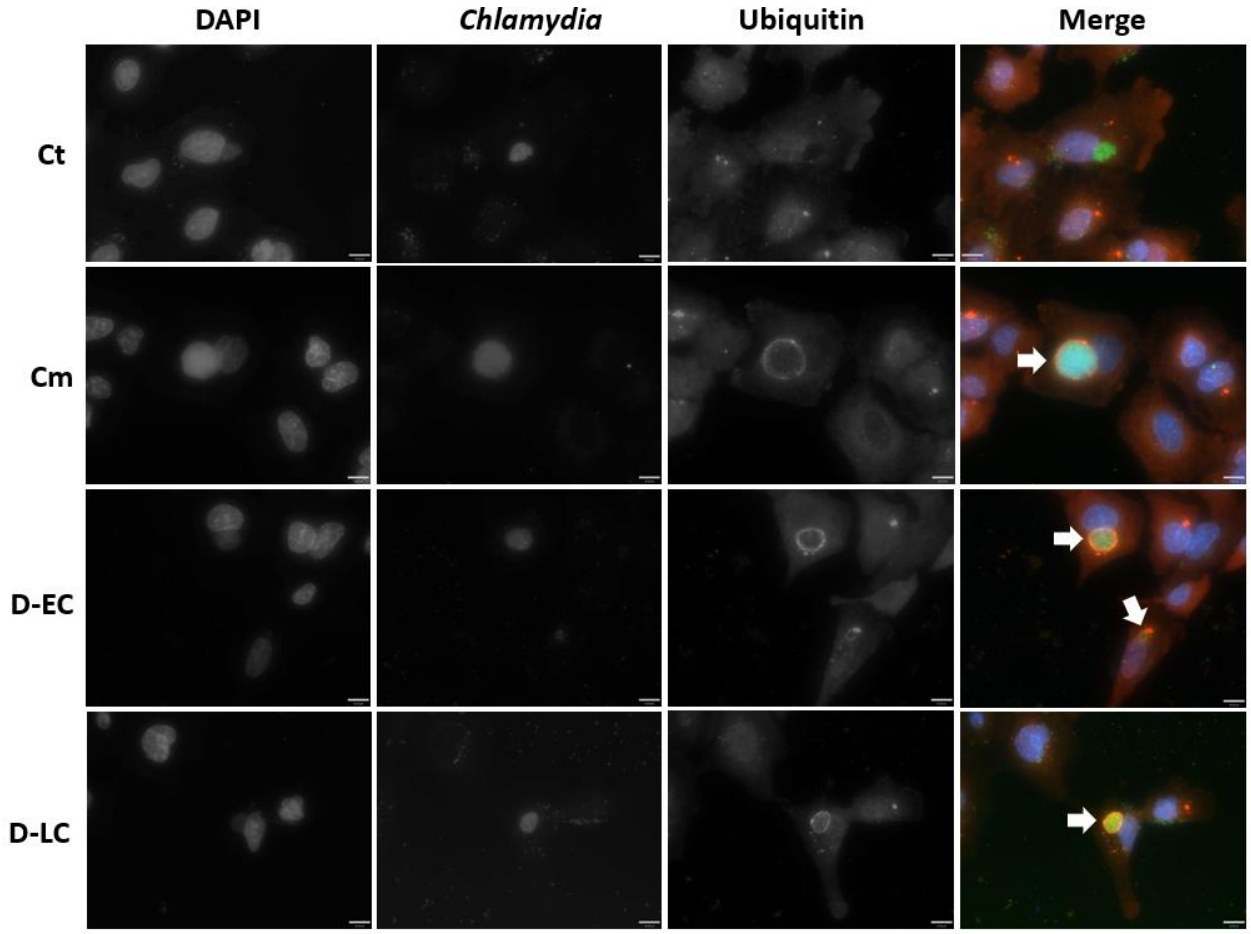

Figure 3.2 Ubiquitin recruitment to inclusions in IFNγ-stimulated human cells. A549 epithelial cells were infected with *C. trachomatis* (Ct), *C. muridarum* (Cm), D-EC, and D-LC and stimulated with IFNγ (100U/mL) 3hpi. Cells were fixed at 20hpi and stained for ubiquitin (red), Ct MOMP (green), and DNA (DAPI, blue). Cm is a transgenic strain expressing GFP (green). Ubiquitinated inclusions are marked with arrows, scale bar = 16µm.

We found that 51.9% of D-EC inclusions and 58.5% of D-LC inclusions were ubiquitinated in IFNγ-stimulated A549 cells (Fig. 3.3A). In unstimulated cells, ubiquitin recruitment was only 2.5% and 5.8%, respectively (Fig 3.3A). 34.7% of *C. muridarum* inclusions were targeted by ubiquitin in stimulated cells versus 11.1% in unstimulated conditions (Fig. 3.3A). Wildtype *C. trachomatis* was completely resistant to inclusion ubiquitination regardless of IFNγ-stimulation of host cells (Fig. 3.3A). The percentage of

ubiquitinated inclusions was higher for D-EC and D-LC than for *C. muridarum* or the chimeras carrying the *C. muridarum ct135* homologue *tc0412*. Because our chimeras are in a *C. trachomatis* serovar L2 background, this difference could reflect serovar-specific susceptibility to cell-autonomous immunity. In contrast, it may indicate that TC0412 confers partial resistance to human cell-autonomous immunity, which would explain why *C. muridarum* and chimera inclusions are targeted by ubiquitin at a lower rate.

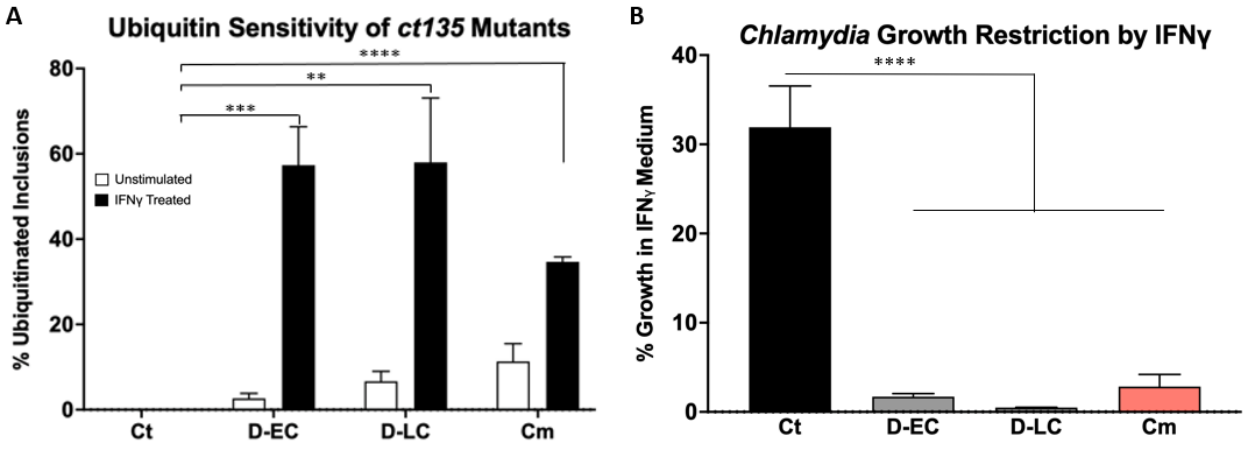

Figure 3.3 *ct135* mutants are susceptible to human cell-autonomous immunity. (A) A549 epithelial cells were infected with *C. trachomatis* serovar D (Ct), *C. muridarum* (Cm), D-EC and D-LC cultured in medium containing IFNγ (100U/mL) or left unstimulated at 3 hpi. Ubiquitinated inclusions were identified via immunofluorescence microscopy to calculate the average percentage of ubiquitinated inclusions. (B) Effect of IFNγ stimulation on progeny production was determined by calculating the percentage of inclusion forming units (IFUs) from infections in IFNγ-primed cells versus IFUs from unstimulated cells. Cell culture medium was supplemented with tryptophan (100ug/mL) to mitigate the effects of IFNγ-induced IDO. Means and standard deviations of 3 technical replicates are shown. Data were analyzed for statistical significance using unpaired two-tailed *t* tests (A) or one-way ANOVA (B): **, P < .005, ***, P < .001; ****, P < .0001

While ubiquitination is the earliest known step in the human cell-autonomous immune response, an important downstream outcome of this pathway is growth restriction of the bacteria. We observed a large growth defect among *ct135* mutants and *C. muridarum* in IFNγ-primed cells compared to wildtype *C. trachomatis*. In IFNγ-primed cells, D-EC, D-LC only grew to 1.7% and 0.5% compared to their growth in untreated host cells (Fig. 3.3B). These rates were similar to the 2.8% growth observed for *C. muridarum* and all were significantly lower than the 31.9% of growth observed for wt *C. trachomatis*. All cells in these experiments were supplemented with tryptophan (Trp) to mitigate bactericidal effects of cytosolic Trp depletion by IFNγ-induced indoleamine-2,3-dioxygenase[58]. The growth restriction of *C. trachomatis* in IFNγ-primed host cells was unexpected and may be due to insufficient Trp supplementation in our culture medium. Taken together, these data implicate *ct135* as a virulence factor that functions to evade cell-autonomous immunity in human cells. D-LC and D-EC were both susceptible to this pathway in IFNγ-stimulated human cells (Fig 3.2A), supporting our prediction that the *ct135* ORFs in both of these strains are disrupted. These data invite a reinterpretation of previous studies that used D-LC as a wildtype control in experiments to characterize the role of *ct135* in *C. trachomatis* virulence. Given its role in preventing inclusion ubiquitination in IFNγ-primed cells, we have named CT135 ‘inclusion membrane protein U’ (IncU), to which it will be referred hereafter.

Structural predictions of IncU

Chlamydial inclusion membrane proteins do not share sequence homology with any other known gene products in nature; thus, inferring their potential functions from sequences has not been possible. Recent computational advances in predicting protein secondary and tertiary structure based on polypeptide folding have made it possible to derive structural models for proteins with no sequence-based homologues. Through an ongoing collaboration with the Seattle Structural Genomics Center for Infectious Disease (SSGCID), we sought to determine the protein structure of IncU by crystallography and computational approaches. We submitted the IncU amino acid sequence to the SSGCID pipeline and worked with them to produce purified full-length protein. Staff at the SSGCID experienced similar difficulties to our own attempts to clone and express the *incU* gene in *E. coli* and thus were unable to proceed with purification and crystallization.

In lieu of this setback, SSGCID submitted the IncU primary sequence to the RobeTTa and AlphaFold servers, which are currently the most accurate *de novo* protein structure prediction software according to the most recent Critical Assessment of Structure Prediction (CASP). Both RobeTTa and AlphaFold predicted a predominantly alpha-helical structure of IncU (Images next to Table 3.2 and Table 3.3, respectively). Our collaborators at the SSGCID identified 4 hydrophobic transmembrane domains with structural characteristics similar to pore-forming proteins in other organisms. Specifically, they determined the AlphaFold IncU predicted structure has structural homology to the helical bundle arrangement found in human Ca^{2+} release-activated Ca^{2+} (CRAC) channels (PDB ID: 4HKR). A late 2021 publication presented the hypothesis that IncU is a pore-forming protein situated in the inclusion membrane for the secretion of *C.*

trachomatis pathogen-associated molecular patterns (PAMPs) into the cytosol of host neutrophils in the mouse model[99]. The authors put forth the idea that IncU-mediated secretion of an outer membrane protein of *C. trachomatis* may activate NLRP3 inflammasomes to promote death of infected mouse neutrophils[99]. We have not observed any host cell death in our experiments using human epithelial cells, suggesting that IncU virulence mechanisms may be tailored to the host species or cell type *C. trachomatis* finds itself in, or alternatively may be multifactorial. Future experiments should perhaps investigate whether a similar IncU-dependent killing occurs in infected human neutrophils. If IncU is indeed a pore-forming inclusion membrane protein, defining substrates that it releases into the host cytosol or internalizes into the inclusion lumen will be critical to inform molecular mechanisms that lead to the killing of murine neutrophils[99] and resisting cell-autonomous immunity in human epithelial cells.

In parallel with our collaborators' analyses, I submitted both RobeTTa and AlphaFold predicted structures to a 3D structure BLAST server (BioXGEM) to generate an alternative list of putative IncU structural homologues. Several proteins were identified as having structural homology to these predictions. The top proteins with homologous structures to the RobeTTa prediction are summarized in Table 3.2, and those with homology to the AlphaFold prediction are summarized in Table 3.3. The reported *E*-values offer a metric to determine the significance of each hit from the structure BLAST. They are calculated based upon the number of common protein substructures that are shared between the input query (IncU) and proteins within a given database. Essentially, smaller E-values correspond to higher confidence of structural homology. Although the tertiary structures are distinct between the two IncU predictions, there was a high degree

of conservation among predicted structural homologues to each predicted structure. While any conclusions based upon these structural similarities are purely speculative, the most interesting result from these unbiased screens was that both predicted structures exhibited some homology to human guanylate binding protein 1 (GBP1). GBP1 is an IFNγ-inducible GTPase that is critical to human cell-autonomous immunity against intracellular pathogens, including *Chlamydia*[76,100].

Table 3.2 3D Structure BLAST results of RobeTTa-predicted IncU structure.

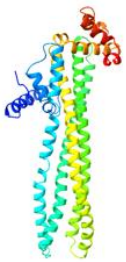
IncU (RobeTTa)

Protein Name	Function	Organism	E-Value
SAV1866	Multidrug transporter	*S. aureus*	4.00E-53
CIP4	Membrane tubulation	*H. sapiens*	2.00E-51
MalT	Transcription factor	*E. coli*	5.00E-50
GBP1	Cell-autonomous immunity	*H. sapiens*	2.00E-49
IRSp53	Adaptor protein	*H. sapiens*	9.00E-47
APPL1	Adaptor protein	*H. sapiens*	2.00E-46

Table 3.3 3D Structure BLAST results of AlphaFold-predicted IncU structure.

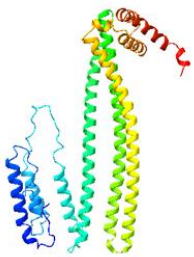
IncU (AlphaFold)

Protein Name	Function	Organism	E-Value
CIP4	Membrane tubulation	*H. sapiens*	2.00E-52
APPL1	Adaptor protein	*H. sapiens*	2.00E-47
GBP1	Cell-autonomous immunity	*H. sapiens*	9.00E-47
IRSp53	Adaptor protein	*H. sapiens*	1.00E-45
SAV1866	Multidrug transporter	*S. aureus*	3.00E-42
Amph	Endocytosis, tubule formation	*D. melanogaster*	2.00E-40

Crystal structures have not been published for any *C. trachomatis* inclusion membrane protein. The difficulty of purifying Incs may be in part due to their being transmembrane proteins that are recalcitrant to protein crystallization methods[101]. Structural analysis of Incs could be a rewarding approach to generate hypotheses regarding their functions. Recent advances in *ab initio* protein structure prediction provide a straightforward approach to predict Incs' tertiary structures in the absence of crystal structures. Analysis of structural homologues of these predictions, as performed here for IncU, may yield meaningful results compared to searching for sequence-based homologues in other organisms.

Conclusion

Dr. Harlan Caldwell's lab previously isolated two clonal mutant populations, D-EC and D-LC, which encode frameshift mutations within the open reading frame (ORF) of *incU*. D-LC was originally described as encoding a functional copy of *incU* and D-EC was considered to encode a nonfunctional *incU*. D-LC was able to infect mice for a longer duration that D-EC, suggesting that this gene is important for *C. trachomatis* infection in mice[88]. Based on our findings, we disagree with the original interpretation of these ORFs, and we predict that the frameshift mutations lead to dysfunction of IncU in both strains. Our *in vitro* characterization of these strains supports our prediction, as D-EC and D-LC are equally susceptible to recognition and growth restriction by human IFNγ-induced cell-autonomous immunity. Importantly, published data have shown that wildtype *C. trachomatis* is susceptible to murine cell-autonomous immunity, suggesting that IncU is a

host-specific virulence factor[62]. It is unclear why D-LC caused a longer-lasting infection than D-EC in the mouse model[88]. *incU* frameshift mutants exhibit a markedly increased growth rate *in vitro*, and in the context of murine infection where IncU does not confer resistance to cell-autonomous immunity[62], the selection for frameshift mutants may be due to faster growing members of the population outcompeting wildtype organisms[102]. In contrast, it is clear that there is sufficient pressure to maintain the integrity of this gene in native human hosts given the lack of deleterious *incU* mutations identified from clinical samples[88].

Following the identification of an 11-gene locus in our chimera screen, we identified a single *C. trachomatis* gene, *incU*, that is responsible for preventing inclusion ubiquitination in IFNγ-stimulated human cells. While this provides a general mechanism for its previously suspected role in virulence, the molecular mechanism remains unknown. *Ab initio* predictions of the IncU tertiary structure may guide future hypotheses regarding its function(s). Interestingly, we identified human GBP1 as a structural homologue to both RobeTTa and AlphaFold predicted structures. GBP1 is an IFNγ-stimulated protein that is critical for cell-autonomous control of *Chlamydia*[76,100], and it readily associates with ubiquitinated *Chlamydia* inclusions to facilitate their clearance through a poorly defined mechanism[59,76]. One of our hypotheses is that IncU mediates resistance to cell-autonomous immunity via molecular mimicry of a host protein. Putative structural homology with GBP1 may inform a more defined hypothesis, wherein *C. trachomatis* expresses IncU to disguise inclusions as already ‘marked’ to cell-autonomous immune machinery. With recent advances in a*b initio* protein structure prediction software,

structural predictions of IncU and other Incs may lead to hypotheses aimed at elucidating their molecular functions.

The data discussed in this chapter invite a reinterpretation of previously published studies that used the D-LC strain of *C. trachomatis* as a wildtype control in their analyses[88,96,97]. One of these studies was performed in the pigtailed macaque model wherein the authors found no difference in virulence between D-EC and D-LC and concluded that *incU* is not important for *C. trachomatis* virulence in this model organism[97]. The absence of a wildtype control in this study makes significant reinterpretation impossible. However, a detailed look at the methods section reveals an unusual aspect of the study: only 3 of 6 animals infected with both D-EC and D-LC were represented in the final data because half of both groups failed to establish a detectable infection[97]. Per communication with the study's lead author, Dr. Dorothy Patton, this was a remarkable outcome, as her group reliably achieves infection following inoculation of NHP with *C. trachomatis*, and 100% infection would have been expected in the wild-type control. Reevaluation of that study in combination with our data led us to hypothesize that infection by *incU* mutants is attenuated in nonhuman primates—which may employ a human-like cell-autonomous immune response.

Materials and Methods

Antibodies and reagents

Information for all primary antibodies: anti-Ubiquitin (Enzo Life Sciences, Farmingdale, NY; BML-PW8810-0500, 1:500) and anti-MOMP (Virostat, Westbrook, ME; 1621, 1:1000). Secondary antibodies were all obtained from Thermo Fisher Scientific (Rockford, IL) and diluted 1:400 for immunofluorescence staining: Donkey anti-Goat Alexa Fluor 488 (A11055) and Rabbit anti-Mouse Alexa Fluor 594 (A11062). 4',6-diamidino-2-phenylindole (DAPI, Fisher Scientific., 1:2000) was used to visualize host nuclei and *Chlamydia* DNA.

Cell culture and bacterial strains

A549 (obtained from Dr. Michael Gale) and McCoy (obtained from Dr. Walt Stamm) cell lines were cultured at 37°C, 5% CO_2 in Dulbecco's modified Eagle medium (DMEM) supplemented with 1x GlutaMax (Gibco) and 10% fetal bovine serum (FBS, HyClone). Fully supplemented medium is referred to as DMEM-complete (DMEMc). *Chlamydia trachomatis* serovars and strains used in this chapter include *Chlamydia trachomatis* D/UW-3/CX, and a *Chlamydia muridarum* strain which encodes green fluorescent protein (GFP) on a transposon inserted in an intergenic region. *incU* mutants D-EC and D-LC were previously isolated by Dr. Harlan Caldwell's lab and were provided to us by Dr. Dorothy Patton[88]. *Chlamydia* strains were propagated by infecting McCoy cells for 48-72 hours. Infected cells were scraped into growth medium and centrifuged at 3500 x *g* for 5 minutes. Pellets were resuspended in a 10% phosphate buffered saline solution and lysed by bead bashing. An equivalent volume of 2x sucrose phosphate buffer

was added to lysates (final concentration: 0.2M sucrose, 8mM sodium phosphate pH 7.1). Lysates were centrifuged at 250 x *g* for 5 minutes and *Chlamydia* elementary bodies (EBs) within supernatants were aliquoted and stored at -80°C. A549 and McCoy cells were inoculated with *Chlamydia* EBs diluted in DMEMc in tissue culture plates or chamber slides then centrifuged at 700 x *g* for 30 minutes and grown at 37°C, 5% CO_2 for the duration of given experiments.

Analysis of Ubiquitin recruitment to inclusions

8-well Nunc Lab-Tek II chambered coverglass slides (Thermo Fisher Scientific, Rockford, IL) were seeded with A549 cells and cultured at 37°C, 5% CO_2. Cells were infected with *Chlamydia* strains (described above) and wells were either left untreated or stimulated with 100U/mL human interferon gamma (IFNγ, R&D Systems, Minneapolis, MN; 285-IF-100) at 3 hours post infection (hpi). Infected cells were fixed at 20 hpi with 3.7% paraformaldehyde for 20 minutes, washed 3 times with phosphate buffered saline (PBS), and permeabilized with 0.5% Triton X-100 for 15 minutes. Wells were washed once more and blocked with 3% bovine serum albumin (BSA) in PBS for one hour. Primary antibodies diluted in 1% BSA-PBS (dilution factors listed under 'Antibodies and reagents') were added to wells and incubated at room temperature for 1 hour, then were washed 3 times with PBS before adding secondary antibodies. Secondary antibodies and DAPI were diluted (dilution factors listed under 'Antibodies and Reagents') in 1% BSA-PBS and incubated for 45 minutes at room temperature in the dark. Wells were washed 3 times and imaged in PBS and stored at 4°C. Stained chamber slides were imaged under oil immersion and 60x magnification on a Nikon Ti-E inverted microscope. The microscopist was not blinded to conditions. A Hamamatsu camera controller C10600 was

used to capture images that were visualized using the software Volocity (PerkinElmer, Waltham, MA). For inclusion-recruitment assays, 50 inclusions were counted per technical replicate, and each inclusion was positive for ubiquitin recruitment if there was a complete ring clearly visible around the inclusion. Three replicates were performed for each target and *Chlamydia* strain combination. Immunofluorescence images in figures are representative.

Growth assay

A549 human epithelial cells were grown in 24-well dishes and were pretreated overnight with either DMEM supplemented with IFNγ (100U/mL) and tryptophan (Trp, 100ug/mL) or DMEM supplemented with Trp only. Pretreated cells were infected with *Chlamydia trachomatis* serovar D, *Chlamydia muridarum*, D-EC, and D-LC at an approximate MOI of 0.5. Infections were incubated for 27 hours, at which point the infected cells were mechanically scraped into media and centrifuged at 3500 x *g*. Infected cell pellets were resuspended in 10% PBS and were lysed by bead bashing. Lysates were centrifuged at 250 x *g* to remove host cell debris and EBs within the supernatants were serially diluted into 96 well plates seeded with confluent monolayers of McCoy cells. These plates were centrifuged at 700 x *g* and incubated at 37C, 5% CO_2. At 24 hpi, these 96 well plates were fixed with 3.7% paraformaldehyde, permeabilized with 0.5% Triton-X 100 and stained with a goat anti-MOMP antibody (Virostat) followed by a secondary donkey anti-goat antibody conjugated to Alexa Fluor 488 (Thermo Fisher Scientific) for visualization of *Chlamydia trachomatis* inclusions. *Chlamydia muridarum* inclusions were visualized through their transgenic expression of GFP. The number of inclusions per field was quantified via immunofluorescence microscopy to calculate inclusion forming units

per mL of the original lysates. Wells containing 10-100 inclusions per field were selected, and three fields were counted per strain/condition. Inclusion forming units (IFU) were calculated based upon the number of inclusions counted and at which dilution factor in the 96 well plates. IFU/mL values calculated for IFNγ + Trp pretreated conditions were divided by the IFU/mL in Trp-only (unstimulated) conditions for each *Chlamydia* strain tested and the resulting ratio was reported as percent growth in IFNγ stimulated cells. Data are representative of three technical replicates.

3D protein structure analysis

We submitted the *C. trachomatis* serovar D IncU amino acid sequence to the SSGCID who uploaded it to AlphaFold (DeepMind) and RobeTTa (Baker lab) protein prediction servers. Predicted structures were modeled using the ChimeraX molecular visualization program (UCSF). To search for structural homologues, we submitted .pdb files of IncU predictions to the 3D-BLAST Protein Structure Search (BioXGEM). We searched for homologues in the SCOP 1.75 (40%) database and set an *E*-value cutoff of 10^{-10}.

Chapter 4. A *C. trachomatis incU* Mutant Fails to Grow in the Nonhuman Primate Model of Infection.

Introduction

Nonhuman primates (NHPs) infected with *C. trachomatis* recapitulate many important facets of human *Chlamydia* infection and disease. In contrast to the mouse model, *C. trachomatis* can readily colonize pigtailed macaque (*Macaca nemestrina*) cervical tissues and maintain infection for up to 15 weeks. Experimental reinfection in macaques can lead to inflammation of upper genital tract tissues and sequelae similar to those in humans experiencing prolonged or repeated *Chlamydia* infections[103]. The NHP model is not without limitations, however these are largely financial and ethical considerations. The use of these animals in research is controversial, and the costs associated are significant[39]. Furthermore, there are only a few research institutions in the US and abroad with facilities to house and support NHP research. Finally, genetic engineering of NHP is extremely challenging, and most research is performed in outbred populations with remarkable intraspecies genetic diversity that can confound analyses of data generated using these model organisms[104]. Despite these limitations, there is no other animal model naturally susceptible to *C. trachomatis* infection that also recapitulates human disease outcomes. In the absence of human challenge studies, the use of NHPs is vital to our understanding of human *Chlamydia* infection.

Innate and adaptive immune cells which secrete IFNγ are critical to controlling *Chlamydia* infection in mice[56,105,106]. Cell-autonomous immunity is a critical component of this immune response as *Chlamydia*-infected epithelial cells stimulated with IFNγ can

independently detect and destroy *Chlamydia*-containing inclusions[62,63]. An association between IFNγ-secreting memory Th1 CD4+ T-cells and partial protection from reinfection has been observed in humans[57]. However, *C. trachomatis* is well documented to evade IFNγ-stimulated immune responses within infected human cells. Indoleamine-2,3-dioxygenase (IDO) is an IFNγ-inducible enzyme in humans that cleaves cytosolic tryptophan to starve auxotrophic intracellular pathogens, including *Chlamydia*[58]. Urogenital and LGV serovars of *C. trachomatis* encode a tryptophan synthase (TrpS) which can overcome this starvation through *de novo* sythesis of tryptophan from scavenged indole obtained from bacteria in the microbiota of the female genital tract[107].

The more recent discovery that *C. trachomatis* evades human cell-autonomous immunity is the second known mechanism by which this bacterium overcomes IFNγ-stimulated immune responses within human cells[59]. Our work along with published findings demonstrate that there is a strict host specificity to *C. trachomatis* resisting IFNγ-stimulated immunity[59,62,107]. Mice are not choice animal models for evaluating the anti-chlamydial effects of IFNγ at the cellular level as they do not encode an IFNγ-inducible IDO and employ a unique family of IRG proteins to mediate cell-autonomous immunity, which *C. trachomatis* fails to evade[62,108]. Thus, a more relevant model is needed to study the nature of immunological protection from *Chlamydia* that is conferred by IFNγ-secreting cells. NHPs are a great model for faithfully replicating important infection and clinical aspects of human chlamydial infections. Like humans, they encode an IFNγ-inducible IDO. However, cell-autonomous immunity in NHP has not been explored. As discussed in the introduction, humans and NHP both lack the IRG family of genes that initiate murine IFNγ -stimulated cell-autonomous immunity[36]. Therefore, we hypothesize

that NHP and humans evolved a distinct, shared mechanism to initiate this response to respond to intracellular pathogens and *C. trachomatis* resists NHP cell-autonomous immunity in an IncU-dependent manner.

We sought to test this hypothesis through analyzing a previous experimental infection of pigtailed macaques with an inoculum containing a mixed population of wildtype organisms and *incU* mutants. To assess whether NHP employ a human-like cell-autonomous immune response, we characterized whether primary NHP fibroblasts possessed the capacity to ubiquitinate *Chlamydia* inclusions in an IFNγ-dependent manner.

Results

A *C. trachomatis incU* mutant fails to grow in nonhuman primates

We investigated an unpublished macaque infection study (courtesy of Dr. Dorothy Patton) wherein an inoculum used to infect a cohort of six female macaques resulted in a poor rate of infection. Animals in this study were sexually mature pigtailed macaques (age range = 5-11 years) and were monitored for one month prior to infection to confirm they displayed normal menstrual cycles. The *C. trachomatis* inoculum used, D/6319, was a clinically isolated serovar D strain propagated *in vitro* to achieve a sufficient titer for infection. Animals were vaginally infected with 1×10^5 inclusion forming units of D/6319. Cervical secretions were collected at baseline and once weekly throughout the 5-week observation period. *C. trachomatis* was detected by culture and nucleic acid amplification

tests (NAATs), and animals were considered infected if they tested positive by culture or NAAT.

Only 2 of the 6 macaques consistently tested positive for *C. trachomatis* infection throughout the 5-week observation period (Fig. 4.1 B). From conversations with our collaborator Dr. Dorothy Patton who ran the study, this was an unusually poor rate of infection compared to routine macaque infection with identical titers of other *C. trachomatis* strains. We hypothesized that the D/6319 inoculum harbored mutants that grew poorly *in vivo*. To address this question, we analyzed D/6319 and 5-week post infection (wpi) populations via whole genome sequencing (WGS). The 5wpi sample was cultured from animal number A11257, one of the two animals that remained infected throughout the duration of this study (Fig 4.1B).

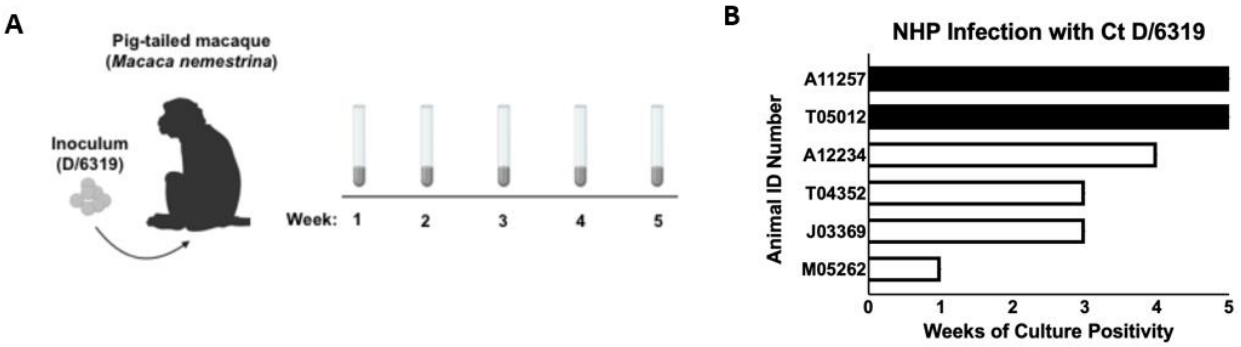

Figure 4.1 Inoculum D/6319 exhibits weak infectivity of NHP. (A) A graphical overview of NHP infection and weekly sample collection. This experiment was previously performed by Dr. Dorothy Patton's group. (B) The number of weeks individual animals were culture and/or NAAT positive for *C. trachomatis* infection throughout the 5-week observation period.

The only mutations observed in the inoculum were within the *incU* open reading frame (ORF). A proportion (27.7%) of *incU* sequences from the inoculum harbored a single base pair deletion at nucleotide (nt) 541, causing a frameshift and an early stop

codon in the ORF (Fig. 4.2, deletion highlighted in yellow, premature stop codon highlighted in red). This population is referred to as CtΔ*incU*. This mutation occurred 3 nt downstream from the frameshift mutation within D-EC, and the predicted protein product is truncated even earlier than in D-EC (compare Fig. 3.1 and Fig. 4.2). Two single nucleotide polymorphisms (SNPs) were also detected in the 3' end of *incU* ORFs in this population (Fig. 4.2). The less represented SNP was a synonymous A1034C nt transition (Fig. 4.2, CtSyn, SNP highlighted in pink), whereas the second SNP resulted in a R284Q mutation in the translated product (Fig. 4.2, CtR284Q, SNP highlighted in green). These SNPs were detected in 1.1% and 16.7% of the inoculum sequences, respectively. Interestingly, the R284Q mutation and the silent SNP were detected at increased rates by WGS of the 5 wpi population, representing 74.8% and 18.6% of sequences, respectively. The frameshift mutation was not detected via WGS of the 5 wpi sample, suggesting that this population failed to establish a productive infection in NHPs. The *incU* allele frequencies within the D/6319 inoculum and 5 wpi populations are summarized in Fig. 4.3A. Considering the *in vitro* results discussed in chapter 3, wherein *C. trachomatis* strains with frameshift mutations in *incU* were susceptible to IFNγ-stimulated cell-autonomous immunity in human cells, we predicted that the *incU* frameshift mutation identified in the D/6319 inoculum would render organisms similarly susceptible to this response.

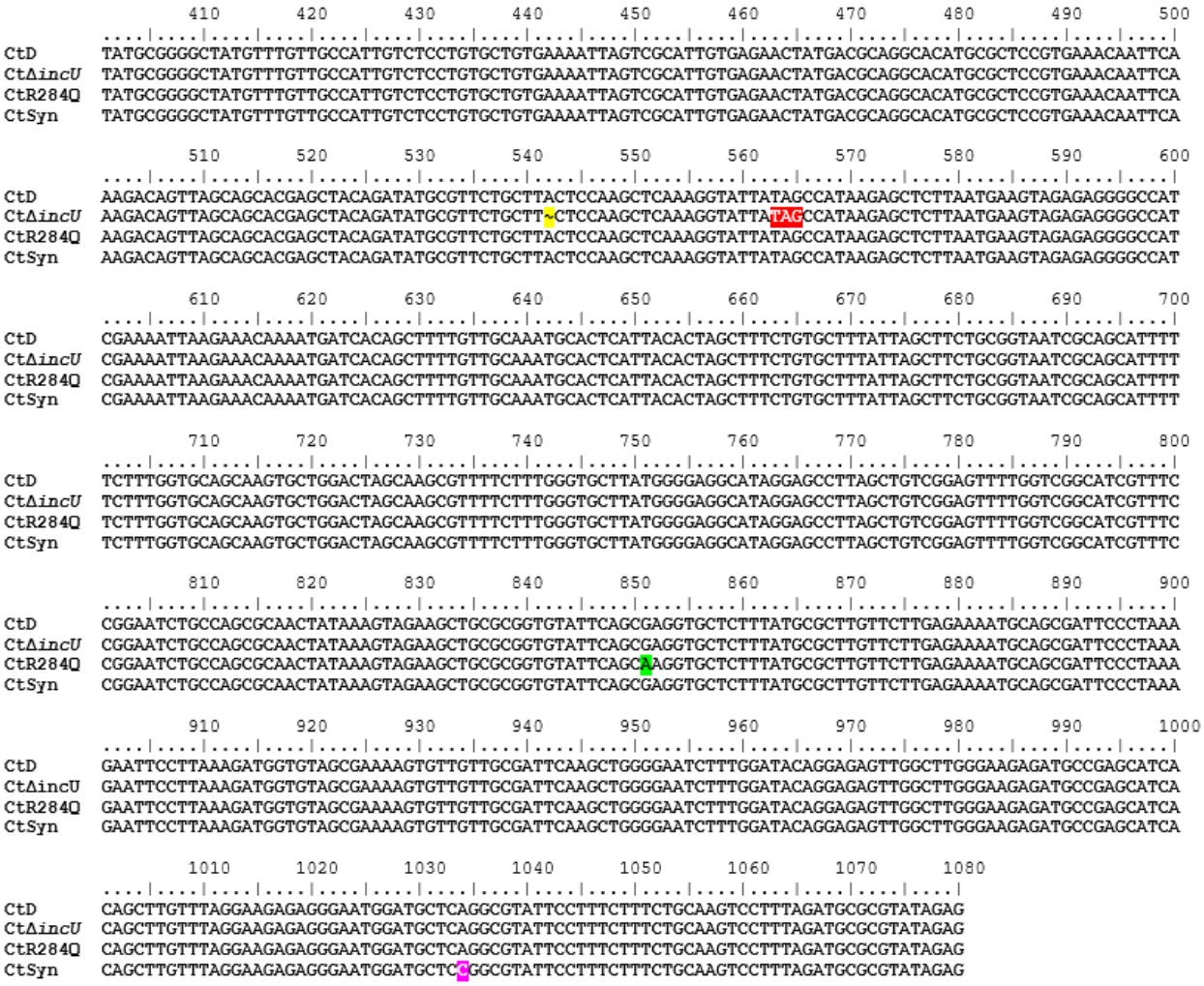

Figure 4.2 Analysis of *incU* mutations identified within the D/6319 inoculum and 5wpi endpoint samples by whole genome sequencing (WGS). Genomic DNA was extracted from EBs of inoculum and endpoint samples and processed for sequencing with an Illumina Nextera XT DNA library preparation kit. WGS was performed on an Illumina HiSeq 3000 and revealed there were 3 unique mutants within these sequenced populations. The most abundant mutant strain within the inoculum, CTΔ*incU*, encoded a single nucleotide (nt) deletion (Δ542, highlighted in yellow) leading to a premature stop codon (highlighted in red).This mutant was not detected via WGS of the endpoint population. The next most abundant mutant determined by WGS was CtR284Q, which carried a SNP (highlighted in green) leading to an R284Q amino acid transition of the encoded protein. CtR284Q made up 16.7% and 74.8% of the inoculum and endpoint populations, respectively. The final mutant identified, CtSyn, encoded a silent A1034C nt transition (highlighted in pink). CtSyn represented 1.1% and 18.6% of the inoculum and endpoint populations, respectively. Estimates of abundances were inferred by the percentage of reads for each SNP identified in our WGS data. Only the 3' end of *incU* is displayed for clarity. No other mutations outside of those displayed here were identified by WGS.

CTΔ*incU* is susceptible to cell-autonomous immunity

The D-EC and D-LC *incU* mutants described in chapter 3 exhibited a clear susceptibility to IFNγ-stimulated cell-autonomous immunity in human cells. However, these strains share additional mutations outside of *incU* (Table 3.1), and it is possible that one or more of these mutations contributed to our observations. CTΔ*incU* is isogenic to wildtype *C. trachomatis* serovar D outside of its *incU* frameshift. We aimed to evaluate whether the CTΔ*incU* population within the D/6319 inoculum was sensitive to IFNγ-stimulated immunity, which would support our hypothesis that intact IncU mediates resistance to cell-autonomous immunity. As a first step, we infected human A549 cells with the D/6319 mixed population used in the Patton lab's original NHP study (Fig. 4.1A) and a 5 wpi sample from animal A11257 (Fig. 4.1B) to assess these populations' sensitivities to inclusion ubiquitination in IFNγ-treated cells. A proportion (14%) of inclusions inhabited by the inoculum population were coated with ubiquitin in IFNγ-stimulated cells, compared to only 3.3% of inclusions in cells infected with the endpoint sample (Fig. 4.3B). In agreement with our findings using D-EC and D-LC strains, the observed ubiquitination was IFNγ-dependent, as less than 1% of inoculum inclusions and 0% of 5wpi inclusions were targeted in unstimulated cells (Fig 4.3B).

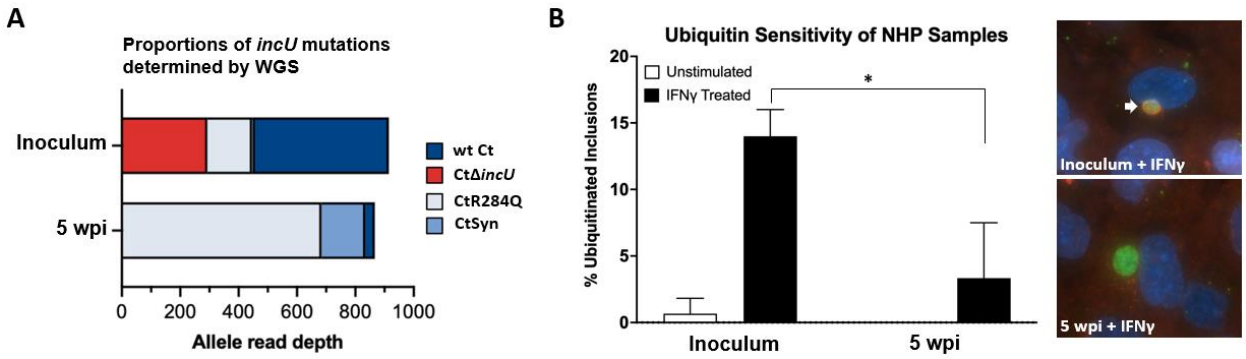

Figure 4.3 Evaluating the sensitivity of D/6319 inoculum and a 5 wpi endpoint sample to cell-autonomous immunity. (A) Raw Illumina reads containing either variant or wt *incU* allele sequences are plotted for the inoculum and 5 wpi NHP samples. (B) Whole populations of the D/6319 inoculum and a 5 wpi sample from one animal (A11257) were used to infect A549 human epithelial cells with or without IFNγ stimulation (given at 3hpi). Cells were fixed at 20 hpi and stained for ubiquitin (red), *C. trachomatis* MOMP (green), and DNA (DAPI, blue). Ubiquitinated inclusions were identified via IF microscopy (arrow in inoculum IF panel). Data represent the means and standard deviations of three technical replicates per condition. Data were analyzed for statistical significance by an unpaired two-tailed *t* test: *, P < .05.

We next isolated clonal populations of CtΔ*incU* and CtR284Q from the *C. trachomatis* D/6319 inoculum via limiting dilution. While the *incU* frameshift mutation was not detected in WGS of the 5 wpi sample, the R284Q allele was detected at the highest frequency at this timepoint, suggesting there was a selection for this mutation *in vivo* (Fig. 4.3A). A high proportion (70%) of CtΔ*incU* inclusions were ubiquitinated in IFNγ-primed A549 human epithelial cells compared to only 1.3% in unstimulated cells (Fig. 4.4). CtR284Q was slightly susceptible to inclusion ubiquitination, with 8% of its inclusions being targeted in IFNγ-stimulated cells compared to 0.67% in unstimulated cells (Fig. 4.4).

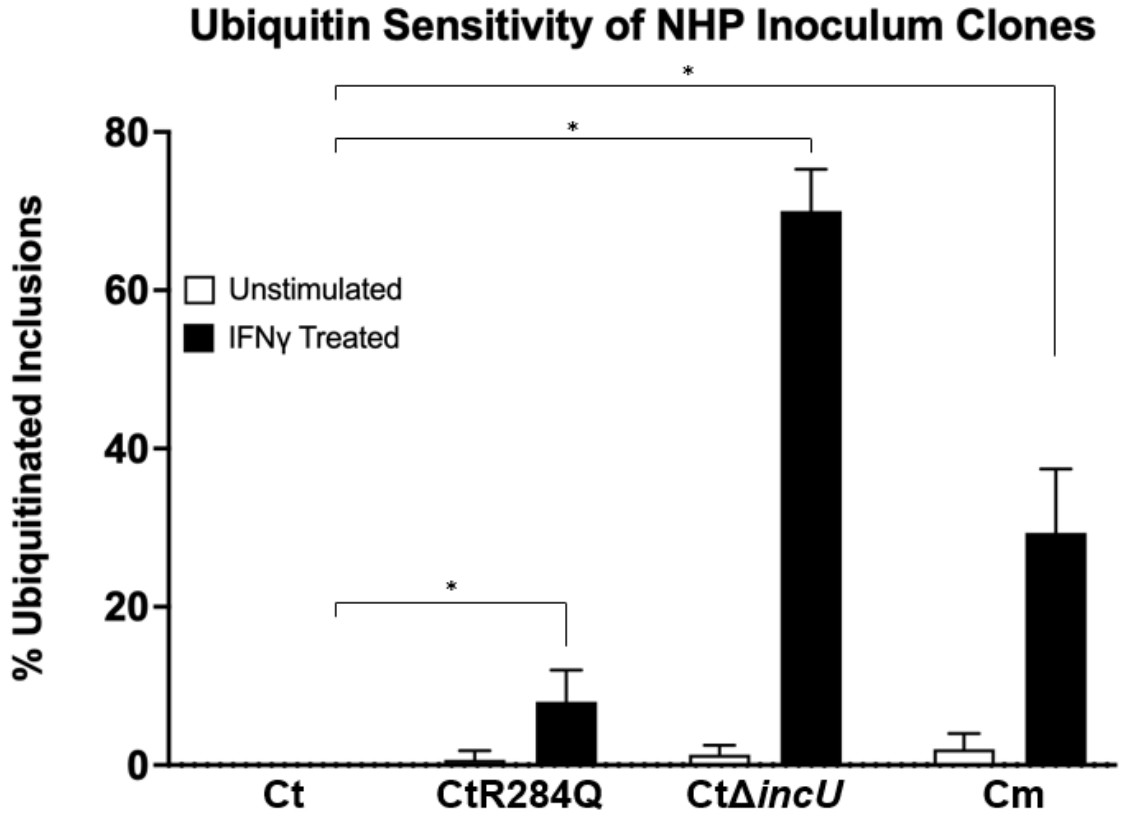

Figure 4.4 Analysis of inoculum clones' ubiquitin sensitivity. *C. trachomatis* serovar D (Ct), CtR284Q, Ct*Δincu*, and *C. muridarum* (Cm) were used to infect A549 human epithelial cells with or without IFNγ stimulation (100U/mL, given at 3hpi). Cells were fixed at 20hpi and stained for ubiquitin, *C. trachomatis* MOMP, and DNA. Ubiquitinated inclusions were identified via IF microscopy. Data represent the means and standard deviations of three technical replicates per condition. Data were analyzed for statistical significance using unpaired two-tailed *t* tests: **, P < .005.

The percentage of ubiquitin-positive CtR284Q inclusions was significantly higher than the completely ubiquitin-devoid wildtype *C. trachomatis* serovar D inclusions (8% vs. 0%, Fig. 4.4). However, compared to Ct*Δincu*, CtR284Q exhibited a relatively low rate of ubiquitination (8% vs. 70%, Fig. 4.4) which suggests why this population was better able to survive *in vivo*, but why it had such a high fitness advantage that it outcompeted wildtype organisms during NHP infection is unclear. It should be noted that nonsynonymous mutations have previously been observed through sequencing low-

passage clinical isolates from human patients[88]. The data described thus far show that Ct∆*incU* failed to grow *in vivo* in the NHP model, and this was associated with this mutant's susceptibility to cell-autonomous immunity. Our Ct∆*incU* strain does not have any mutations outside of its *incU* frameshift, giving us the opportunity to clearly link *in vitro* phenotypes to the *incU* mutation. This linkage was not possible with mutant strains D-EC and D-LC analyzed in chapter 3 (Table 3.1). Considering this, we sought to evaluate whether additional cell-autonomous immunity proteins colocalize with Ct∆*incU* inclusions in IFNγ-stimulated cells.

We analyzed whether two autophagy proteins known to be involved in cell-autonomous immunity, p62 and NDP52, associated with Ct∆*incU* inclusions in IFNγ-stimulated human cells. Previously, p62 was shown to redistribute to the cytosolic face of *C. muridarum* inclusion membranes in an IFNγ-dependent manner in human cells[62]. The specific role p62 plays in the greater cell-autonomous immune clearance of *Chlamydia* is not clear. However, infection of mouse cells with another vacuolar pathogen, *Toxoplasma gondii*, revealed that p62 promoted MHC-I antigen presentation in IFNγ-stimulated host cells leading to enhanced activation of CD8+ T-cells *in vivo*[65]. We found that 28.7% of *C. muridarum* and 60% of Ct∆*incU* inclusions were labeled by p62 in IFNγ-stimulated A549 cells (Fig. 4.5A, Fig. 4.6A). This recruitment was IFNγ-dependent, as recruitment rates dropped to 5.3% and 4.7% in unstimulated cells, respectively, and wt *C. trachomatis* serovar D inclusions were completely resistant to p62 recruitment regardless of IFNγ-stimulation (Fig. 4.5A, Fig 4.6A)

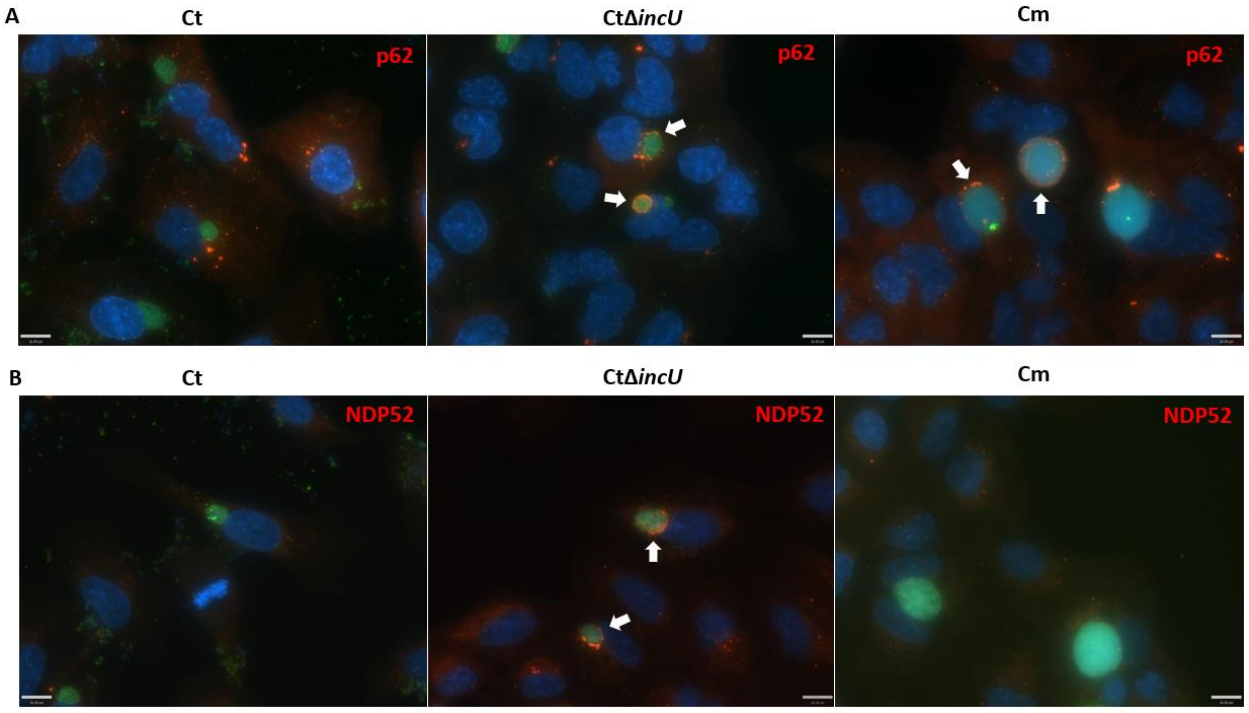

Figure 4.5 Autophagy-associated proteins traffic to CtΔIncU inclusions in IFNγ stimulated cells A549 human cells were infected with *C. trachomatis* (Ct), *C. muridarum*, or CtΔIncU and stimulated with IFNγ at 3 hpi. Cells were fixed at 20 hpi and stained for *C. trachomatis* MOMP (green), p62 (A, red), NDP52 (B, red), and DNA (DAPI, blue). The Cm strain used encodes GFP on a transposon inserted into an intergenic region of its genome. Inclusions with p62 (A) or NDP52 (B) deposited on their surface are marked with white arrows. Scale bar = 16 µm.

NDP52 does not have a defined role in cell-autonomous defense against *Chlamydia* spp., but its ubiquitin binding domain may function to deliver other effector proteins important for microbial killing, such as guanylate binding proteins (GBPs), to inclusions[62]. We observed 38% of CTΔ*incU* inclusions were bound by NDP52 in IFNγ-stimulated cells, compared to 1.3% in unstimulated cells (Fig.4.5B, Fig. 4.6B). Wildtype *C. trachomatis* inclusions were devoid of NDP52 in stimulated and unstimulated cells (Fig. 4.5B, Fig. 4.6B). Interestingly, only a small subset of *C. muridarum* inclusions had NDP52 on their surface in both conditions (2.7% and 2% in IFNγ-stimulated and unstimulated conditions, respectively), which does not agree with previously published data showing

they are susceptible to NDP52 recruitment following IFNγ-stimulation of human cells[86]. We are unsure of the reasons behind these differences, but it may be valuable to determine the recruitment kinetics of all known cell-autonomous immunity effectors, as the time at which infected cells are fixed and analyzed may represent timepoints where some factors have not yet been recruited to inclusions. This discrepancy makes interpretation of our NDP52 recruitment data difficult. However, the IncU-dependent resistance to p62 recruitment to *C. trachomatis* inclusions supports our hypothesis that this virulence factor functions to evade the broader cell-autonomous immune response in human cells.

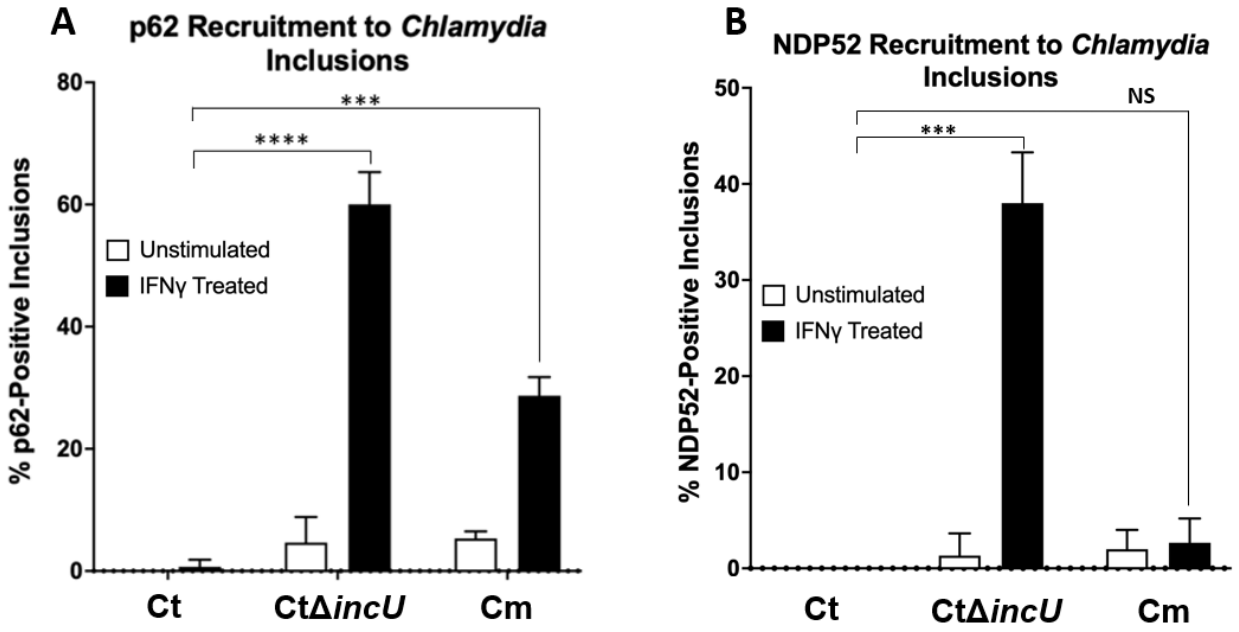

Figure 4.6 Quantification of p62 and NDP52 recruitment to inclusions. A549 epithelial cells were infected with *C. trachomatis* serovar D (Ct), Ct*ΔincU*, or *C. muridarum* (Cm) and were either untreated or stimulated with IFNγ at 3 hpi. Percentages of inclusions targeted by either protein were calculated by counting 50 inclusions for each replicate. Data represent the means and standard deviations of 3 technical replicates. Data were analyzed for statistical significance using unpaired two-tailed *t* tests: P < .005, ***, P < .001; NS = not significant

The isolation of CtΔ*incU* from a poorly infectious inoculum (D/6319, Fig. 4.1) and its characterized susceptibility to cell-autonomous immunity suggests that IncU may be an important virulence factor for infection of NHP. To support our hypothesis that the *in vivo* attenuation of *incU* mutants is a direct result of their susceptibility to cell-autonomous immunity, it was next important to determine whether nonhuman primate cells possess the capacity to target *Chlamydia* inclusions by a human-like cell-autonomous immune pathway, and whether the IncU-mechanism of resistance is functional in NHPs.

NHPs employ a human-like cell-autonomous immune response that is resisted by *C. trachomatis.*

The genes important for human cell-autonomous immunity are conserved in NHP, but functional evidence of this immune response in this model organism is lacking. We aimed to determine whether this pathway is conserved between humans and NHP, specifically in the context of host-mediated clearance of *C. trachomatis incU* mutant strains and the ability of wildtype *C. trachomatis* to subvert these pathways. Such conservation would support our hypothesis that the *in vivo* attenuation of CTΔ*incU* in NHP is due to its being unable to overcome IFNγ-stimulated cell-autonomous immunity.

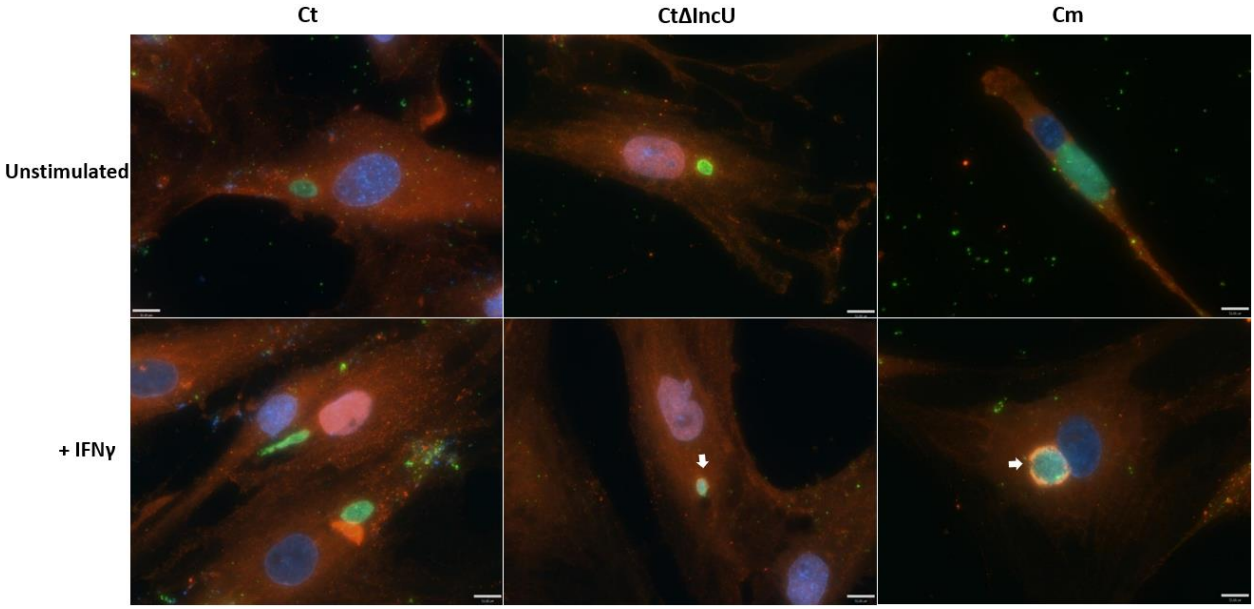

Figure 4.7 Immunofluorescence microscopy of IFNγ-treated NHP fibroblasts infected with *Chlamydia*. Primary NHP fibroblasts were infected with *C. trachomatis* (Ct), CtΔ*incU*, and *C. muridarum* (Cm) strains then fixed and permeabilized at 20 hpi. Cells were stained for ubiquitin (red), *C. trachomatis* MOMP (green), and DNA (DAPI, blue). The Cm strain used encodes GFP (green) on a transposon inserted into an intergenic region of its genome. Ubiquitinated inclusions are marked by white arrows. Scale bars = 16μm.

We isolated pigtailed macaque fibroblasts from a skin biopsy obtained from the Washington National Primate Research Center and evaluated whether they were capable of ubiquitinating *Chlamydia* inclusions following IFNγ stimulation. Immunofluorescence microscopy revealed specific targeting of ubiquitin to CtΔ*incU* and *C. muridarum* inclusions (Fig. 4.7). Wildtype *C. trachomatis* resisted inclusion ubiquitination in IFNγ-stimulated NHP fibroblasts: 6.7% of its inclusions were ubiquitinated compared to 26.7% of *C. muridarum* inclusions (Fig 4.8). Only 2% of *C. muridarum* inclusions were ubiquitinated in unstimulated fibroblasts whereas *C. trachomatis* inclusions were completely devoid of ubiquitin in unstimulated cells (Fig. 4.8). These NHP fibroblast data agree with findings in human cells (Fig. 3.2 A)[59]. 42.7% of CTΔ*incU* inclusions were

ubiquitinated in IFNγ-stimulated fibroblasts compared to 0.67% in unstimulated cells. The IFNγ-dependent manner of ubiquitin recruitment to CTΔ*incU* and *C. muridarum* inclusions (Fig. 4.8) supports the hypothesis that NHP cells carry out a cell-autonomous immune response that is functionally similar to the human pathway. This is the first direct evidence of IFNγ-stimulated NHP cell-autonomous immunity and directly links the *in vivo* growth defect of CTΔ*incU* mutants with a failure to evade this pathway.

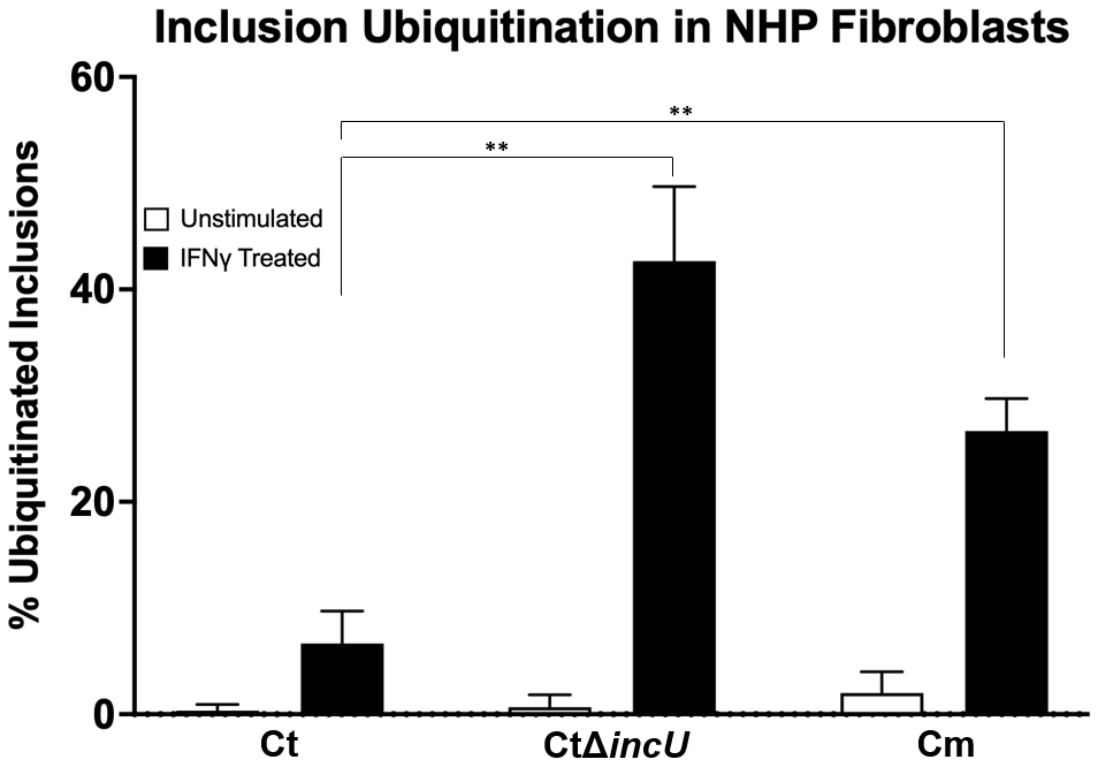

Figure 4.8 NHP fibroblasts employ an IFNγ-inducible cell-autonomous immune response that is sensitive to IncU-mediated resistance. Primary NHP fibroblasts were infected with *C. trachomatis* serovar D (Ct), *C. muridarum* (Cm), and CtΔ*incU* and supplemented with IFNγ (100U/mL) at 3 hpi or left unstimulated. Percentages of ubiquitin-positive inclusions represent the means and standard deviations of three technical replicates. Data were analyzed for statistical significance using unpaired two-tailed *t* tests: **, P < .005

Cis-complementation of CTΔ*incU* rescues ubiquitin resistance in IFNγ-stimulated cells

While our data thus far support the importance of IncU in mediating resistance to cell-autonomous immunity, we next sought to confirm this hypothesis by complementing the frameshift mutation within the CTΔ*incU* strain and testing whether this action rescued ubiquitin resistance in IFNγ-stimulated cells. To circumvent the difficulties associated with transforming *C. trachomatis*, we designed an approach to complement CTΔ*incU* in *cis* by leveraging the expertise of our group with homologous recombination. As discussed in chapter 2, we have generated a large library of tetracycline resistant (tet^R) *C. trachomatis* serovar L2 transposon mutants. One such mutant, CtL2Tn386-tet^R, encodes a transposon in the 5' region of *ctl0386* (*ct131* homologue). This transposon encodes a tetracycline resistance marker (tet^R). Given the proximity of this transposon to the *incU* homologue *ctl0390*, we reasoned that homologous recombination between CtL2Tn386 and CTΔ*incU* would yield recombinant strains carrying *ctl0390* in place of the latter's frameshifted *incU*. To facilitate isolation of recombined mutants via dual-antibiotic selection, we derived an oflaxacin-resistant (ofl^R) strain of CTΔ*incU* by culturing this strain in subinhibitory levels of ofloxacin—a previously published method to induce spontaneous mutations in *gyrA* of *C. trachomatis* which confer ofloxacin resistance[109,110]. We coinfected murine fibroblasts (McCoy cell line) with CTΔ*incU*-ofl^R (*C. trachomatis* serovar D background) and CtL2Tn386-tet^R (*C. trachomatis* serovar L2 background) to facilitate homologous recombination between these strains[82]. Dual tet^R/ofl^R recombinants were clonally isolated via limiting dilution, and serovar D strains were selected for downstream

analysis by immunofluorescence microscopy using a MOMP specific antibody with specificity for *C. trachomatis* serovar D.

Whole genome sequencing revealed one of our isolated recombinant strains, CtΔ*incU*::*incU*, had a recombined locus spanning *ct131* through *incU/ct135*. *incU* and the serovar L2 homologue *ctl0390* are highly conserved, however their 11 unique SNPs allow for their differentiation (Fig 4.9). We found that CtΔ*incU*::*incU* encoded a hybrid *incU*/*ctl0390* ORF (Fig. 4.9, graphical summary in Fig. 4.10). It carried unique serovar L2 SNPs at nt positions 33, 212, 343, 379, and 558 (Fig. 4.9, highlighted in yellow), and serovar D-specific SNPs at nt positions 657, 660, 705, 933, 1026, and 1055 (Fig 4.9, bases highlighted in green). Therefore, the 3' margin of recombination occurred between nt558 and nt657 (underlined sequence in Fig. 4.9), just downstream from the ΔA542-induced frameshift within the CtΔ*incU* parent strain. This deletion was absent in CtΔ*incU*::*incU*, which carries an intact, hybrid gene. In chapter 2, we showed that *ctl0390* confers *C. trachomatis* with the ability to resist human cell-autonomous immunity (Fig 2.2A), mirroring our conclusions on the function of *incU* in serovar D strains in chapter 3. Given the high genomic conservation between these two serovars, mosaic recombination of multiple loci is not uncommon. We did observe two additional recombination events within CtΔ*incU*::*incU*: the first between *ct119* and *ct122* and a second between *ct114* and *ct115*. These regions were recombined in one of our ubiquitin-susceptible chimeras discussed in chapter 1, RC7, but not in any of the other four susceptible chimeras, and they are unaltered in D-EC, D-LC, and CtΔ*incU* genomes so we do not believe they are involved in *C. trachomatis* resistance to cell-autonomous immunity.

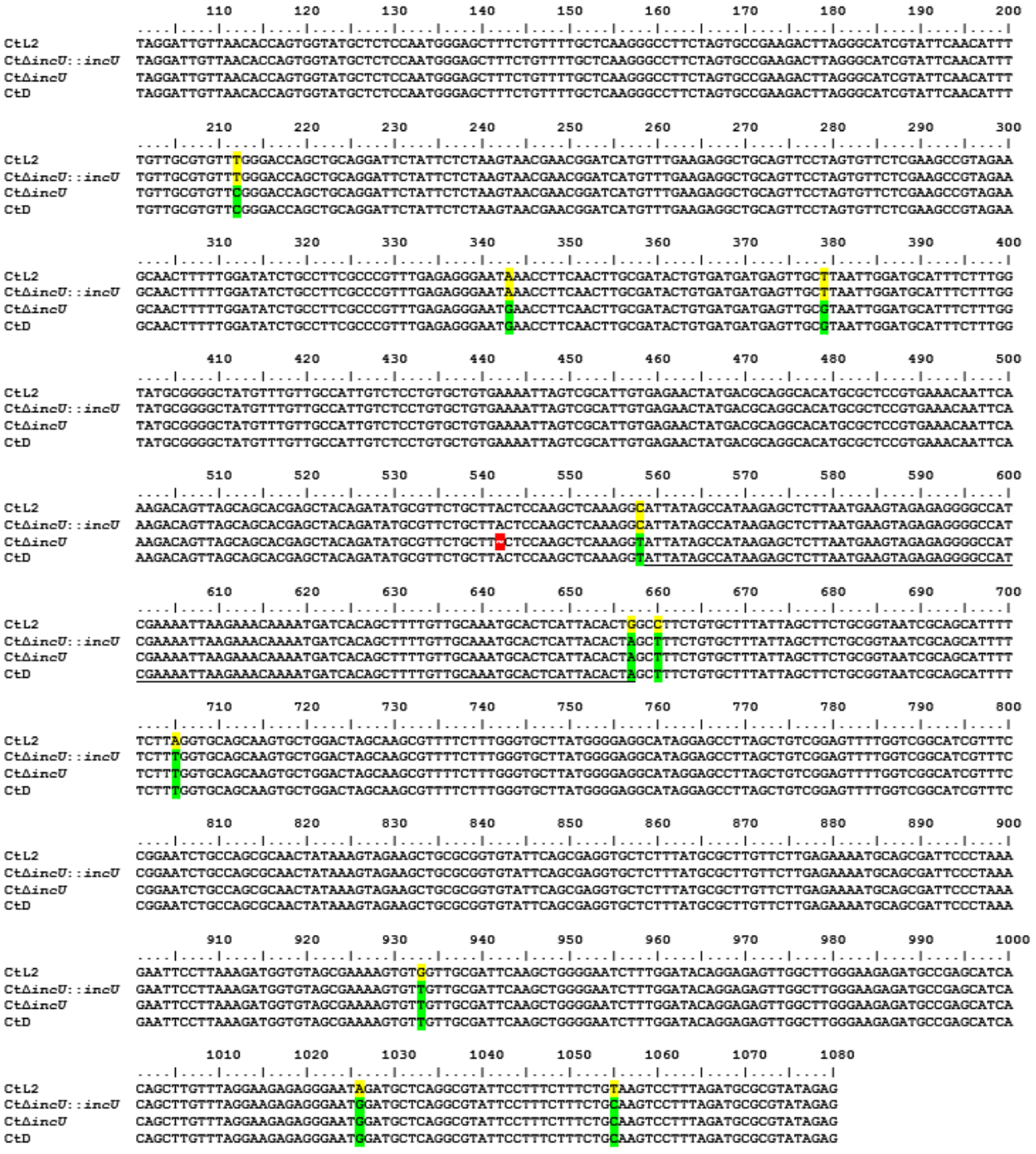

Figure 4.9 Analysis of CtΔ***incU*****::*incU* ORF.** *incU* ORFs of CtΔ*incU* and CtΔ*incU*::*incU* are aligned to *C. trachomatis* serovar L2 (CtL2) and serovar D (CtD) reference genes. Serovar L2 specific SNPs are highlighted in green, serovar D SNPs are highlighted in green. The ΔA542 frameshift mutation encoded by CtΔ*incU* is highlighted in red. The predicted 3' margin of the recombined locus within CtΔ*incU*::*incU* is underlined.

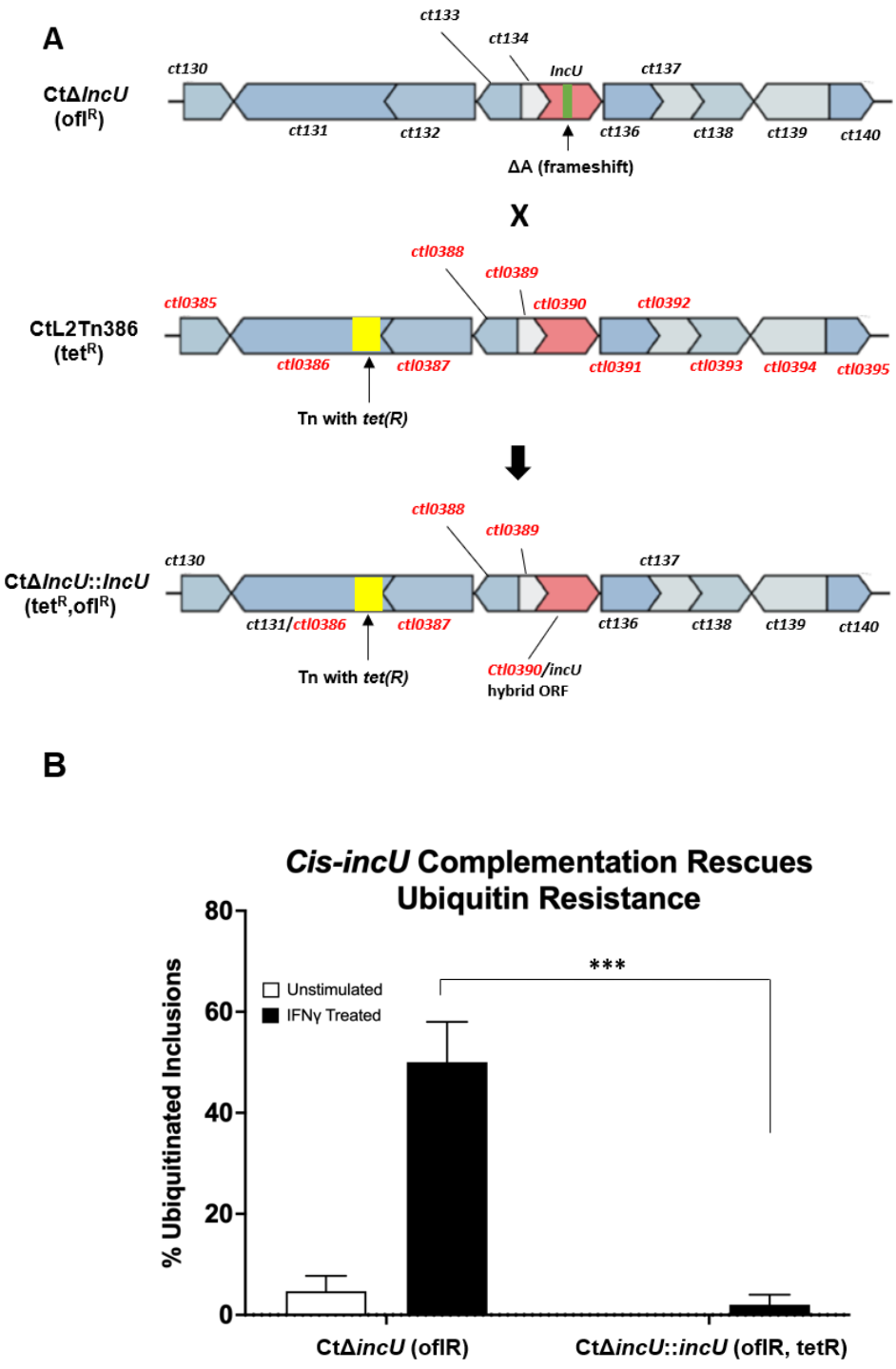

Figure 4.10 Complementation of *incU* restores ubiquitin resistance. (A) graphical summary of recombination strategy and WGS data of CTΔ*incU*::*incU*. (B) Human A549 cells were infected with CTΔ*incU* and CTΔ*incU*::*incU* and stimulated with IFNγ at 3hpi or left unstimulated. Percentages of ubiquitin-positive inclusions represent the means and standard deviations of three technical replicates. Data were analyzed for statistical significance by an unpaired two-tailed *t* test: ***, P < .001

We hypothesized that CtΔ*incU*::*incU* would resist inclusion ubiquitination in IFNγ-stimulated human cells. 50% of CtΔ*incU*-ofl^{R} inclusions were coated with ubiquitin in IFNγ-stimulated human cells in contrast to 4.7% in unstimulated cells (Fig. 4.10B). 2% of CtΔ*incU*::*incU* inclusions were ubiquitinated in stimulated cells vs. 0% in unstimulated cells(Fig. 4.10B). Therefore, restoring the open reading frame of CtΔ*incU* by *cis*-complementation rescues its ability to block inclusion ubiquitination in IFNγ-stimulated cells. Taken together with the findings presented in this dissertation, we conclude that IncU is a *C. trachomatis* virulence factor that confers resistance to cell-autonomous immunity in human and nonhuman primate host cells.

Conclusion

Protective immunity against *C. trachomatis* infection in humans is not completely understood. While IFNγ production is central to protective immunity in the murine model, there has been only a limited association to suggest a similar outcome in humans. Following antibiotic treatment of primary infection, women with peripheral blood *C. trachomatis*-specific Th1 type CD4+ T-cells that secrete IFNγ were shown to have lower rates of reinfection 3 months after treatment, compared to women lacking these specific T-cells (33% vs. 60%)[57]. However, the differences in reinfection rates between the two groups were not significantly different 6 months after their initial treatment[57]. In the mouse model, sterilizing immunity against *Chlamydia* infection has been linked to IFNγ-secretion by CD4+ T-cells and other immune cells[49,105]. CD4+ T-cell immunity appears to be relatively long-lived, as adoptive transfer of these cells from previously infected mice (4

months after primary infection) led to a reduction in bacterial burden among naïve mice infected with *C. trachomatis*[111]*.* The protection conferred by CD4+ T-cells in the mouse model has been proposed to be partially driven by IFNγ-stimulated IRG-mediated cell-autonomous immunity[49,62]. In addition to its well documented mechanism to overcome IFNγ-induced tryptophan starvation in human cells, the recent finding that *C. trachomatis* evades IFNγ-stimulated cell-autonomous immunity in its native human host complicates the picture, making a clear explanation of the role of IFNγ-secretion in immunity elusive[59].

In this chapter, we identified a population of *incU* frameshift mutants within the D/6319 inoculum causing attenuated infection in the NHP model. This mutant Ct∆*incU* population was susceptible to cell-autonomous immune recognition in both human epithelial cells and primary NHP fibroblasts, thus reducing the effective infectious dose inoculated. In a cloned frameshift mutant from this inoculum, we restored the *incU* ORF via homologous recombination with a *C. trachomatis* serovar L2 transposon mutant and showed that this complementation rescued resistance to inclusion ubiquitination in IFNγ-stimulated human cells. These data support our hypothesis that *incU* is a virulence factor that is required for *C. trachomatis* resistance to cell-autonomous immunity.

An important outcome of this work is the finding that NHP cells recognize intracellular *C. trachomatis* by a cell-autonomous immune response that is similar to that of humans; we hypothesize that this common pathway will extend to other intracellular pathogens. The pigtailed macaque used in our experiments is therefore a valuable model for studying the role of cell-autonomous immunity against *Chlamydia*. The murine cell-autonomous immune pathway is initiated by a specific and distinct family of IRGs that are not encoded in either the human or the pigtailed macaque genome. We hypothesize that

humans and NHP employ a shared, IRG-independent molecular mechanism to initiate this process following IFNγ-stimulation of *Chlamydia* infected cells[36]. If CtΔ*incU* was the driving force behind the partial attenuation observed in animals infected with our D/6319 inoculum, CtΔ*incU* could perhaps be investigated as a candidate live-attenuated vaccine in future studies.

Materials and Methods

Antibodies and reagents

Information for all primary antibodies: anti-Ubiquitin (Enzo Life Sciences, Farmingdale, NY; BML-PW8810-0500, 1:500), anti-MOMP (Virostat, Westbrook, ME; 1621, 1:1000), p62 (Abcam, Cambridge, United Kingdom; ab109012, 1:500), and NDP52 (Abcam; TA501971, 1:500). Secondary antibodies were all obtained from Thermo Fisher Scientific (Rockford, IL) and diluted 1:400 for immunofluorescence staining: Donkey anti-Goat Alexa Fluor 488 (A11055), Donkey anti-Rabbit Alexa Fluor 594 (A21207), and Rabbit anti-Mouse Alexa Fluor 594 (A11062). 4',6-diamidino-2-phenylindole (DAPI, Fisher Scientific, 1:2000) was used to visualize host nuclei and *Chlamydia* DNA.

Human cell culture and bacterial strains

A549 (obtained from Dr. Michael Gale) and McCoy (obtained from Dr. Walt Stamm) cell lines were cultured at 37°C, 5% CO_2 in Dulbecco's modified Eagle medium (DMEM) supplemented with 1x GlutaMax (Gibco) and 10% fetal bovine serum (FBS,

HyClone). Fully supplemented medium is referred to as DMEM-complete (DMEMc). *Chlamydia trachomatis* serovars and strains used in this chapter include *Chlamydia trachomatis* D/UW-3/CX, a *C. trachomatis* serovar L2 transposon mutant (CtL2Tn386) and a *Chlamydia muridarum* strain which encodes green fluorescent protein (GFP) on a transposon inserted in an intergenic region. *incU* mutants CtΔ*incU* and CtR284Q were isolated from the D/6319 inoculum by two-fold limiting dilution. *Chlamydia* strains were propagated by infecting McCoy cells for 48-72 hours. Infected cells were scraped into growth medium and centrifuged at 3500 x *g* for 5 minutes. Pellets were resuspended in a 10% phosphate buffered saline solution and lysed by bead bashing. An equivalent volume of 2x sucrose phosphate buffer was added to lysates (final concentration: 0.2M sucrose, 8mM sodium phosphate pH 7.1). Host cell debris was cleared by centrifugation at 250 x *g* for 5 minutes and supernatants containing *Chlamydia* elementary bodies (EBs) were aliquoted and stored at -80°C. A549 and McCoy cells were inoculated with *Chlamydia* EBs diluted in DMEMc in tissue culture plates or chamber slides, which were centrifuged at 700 x *g* for 30 minutes and grown at 37°C, 5% CO_2 for the duration of given experiments.

Isolation of primary macaque fibroblasts

A skin biopsy from a 5-year-old female pig-tailed macaque was acquired from the Washington National Primate Research Center's Tissue Distribution Program. The skin was immediately submerged in 30mL of DMEM supplemented with GlutaMax and 20% FBS (DMEMp) and transported on ice for processing. The skin was dissected into ~2mm^3 sections, and 2-3 pieces were added to each well of 6-well plates that had been coated with a 1% gelatin solution for 30 minutes at room temperature. The sections were partially

submerged in 800uL of DMEMp supplemented with 1x PenStrep (Thermo Fisher Scientific) and incubated at 37°C, 5% CO_2 for one week to allow attachment of skin and outgrowth of fibroblasts. After one week, the volume of DMEMp + 1x PenStrep was increased to 2mL/well. Once confluent, cells were trypsinized and each 6-well plate was split into two 75cm^2 tissue culture flasks. These cells were washed thoroughly with PBS and passaged into a 75cm^2 flask and grown in DMEMc (without PenStrep).One additional passage was performed in the absence of PenStrep, and once cells were ~70-80% confluent, flasks were washed with PBS, trypsinized, and cells were either passaged into 75cm^2 flasks or used to seed 8-well chamber slides for ubiquitination assays as described above. Infection with *Chlamydia* strains was performed as described above for human cells.

Macaca nemestrina **infection**

In a previous experiment performed by Dr. Dorothy Patton's group, six pig-tailed macaques were infected with a single *C. trachomatis* serovar D inoculum (D/6319). Animals were inoculated with 1mL (10^5 inclusion forming units (IFU)) of *C. trachomatis* using a 1cc tuberculin syringe inserted into the vaginal fornix. Animals were monitored weekly for active chlamydia infection by culture and nucleic acid amplification tests (NAATs). Animals were considered actively infected if they were culture and/or NAAT positive in weekly tests. At the end of the study, infected animals were treated with a curative dose of azithromycin (14mg/kg/day for 5 days) regardless of positivity by culture or NAAT and returned to the colony.

Analysis of ubiquitin, p62, and NDP52 recruitment to inclusions

Chambered coverglass slides (8-well Nunc Lab-Tek II; Thermo Fisher Scientific, Rockford, IL) were seeded with A549 cells or primary NHP fibroblasts and cultured at 37°C, 5% CO_2. Cells were infected with *Chlamydia* strains such that three technical replicates are represented in final data. Wells were left either untreated or stimulated with 100U/mL human interferon gamma (IFNγ, R&D Systems, Minneapolis, MN; 285-IF-100) at 3 hours post infection (hpi). Infected cells were fixed at 20 hpi with 3.7% paraformaldehyde for 20 minutes, washed 3 times with phosphate buffered saline (PBS), and permeabilized with 0.5% Triton X-100 for 15 minutes. Wells were washed once more and blocked with 3% bovine serum albumin (BSA) in PBS for one hour. Primary antibodies were diluted (dilution factors listed under 'Antibodies and Reagents') in 1% BSA-PBS and incubated at room temperature for 1 hour, after which we performed 3 5-minute washes before adding secondary antibodies. Secondary antibodies and DAPI were diluted (dilution factors listed under 'Antibodies and Reagents') in 1% BSA-PBS and incubated for 45 minutes at room temperature in the dark. We performed 3 5-minute washes with PBS and slides were imaged in PBS and stored at 4°C. A Nikon Ti-E inverted microscope was used to image stained chamber slides. A Hamamatsu camera controller C10600 was used to capture images that were visualized using the software Volocity (PerkinElmer, Waltham, MA). For inclusion-recruitment assays, 50 inclusions were counted in each well, and each inclusion was positive for ubiquitin or p62 recruitment if there was a complete ring clearly visible around the inclusion. Inclusions were called positive for NDP52 if there were complete or partial rings around around them, which is consistent with published findings[59]. The data in our recruitment assay represent the

number of ubiquitin, p62, or NDP52-positive inclusions divided by 50 (the total number of inclusions counted in each well). Data are representative of 3 technical replicates. Immunofluorescence images in figures are representative of the annotated strains/conditions. The microscopist was not blinded to conditions.

Derivation of ofl^R CtΔ*incU*

To derive an oflaxacin-resistant (ofl^R) strain of our CtΔ*incU* mutant, we inoculated McCoy cells with CtΔ*incU* (serovar D background) EBs in 75cm^2 flasks and initiated infection by centrifuging the flasks at 1,200 x *g* for 1 h at 37°C. Infected cells were fed with subinhibitory levels of ofloxacin equivalent to half of its MIC (0.25 ug/mL) and incubated at 37°C and 5% CO_2 for 48 hours. Cells were lysed by freeze-thawing at -80°C and 37°C, then aspirated and centrifuged at 200 x *g* to remove host cell debris. Isolated EBs within the supernatants were used to infect new McCoy cells in shell vials. Serial two-fold dilutions of ofloxacin diluted in minimal essential medium supplemented with 10% fetal bovine serum and cycloheximide (1ug/mL) (MEM-10) were added to infected cells. When resistant inclusions were observed by immunofluorescence microscopy using an anti-LPS antibody, CtΔ*incU*-ofl^R was clonally isolated by limiting dilution.

Recombination-mediated rescue of the CtΔ*incU incU* open reading frame.

Recombination experiments were performed as previously described[82]. Briefly, shell vials (12mm^2) were seeded with 4.0 x 10^5 McCoy cells. These monolayers were coinfected with CtΔ*incU*-ofl^R and a previously generated tetracycline-resistant (tet^R) transposon mutant in a *C. trachomatis* serovar L2 serovar (CtL2Tn). CtL2Tn encodes a tet^R transposon in *ctl0386* (homolog of serovar D *ct131*). Monolayers of McCoy cells were infected with approximate multiplicity of infection of 2.0 of each CtΔ*incU* and CtL2Tn.

Cultures were incubated for 48 hours at 37°C and 5% CO_2 in the absence of antibiotics, then they were harvested by the freeze-thaw method described above. Recombinant strains were isolated by inoculating 50uL of lysates from shell vials into McCoy monolayers in new shell vials and were incubated at 37°C and 5% CO_2 in MEM-10 supplemented with 2ug/mL ofloxacin and 0.5ug/mL tetracycline—representing 4x and 2x respectively the MIC of parental strains. Cultures were grown for 48 hours and surviving bacteria were detected by immunofluorescence. Infected cells were lysed by the freeze-thaw method and blindly passaged until inclusions were observed by immunofluorescence microscopy. Recovered dual-resistant strains were cloned by limiting two-fold dilution and recombinants with a predominantly Ct*Δincu* genome were determined by serological typing of MOMP by immunofluorescence microscopy. A total of ten tet^R/ofl^R recombinants were isolated, and we screened for *incU* rescue by Sanger sequencing followed by a phenotype screen performing our ubiquitination assay detailed above.

Whole genome sequencing.

Chlamydia EBs were centrifuged at 16,000 x *g* for 10 minutes and supernatants were discarded. EB pellets were resuspended in water and treated with RQ1 DNase (Promega) at 37°C for 30 minutes. Reactions were terminated by adding RQ1 stop solution and incubating at 65°C for 10 minutes. EBs were supplemented with 5mM dithiothreitol and incubated at 56°C for 1 hour, and genomic DNA (gDNA) was extracted using a DNeasy blood and tissue kit (Qiagen). gDNA was prepared for sequencing with a Nextera XT DNA library preparation kit (Illumina), and whole genome sequencing was performed on an Illumina HiSeq 3000 at the Oregon State University Center for Genome

Research and Biocomputing Core. Raw sequence reads were trimmed using Trimmomatic[92] and processed sequences were mapped to *C. trachomatis* serovar D (NC_000117) and serovar L2 (CP042653) genomes using Bowtie2[93] and Trinity[94] programs. Final assemblies were analyzed with the sequence analysis software Geneious. Given the high genomic similarities between L2 and serovar D, recombination ends were approximated by determining the presence of differentiating SNPs of sequenced strains.

Chapter 5. Development of a system for proteomic identification of host proteins that directly interact with *Chlamydia* inclusions

Introduction

Human cell-autonomous immunity is poorly understood compared to the murine pathway. The core factors which initiate recognition of intracellular pathogen-containing vacuoles, including chlamydial inclusions, are largely unknown, as is the complete suite of human proteins that are recruited to these sites to mediate pathogen clearance. The *C. trachomatis incU*-mutants characterized in this dissertation offer a unique opportunity to answer some of these questions through differential analysis of host factors recruited to the cytosolic faces of mutant versus wildtype inclusion membranes in IFNγ-stimulated cells.

Proteomic characterization of discrete microenvironments within a cell has been accomplished through a variety of methods, ranging from mechanical isolation of these sites or through biochemically labelling them for downstream isolation. Recently in the *Chlamydia* field, a unique methodology of proximity labeling inclusions was developed by genetically engineering *C. trachomatis* to express a recombinant inclusion membrane protein fused to an ascorbate peroxidase (APEX), to enable *in situ* biotinylation of neighboring proteins to the inclusion membrane protein in living cells, within a biologically-relevant 20 nm radius[112]. These fusion proteins biotinylate host proteins that are in close proximity to inclusions, and mass spectrometry of streptavidin bead-purified proteins was used to reveal the identity of host factors recruited to inclusions. Our lab applied this

method to discover the essentiality of endoplasmic reticulum exit sites in supporting *C. trachomatis* growth[112]. One major caveat of this approach is the need for a genetically tractable strain of *C. trachomatis,* for example the lab-adapted L2 strain which has been used in all APEX studies to-date. Our *incU* mutants are in a serovar D background, and these strains are more fastidious than the L2 strain and, in our experience, present a greater challenge when it comes to genetic manipulation. To leverage our unique *C. trachomatis* serovar D mutants to annotate host proteins recruited to inclusions in IFNγ -stimulated cells, we explored the utility of a novel proximity labeling protocol which does not require genetic manipulation of *Chlamydia.*

Biotinylation by antibody recognition (BAR) is a technology platform that is functionally similar to the APEX-mediated approach, with the difference of a horseradish-peroxidase (HRP)-conjugated antibody that is used to facilitate biotinylation of proximal proteins in fixed cells[113]. Therefore, the only requirement to label a given intracellular niche is an antibody to a target specific to that microenvironment. We propose using BAR to generate proteomic datasets of proteins involved in the human cell-autonomous immune response against *Chlamydia*. Specifically, we hope to label inclusion membrane proteins with BAR using an antibody against a highly abundant inclusion membrane protein, IncA, to label IFNγ-stimulated human cells infected with our *C. trachomatis incU* mutants and an isogenic wildtype serovar D control. Differential analysis of these datasets will provide an unbiased means to identify the complete suite of human cell-autonomous immunity factors which traffic to susceptible *Chlamydia* inclusions to mediate their clearance.

We first wanted to test this new approach in a way that could be benchmarked against previously generated datasets using alternative proximity labeling methods. Our group previously generated a *C. trachomatis* serovar L2 strain which expressed IncA fused to an APEX molecule (IncA-APEX)[112]. This strain allowed us to induce biotinylation of proteins within or near the inclusion membrane at various infection timepoints in live cells. Pulldown and LC-MS/MS of biotinylated proteins provided rich datasets annotating temporal host-pathogen interactions at the interface of the *Chlamydia* inclusion and host cytosol[112]. We aimed to test BAR-mediated proximity labeling using the same *C. trachomatis* L2 strain and HeLa host cell line. Additionally, protein purification and mass spectrometry in our previous study was performed by the Pacific Northwest National Laboratory, and we aimed to perform BAR-MS with their LC-MS/MS pipeline[112]. In this pilot study, we decided to evaluate a BAR approach using an antibody against the major outer membrane protein (MOMP) of *C. trachomatis*. MOMP is highly expressed on the outer membrane of resident EBs and RBs and thus fairly ubiquitous within the inclusion lumen[114]. Because BAR requires fixation and permeabilization of infected cells prior to labeling, we reasoned that MOMP-mediated BAR would provide an opportunity to simultaneously label proteins within the inclusion lumen and those associated with the inclusion membrane during infection to elucidate the global host proteins which interact with inclusions during *Chlamydia* infection.

Results

BAR results in robust and specific labeling of the inclusion microenvironment.

Our BAR approach requires fixation and permeabilization of infected host cells prior to labeling and downstream purification of biotinylated proteins. These conditions have been shown to cause inclusions to 'leak'—contents inside may escape the inclusion and host factors outside may aberrantly enter, leading to potential off-target labeling of the host cytosol or artifactual labeling of translocated proteins[115].

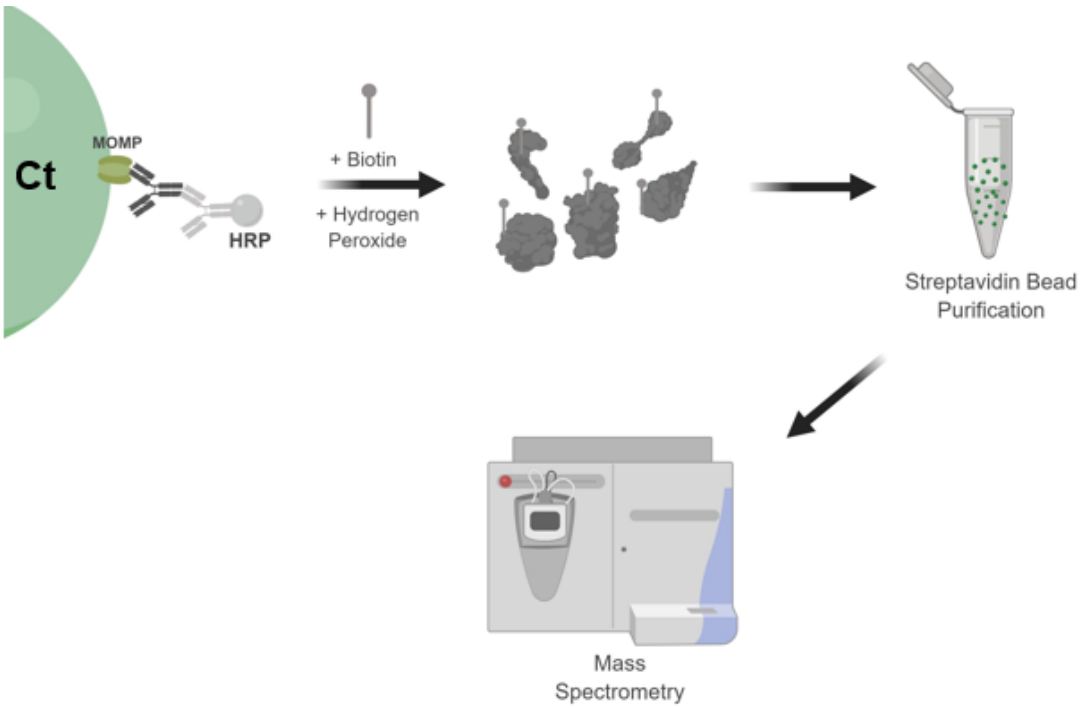

Figure 5.1 Overview of biotinylation by antibody recognition (BAR). After infected cells are fixed and permeabilized, they are incubated with a primary antibody against a specific target (anti-MOMP, dark grey antibody binding Ct MOMP). A secondary horseradish peroxidase-conjugated antibody specific to the primary antibody's host species. Biotin tyramide and hydrogen peroxide are added to the cells, allowing HRP to generate free radicals on biotin tyramide and proteins in close proximity. Biotinylated proteins are pulled down with streptavidin coated beads and are identified by mass spectrometry. Ct = *C. trachomatis* bacterium, MOMP = major outer membrane protein.

We first sought to determine the specificity of labeling by immunofluorescence microscopy. HeLa cells were infected with *C. trachomatis* serovar L2 and fixed at either 16 or 24 hours postinfection (hpi). BAR using a primary anti-MOMP antibody revealed robust and specific labeling of the inclusion lumen (Fig 5.2A). Infected cells fixed at 16 hpi show diffuse labeling throughout the inclusion lumen, whereas those fixed at 24 hpi elicited fainter labeling in the center of inclusions (Fig 5.2A). The latter observation may be due to steric hindrance by the increased population of *Chlamydia* preventing efficient antibody penetration into this region. A small number of biotin positive puncta were observed outside of inclusions, and they were in close proximity to DAPI-labeled nucleic acids far away from host cell nuclei. We believe that a subset of these represents BAR-labeling by chlamydial EB debris in the imaged wells.

Our ultimate goal with BAR will be to label host proteins on the cytosolic face of the inclusion membrane, therefore we assessed whether using an anti-incA primary antibody would yield specific labeling the inclusion membrane. IncA-mediated BAR resulted in high fidelity labeling of inclusions (Fig 5.2B) like what we observed in our MOMP trial. Unexpectedly, some biotin-positive puncta appeared to be in the lumen of inclusions (Fig 5.2B), which could have been due to several reasons. Primary antibodies may have bound to newly synthesized IncA molecules which were not fully secreted outside of the *C. trachomatis* RBs, allowing them to facilitate BAR within the inclusion lumen. Alternatively, permeabilization of cells prior to BAR may have exposed contents within the inclusion lumen to HRP-conjugated antibodies on the inclusion membrane—this could explain why we did not see a similar outcome using IncA-APEX-mediated biotinylation using live, unpermeabilized cells. Finally, fixation can cause leakage of

cytosolic proteins into inclusions, and it is possible that the biotinylation within the lumen is caused by IncA which entered this compartment following fixation[115]. Importantly, we did not observe off-target labeling of the host cytosol, suggesting that BAR using antibodies specific to *Chlamydia* proteins is a viable strategy to label the inclusion microenvironment, although specific labeling of the lumen versus the inclusion membrane may be challenging.

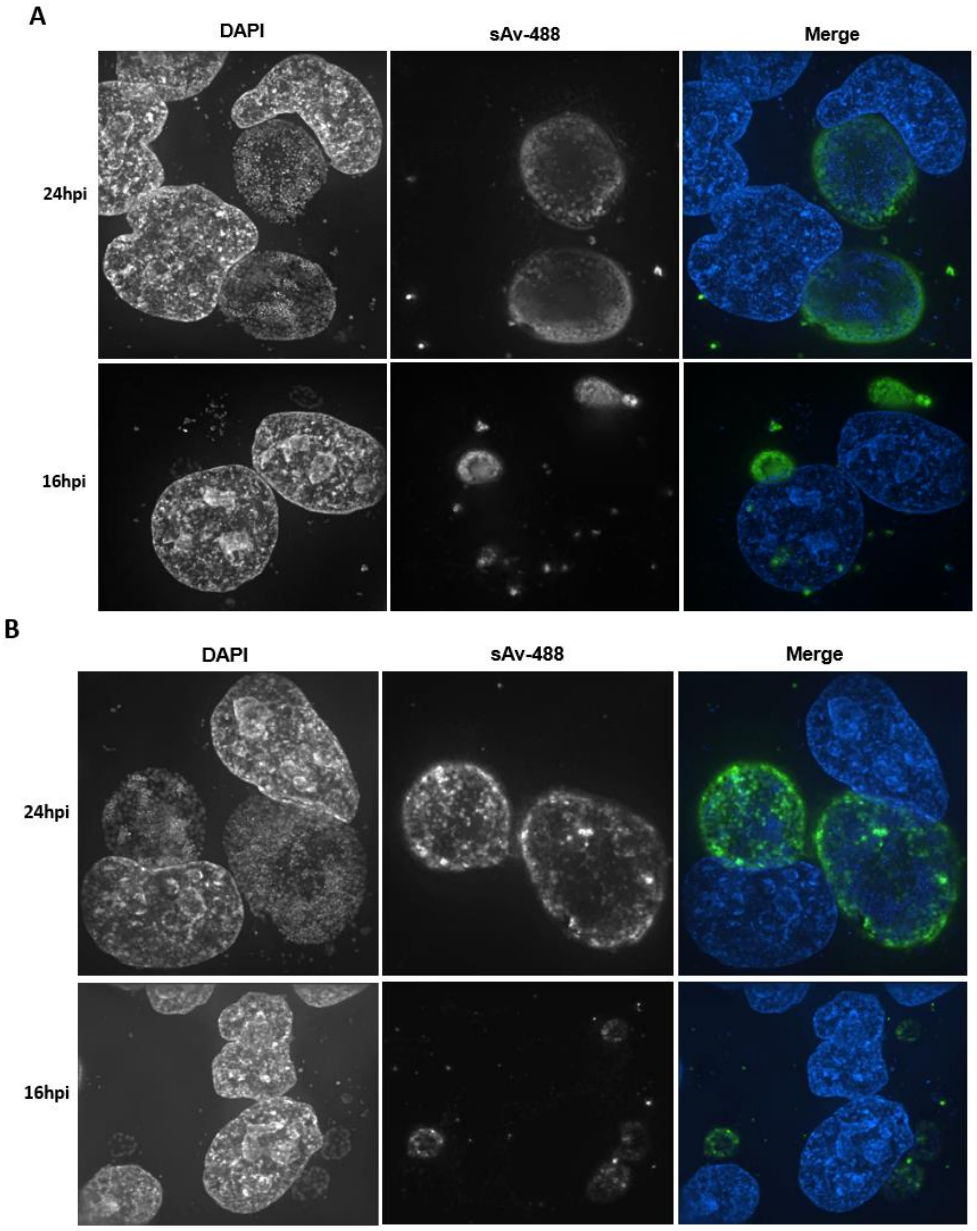

Figure 5.2 (A) MOMP and (B) IncA mediated BAR labeling of inclusions. HeLa cells infected with *C. trachomatis* were fixed and permeabilized at either 16 or 24hpi. Cells were stained with an anti-MOMP (A) or anti-IncA (B) antibody which were subsequently detected with a secondary HRP-conjugated antibody. Cells were incubated with biotin tyramide and hydrogen peroxide for 10 minutes then reactions were stopped by adding sodium ascorbate (500mM). Localization of biotinylated proteins was determined by incubating stained cells with Alexa 488-conjugated streptavidin (green) and human/*C. trachomatis* DNA was stained with DAPI (blue). Images were captured under 60x magnification under oil immersion.

Mass spectrometry of biotinylated proteins labeled by BAR and overrepresented KEGG ontologies within identified host proteins.

Protein extracts from MOMP-BAR labeled cells (2 replicates per condition) were processed at the Pacific Northwest National Laboratory to determine the identity of biotinylated proteins via liquid chromatography with tandem mass spectrometry (LC-MS-MS). Control samples were prepared for each timepoint and consisted of identical labeling steps except that they were not incubated with an anti-MOMP antibody. These controls allowed us to assess the level of nonspecific background due to endogenous peroxidases, non-specific labeling with our HRP-conjugated antibody, or other factors leading to noise in our datasets. For this pilot study, we averaged data from two replicates per timepoint to obtain a mean spectral count for each identified host protein and subtracted spectral counts from corresponding negative controls to minimize errant detection of background labeling. A total of 1204 human proteins were identified above background in the 16 hpi samples and 1182 proteins were identified in the 24 hpi samples. Many of these are low confidence hits, as only 139 (16 hpi) and 153 (24 hpi) of identified proteins have normalized spectral counts of 10 or greater. We selected 100 human proteins from each dataset that represented the highest spectral counts identified for further analysis (16 hpi spectral counts: range = 12-87, median = 19; 20 hpi spectral counts: range = 13-161, median = 20).

We are hesitant to make any over-reaching conclusions based upon the presence of specific proteins in this preliminary dataset, as the data need to be strengthened with additional controls and a higher number of replicates. The primary purpose of this pilot effort was to evaluate the feasibility of the BAR approach for proteomic discovery of

chlamydial and host proteins recruited to specific spatial regions of the *Chlamydia* inclusions, through analyzing overrepresented KEGG pathways in these datasets with InnateDB[116] and broadly defining the host pathways recruited to inclusions during infection. We chose this approach because it is bioinformatically analogous to a previous analysis the laboratory performed to evaluate KEGG pathways enriched on inclusions using an APEX-labeling approach[112]. Those published data were more stringently controlled than our current BAR dataset, and we reasoned that if we observed significant overlap between KEGG pathways identified it would provide confidence to optimize and pursue BAR further.

Table 5.1 KEGG pathways representing human proteins recruited to *C. trachomatis* inclusions at 16hpi

KEGG Pathway	BAR-MS identified proteins	Genes in pathway	p-value (corrected)
Pathogenic Escherichia coli infection	10	56	6.84E-09
Protein processing in endoplasmic reticulum	11	171	1.79E-05
Antigen processing and presentation	7	71	7.19E-05
Phagosome	9	152	1.90E-04
Regulation of actin cytoskeleton	10	217	4.63E-04
Adherens junction	6	73	5.96E-04
Leukocyte transendothelial migration	7	120	1.01E-03
Tight junction	7	135	1.70E-03
Glycolysis / Gluconeogenesis	5	67	2.22E-03
Arrhythmogenic right ventricular cardiomyopathy (ARVC)	5	74	3.42E-03
Bacterial invasion of epithelial cells	5	77	3.98E-03
Focal adhesion	8	210	4.32E-03
Shigellosis	4	62	9.58E-03
Pyruvate metabolism	3	39	1.69E-02
Gastric acid secretion	4	76	1.69E-02
Hypertrophic cardiomyopathy (HCM)	4	83	2.17E-02
Aminoacyl-tRNA biosynthesis	3	45	2.27E-02
Dilated cardiomyopathy	4	90	2.61E-02
Gap junction	4	90	2.61E-02
Viral myocarditis	3	56	3.64E-02
NOD-like receptor signaling pathway	3	57	3.77E-02
RNA transport	5	170	4.74E-02

Table 5.2 KEGG pathways representing human proteins recruited to *C. trachomatis* inclusions at 24hpi

KEGG Pathway	BAR-MS identified proteins	Genes in pathway	p-value (corrected)
Pathogenic Escherichia coli infection	7	56	1.63E-05
Glycolysis / Gluconeogenesis	7	67	5.25E-05
Protein processing in endoplasmic reticulum	10	171	7.30E-05
Antigen processing and presentation	6	71	5.32E-04
Regulation of actin cytoskeleton	9	217	1.41E-03
Pyruvate metabolism	4	39	2.65E-03
Adherens junction	5	73	3.18E-03
Leukocyte transendothelial migration	6	120	4.38E-03
Propanoate metabolism	3	27	6.06E-03
Phagosome	6	152	8.59E-03
Arrhythmogenic right ventricular cardiomyopathy (ARVC)	4	74	1.30E-02
RNA degradation	4	74	1.30E-02
Valine, leucine and isoleucine degradation	3	44	1.88E-02
Aminoacyl-tRNA biosynthesis	3	45	1.94E-02
Focal adhesion	6	210	2.87E-02
NOD-like receptor signaling pathway	3	57	3.26E-02
Pentose phosphate pathway	2	28	4.90E-02

We identified 22 and 17 KEGG pathways that were enriched in our 16 hpi and 24 hpi BAR-MS samples, respectively ($P < .05$). There was significant overlap between the two groups, as they shared enrichment of host proteins involved in 12 different KEGG pathways (Tables 5.1 and 5.2). Given that the focus of our greater research interests involves mechanisms of *C. trachomatis* resistance to host immunity, we were intrigued to find an enrichment of host proteins involved in antigen processing and presentation in both of our datasets (Table 5.1 and Table 5.2). The identified proteins representing this pathway were calreticulin (CALR), protein disulfide isomerase family A member 3 (PDIA3), heat shock protein 90 alpha family class A member 1 (HSP90AA1), heat shock protein 90 alpha family class B member 1 (HSP90AB1), heat shock protein family A member 5 (HSPA5), and heat shock protein family A member 8 (HSPA8). Calnexin (CANX) was uniquely identified in our 16 hpi dataset. CALR, PDIA3, and CALX were

identified in our group's previously generated IncA-APEX[112] MS dataset and also in a third MS dataset that was generated by evaluating protein contents of mechanically isolated inclusions[117]. HSP90AA1, HSP90AB1, and HSPA8 were also identified in the latter study[117]. Calreticulin was identified in all three datasets, and plays an important role in antigen presentation by MHC-I molecules[118]. *C. trachomatis* is known to downregulate MHC-I presentation by infected cells[51], and the observation that calreticulin is associated with inclusions by three independently generated MS datasets encourages future experiments to determine whether sequestration of calreticulin into or onto *C. trachomatis* inclusions contributes to chlamydial subversion of MHC-I presentation[51,119]. It is promising that, with the exception of HSPA5, all BAR-identified proteins representing this KEGG pathway were also identified in previous publications that used alternative methods to annotate the inclusion proteome[112,117]. The data presented here are preliminary and must be strengthened by additional replicates and controls prior to making any conclusions regarding inclusion-associated proteins identified by BAR. However, we believe that this method has the potential to be an important tool with which to study the *C. trachomatis* inclusion microenvironment and inform host-pathogen interactions that occur during the *Chlamydia* developmental cycle.

Conclusion

Biotinylation by antibody recognition (BAR) was originally developed as a method to annotate protein contents of specific microenvironments within eukaryotic cells[113]. Its utility in microbiology and infectious disease research has yet to be evaluated. In our

study, we were able to label *C. trachomatis* inclusions by this method using either anti-MOMP or anti-IncA antibodies (Fig 5.2). LC-MS/MS analysis of biotinylated proteins labeled by MOMP-BAR yielded many host proteins that were recruited into or onto inclusions 16 and 24 hpi, which represent specific families of proteins identified by KEGG ontology analysis (Table 5.1 and Table 5.2). In our preliminary analysis of one identified KEGG pathway, “antigen processing and presentation”, we were encouraged to find overlap with the proteins we identified and two previously published proteomic studies[112,117]. There are, however, several limitations to the data presented in this chapter and to this approach in general. BAR-MS-identified KEGG pathways (Table 5.1 and Table 5.2) did not completely overlap with our previous APEX study, especially comparing KEGG ontology analysis of our 24hpi samples[112]. While we anticipate identifying more proteins and KEGG pathways with MOMP-BAR because proteins within and on the surface of inclusions are labeled, the fact that we failed to identify most KEGG pathways from our previous study at 24hpi suggests there may be significant background in our datasets precluding the identification of true ‘hits’. This is likely the case in the data presented here, as the data represent averages of only two replicates normalized to a single control. In the future, we should aim to improve this approach by increasing the number of experimental replicates and designing careful controls to improve confidence in our final MS datasets.

We hope to optimize our BAR protocol such that we can confidently perform parallel proximity-labeling experiments on IFNγ-treated cells infected with our CtΔ*incU* strain or an isogenic wildtype control. Differential analyses of BAR-MS datasets from these conditions will provide a unique opportunity to weed-out artifacts. Given the nature

of cell-autonomous immune resistance by wildtype *C. trachomatis*[59], we anticipate that analyzing host proteins recruited only to CtΔIncU inclusions and not to those of our control strain in IFNγ-stimulated cells could facilitate high-fidelity identification of the human cell-autonomous immunity repertoire while minimizing errant hits from background labeling or other factors.

Human proteins that facilitate cell-autonomous immune clearance of intracellular pathogens are largely enigmatic. Our preliminary BAR data provides an important proof-of-concept that this recently published methodology reliably labels the inclusion microenvironment. Current methods to label or isolate inclusions or inclusion membranes are technically challenging, requiring genetic manipulation of *Chlamydia* or laborious mechanical isolation of whole inclusions[112,117]. Our experimental approach here provides the field with a new tool with promise to perform proximity labeling cheaply and efficiently in fixed infected cells, and the specific nature of this labeling provides promise in the utility of this methodology for future research into *Chlamydia* biology.

Materials & Methods

Antibodies and reagents

Information for all primary antibodies: goat anti-MOMP (Virostat, Westbrook, ME; 1621, 1:1000), mouse anti-IncA (gift from Daniel Rockey, Oregon State University, 1:50). Information for all secondary antibodies: rat anti-goat HRP (Thermo Fisher Scientific, Rockford, IL, 1:500), goat anti-mouse-HRP (Thermo Fisher Scientific, Rockford, IL,

1:500). An Alexa Fluor 488-conjugated streptavidin (Thermo Fisher Scientific, Rockford, IL) was used to detect of biotin by IF microscopy, and 4',6-diamidino-2-phenylindole (DAPI, Fisher Scientific, 1:2000) was used to visualize host nuclei and *Chlamydia* DNA.

Chlamydia infection and cell culture

HeLa cells (ATCC) were cultured at 37°C, 5% CO_2 in Roswell Park Memorial Institute 1640 (RPMI, Gibco) medium supplemented with 1x GlutaMax (Gibco) and 10% fetal bovine serum (FBS, HyClone). *Chlamydia trachomatis* LGV L2 434/Bu was propagated by infecting McCoy cells for 48 hours, then infected cells were scraped into growth medium and centrifuged at 3500 x *g* for 5 minutes. Pellets were resuspended in 10% phosphate buffered saline and lysed by bead bashing. An equivalent volume of 2x sucrose phosphate buffer was added to lysates (final concentration: 0.2M sucrose, 8mM sodium phosphate pH 7.1). Lysates were centrifuged at 250 x *g* for 5 minutes and *Chlamydia* elementary bodies (EBs) within supernatants were aliquoted and frozen at -80°C. Infection of host cells in this study was performed by diluting *Chlamydia* EBs in Hank's buffered salt solution (HBSS, Gibco) and adding to adherent HeLa cells in tissue culture flasks or chamber slides at an approximate multiplicity of infection of 1. Cells were incubated at room temperature for 2 hours, then HBSS was replaced with RPMI, and cells were incubated at 37°C, 5% CO_2.

Biotinylation by antibody recognition

Chlamydia infected cells in 25 cm^2 tissue culture flasks or 8-well chamber slides were fixed at either 16 or 24hpi with 3.7% paraformaldehyde for 20 minutes, washed 3 times with PBS, and permeabilized with 0.5% Triton X-100 for 15 minutes. Wells were

washed once more and blocked with 3% bovine serum albumin (BSA) in phosphate buffered saline (PBS) for one hour. Primary antibodies against MOMP and IncA were diluted (dilution factors listed under 'Antibodies and Reagents') in 1% BSA-PBS and incubated at room temperature for 1 hour, after which we performed 3 five-minute washes before adding secondary antibodies. Secondary HRP-conjugated antibodies were diluted (dilution factors listed under 'Antibodies and Reagents') in 1% BSA-PBS and incubated for 45 minutes at room temperature in the dark, followed by 3 five-minute washes with PBS. Biotinylation by antibody recognition was performed on 25 cm^2 flasks using a TSA Biotin Kit (Perkin Elmer, Waltham, MA) according to manufacturer's instructions. Briefly, biotin-tyramide was diluted 1:50 in TSA dilution buffer containing H_2O_2 and added to 8-well chamber slides and 25 cm^2 flasks for 10 minutes. Sodium ascorbate (500mM) was added to stop reactions, then we performed 3 washes with PBS (5 minutes each). Lysis buffer (2% SDS, 1.3% sodium deoxycholate) was added to cells in 25 cm^2 8-well chamber slides, and these lysates were stored at -80°C until they were shipped to the Pacific Northwest National Laboratory (PNNL) for processing and mass spectrometry. Cells in 8-well chamber slides were stained with Alexa Fluor 488-conjugated Streptavidin and DAPI and analyzed via immunofluorescence microscopy to qualitatively assess the specificity of biotin labeling.

Mass Spectrometry

Collaborators at the PNNL prepared BAR-labeled lysates for mass spectrometry (MS) analysis as previously described[112]. Briefly, whole cell lysates were sonicated at 20% amplitude on ice, then were centrifuged at 15,000 x *g* for 10 minutes at 4°C to clear cell debris. Protein concentrations were determined for each sample by BCA. 1000 µg of

each sample was enriched with streptavidin agarose resin (Thermo Fisher Scientific, Rockford, IL) to isolate biotinylated proteins. Isolated proteins were digested with trypsin, and tryptic peptides were dried using a speed vacuum, suspended in 25 mM sodium bicarbonate, and centrifuged at 53,000 x *g* for 20 minutes at 4°C to remove debris. Digested peptides were separated by PNNL using their reverse-phase resin columns by liquid chromatography (LC) and analyzed on a Thermo Fisher Velos Orbitrap MS[120]. The MS/MS spectra, identified through an accurate mass and time (AMT) methodology, were compared against *Chlamydia trachomatis* serovar L2 434 Bu pL2Plasmid 2018-01-05 and *Homo sapiens* Uniprot SPROT 2017-04-12 FASTA files[121]. Results were filtered on a false discovery rate less than or equal to 1%. Relative peptide abundances between replicate samples were log transformed and subjected to quality control. KEGG ontology analysis was performed by uploading the top 100 identified hits from our MOMP-BAR-MS dataset to InnateDB pathway analysis server, and we processed these data using the InnateDB overrepresentation analysis tool. We used their recommended settings for statistical analysis and selected for pathways that were statistically significant ($P < 0.05$).

Chapter 6. Conclusions and Future Directions

The work described herein documents several important findings informing *Chlamydia trachomatis* virulence. Initial experiments involving a unique interspecies chimera library led us to identify a discrete genetic locus within the *C. trachomatis* genome that confers resistance to IFNγ-stimulated cell-autonomous immunity in its natural human host cells. Support from the literature led to our hypothesis that a single divergent gene within this locus, *incU*, conferred this resistance. Follow up experiments using *C. trachomatis incU* mutants consistently supported this hypothesis. Our experiments performed in the nonhuman primate (NHP) model showed for the first time that pigtailed macaques employ an IFNγ-inducible cell-autonomous immune response that is similar to the human pathway, and *C. trachomatis* resists pigtailed macaque cell-autonomous immunity in an IncU-dependent manner, as it does in humans. Infection of macaques with a heterogenous *C. trachomatis* inoculum revealed that deleterious *incU* mutations appear to be attenuating to infection *in vivo*. Finally, we introduce a new technique to biochemically label and annotate the protein contents of the *Chlamydia* inclusion; as a future step, this technology could facilitate the discovery of the full panel of host factors that are mobilized to the inclusion membrane interface as a result of cell-autonomous immune activation.

Chapter 2 describes how we exploited a novel interspecies chimera library to identify a finite genetic locus which was required for *C. trachomatis* resistance to IFNγ-stimulated inclusion ubiquitination. Chimeras which inhabited ubiquitin-positive inclusions

lacked a shared locus of 11 *C. trachomatis* genes, instead carrying the *C. muridarum* homologues. Analysis of these genes yielded two priority candidates, *ct134* and *incU* (*ct135*) that are type-III secreted inclusion membrane proteins and were the most divergent of the candidate genes between *C. trachomatis* and *C. muridarum*.

Interestingly, *incU* has previously been implicated as a *C. trachomatis* virulence factor in the mouse model, and we evaluated whether this gene was required for *C. trachomatis* resistance to cell-autonomous immunity. For the work described in chapter 3, we obtained two *incU* mutants from Dr. Harlan Caldwell, D-EC and D-LC. Both strains carry frameshift mutations in their *incU* open reading frames (ORFs), and we predicted that the mature IncU encoded by D-EC is missing the majority of its carboxyl end, whereas D-LC encodes a much more severe IncU truncation. We showed that D-EC and D-LC inhabited inclusions that were susceptible to ubiquitination in IFNγ-primed epithelial cells, and that this recognition by cell-autonomous immunity led to a severe growth restriction *in vitro*. Our findings invite a reinterpretation of previously published studies which used D-LC as a wildtype control to compare against D-EC to determine the virulence characteristics of IncU in mouse and nonhuman primate models of *Chlamydia*[88,96,97]. Our data suggest that *incU* encoded by D-LC does not confer resistance to cell-autonomous immunity, similar to the other *incU* frameshift mutants we characterized. These historical studies led to the conclusion that IncU is a virulence factor in the mouse model, as D-LC-infected mice shed higher levels of bacteria and were infected for a longer duration compared to D-EC. We speculate this outcome could be due to faster growth of D-LC, or potentially other unidentified properties of IncU. A previous study showed that frameshift mutations within *incU* conferred faster replication *in vitro*[102]. It is possible that earlier

disruption of the *incU* open reading frame within D-LC confers a greater growth advantage compared to D-EC. It will be informative to repeat the mouse infection experiments and include true wildtype *C. trachomatis* control groups. We predict that wildtype organisms will cause a shorter infection than both D-EC and D-LC in the mouse model due to the faster growth of *incU* frameshift mutants[102].

Prior to our studies, the literature states that *incU* is unimportant to *C. trachomatis* virulence in NHPs[97], however the 2018 study leading to this conclusion used the mutant strain D-LC as a wildtype control as it was thought at the time to encode a functional copy of *incU*[88,97]. In chapter 4, we show that an inoculum containing a subpopulation of *incU* frameshift mutants (CtΔ*incU*) was poorly infectious in an experimental infection of pigtailed macaques, compared to wildtype *C. trachomatis* or organisms with *incU* mutations that do not lead to early truncations of the mature protein. WGS analysis suggested CtΔ*incU* made up ~27.7% of the inoculum population yet was not detected in a 5 wpi sample from an animal that remained positive at that timepoint. These data suggest that CtΔ*incU* organisms failed to establish infection in the macaque model. We linked this *in vivo* phenotype to CtΔ*incU* susceptibility to IFNγ-stimulated cell-autonomous immunity in primary macaque fibroblasts, which were capable of ubiquitinating CtΔ*incU* inclusions following IFNγ stimulation *in vitro*. The characterization of CtΔ*incU*, which does not encode any mutations outside of a single nucleotide deletion in the *incU* open reading frame, offered the opportunity to directly implicate this gene as a virulence factor—which was not possible with the D-EC and D-LC strains that encode additional mutations[88]. Interestingly, in the aforementioned 2018 study the authors mentioned an unusual outcome wherein half of monkeys infected with either D-EC or D-LC failed to become

infected. Repeating this study with a true wildtype *C. trachomatis* serovar D control group should be prioritized to definitively evaluate in a controlled study whether *incU* mutant strains cause attenuated infection in the female macaque cervical infection model.

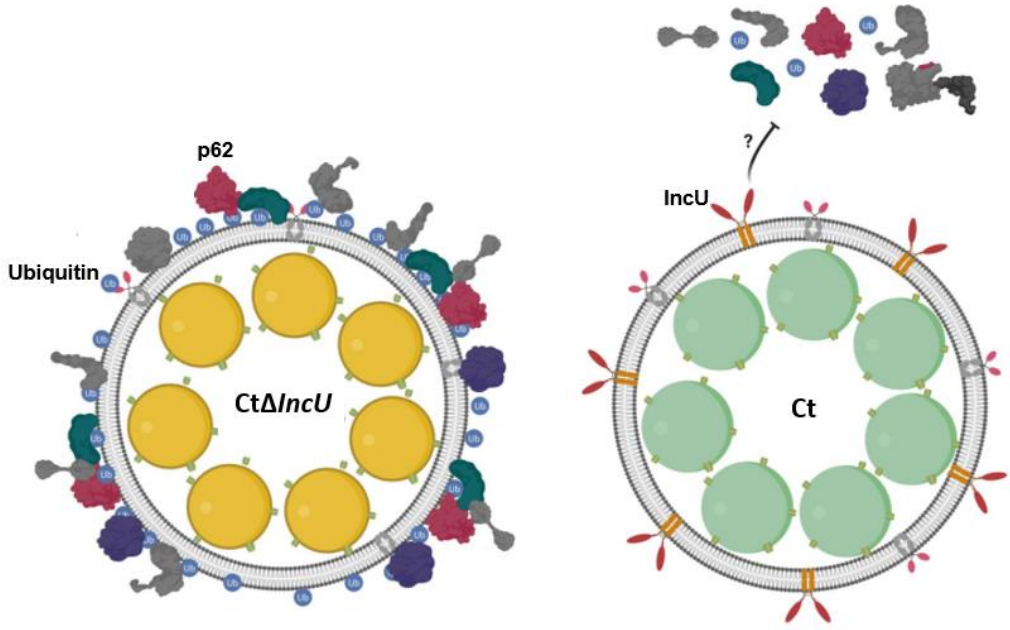

Figure 6.1 Graphical summary of findings. *C. trachomatis* organisms with frameshift mutations in *incU* (CtΔ*incU*) are susceptible to human and nonhuman primate (NHP) cell-autonomous immunity, evidenced by ubiquitin (blue protein) and p62 (pink protein) recruitment to their inclusion membranes in IFNγ-stimulated host cells. This susceptibility is associated with impaired growth *in vitro* and a failure to grow and replicate in the NHP model. Wildtype *C. trachomatis* (Ct) resists recognition by this pathway via its secretion of the inclusion membrane protein IncU.

We discovered that IncU also prevented association of p62 with inclusions in IFNγ-stimulated cells. p62 was previously reported to have a unique role in cell-autonomous immunity that was separate from restricting the growth of pathogens. In the murine model, IFNγ-induced p62 association with *Toxoplasma gondii* pathogen-containing vacuoles (PCVs) led to increased antigen presentation by MHC-I which enhanced CD8+ T-cell

activation *in vivo*[65]. If p62 has a similar function in human cell-autonomous immunity, the outcomes of IncU-mediated immune evasion by *C. trachomatis* may include thwarting a unique adaptive immune response mediated by CD8+ T-cells. *Cis*-complementation of CtΔ*incU* via homologous recombination rescued its ability to resist IFNγ-stimulated inclusion ubiquitination in human cells, and we conclude that IncU is a *C. trachomatis* virulence factor which functions to evade cell-autonomous immunity in its native human and NHP hosts.

In chapter 5, we described a novel method for defining host proteins which are recruited into the lumen or onto the cytosolic face of *C. trachomatis* inclusions during infection. Biotinylation by antibody recognition (BAR) was originally developed to define protein-protein interactions within specific microenvironments of eukaryotic cells[113], and our application is the first described to study pathogen-host interactions by this method. *C. trachomatis* MOMP antibody-mediated proximity labeling resulted in specific biotinylation of proteins comprising the *Chlamydia* inclusion microenvironment. The benefit of BAR compared to other proximity labeling methods is its relative ease-of-use and wide applicability. It circumvents the need to genetically manipulate *Chlamydia*, so it can feasibly be used to study fastidious or genetically intractable *C. trachomatis* serovars. Following our proof-of-principle analysis of this method, we propose a future experiment wherein we BAR-label wildtype *C. trachomatis* and CtΔ*incU* inclusions in IFNγ-stimulated human cells. Differential analysis of MS data between these two groups may yield a broad characterization of host factors involved in cell-autonomous immunity. Characterization of this poorly understood pathway will further our understanding IFNγ-mediated control of intracellular pathogens.

Molecular mechanism of IncU-mediated immune evasion

We have demonstrated that IncU is required for inhibiting IFNγ-stimulated cell-autonomous immunity in human cells, however the underlying molecular mechanism driving this evasion remains unknown. Resistance to IFNγ-induced cell-autonomous immunity is not unique to *Chlamydia*, as multiple pathogens employ a variety of strategies to interfere with this pathway. The cytoplasmic pathogen *Shigella flexneri* is a bacterium which actively degrades GBP1 in human cells through secretion of a virulence factor IpaH9.8[122]. IpaH9.8 is a type-III secreted ubiquitin ligase which ubiquitinates GBP1 resulting in its proteasomal degradation. IpaH9.8-mediated degradation of GBPs was also observed in the non-native mouse model[122]. Similarly, the human pathogen *Mycobacterium tuberculosis* was recently shown to evade GBP-mediated immunity in the mouse model, although the specific virulence factors mediating this evasion are unknown[123]. The ability of these intracellular pathogens to overcome IFNγ-mediated cell-autonomous immunity in a non-native host is distinct from our observations of IncU-mediated immune evasion by *C. trachomatis*, which is susceptible to this response in mouse cells[59,62]. This discrepancy may be due to the specific steps of cell-autonomous immunity (Fig. 1.1) that are inhibited by *S. flexneri* and *M. tuberculosis*. GBPs are partially conserved between mice and humans, which may suggest that *S. flexneri* and *M. tuberculosis* have evolved strategies to overcome components of GBP-mediated immunity that are conserved in both host species. Alternatively, the human-restricted nature of IncU-mediated immune evasion suggests that IncU interferes with a stage of cell-autonomous immunity that is not shared between humans and mice.

We and others have shown that *C. trachomatis* inclusions are devoid of ubiquitin in IFNγ-stimulated human cells, and we hypothesize that IncU interferes with cell-autonomous immunity at a step that precedes inclusion ubiquitination. These early events are well defined in the mouse pathway, wherein immunity related GTPases (IRGs) recognize *Chlamydia* inclusions and other PCVs via a missing-self phenomenon to promote their ubiquitination and clearance (Fig. 1.1). The human genome does not encode these IRGs, and by necessity must have evolved a novel mechanism to recognize PCVs and initiate downstream events of cell-autonomous immunity[36]. A previous study evaluated the interactions of multiple Incs, including IncU, in human HEK293T cells[124]. Affinity purification of IncU followed by mass spectrometry (AP-MS) revealed protein-protein interactions with 4 host proteins: Atlastin-3 (ATL3), Exportin4 (EXPO4), and V-type proton ATPase subunit H (ATP6V1H)[124]. Interestingly, atlastins are dynamin GTPases which are highly related to GBPs[125]. Because the events following PCV ubiquitination are similar in human and murine cell-autonomous immunity, it is possible that the general mechanism of PCV recognition by GTPases is shared between mice and humans. This would necessitate an IRG-independent GTPase or set of GTPases driving this process in humans. Future experiments should evaluate whether ATL3 is involved in human cell-autonomous immunity, and whether its interaction with IncU is important to *C. trachomatis* evasion of this pathway. It is also possible that IncU interacts with human proteins that are induced by IFNγ-stimulation. Repeating the aforementioned AP-MS in IFNγ-stimulated human cells may reveal additional IncU interaction partners that are more relevant to its molecular function[124].

An alternative hypothesis is that IncU-mediated immune evasion does not require interactions with host factors, but instead occurs through passive molecular mimicry. In mouse cells, recognition of *C. trachomatis* inclusions by cell-autonomous immunity occurs through a missing-self phenomenon mediated by IRGs[66]. It is possible that the human pathway recognizes PCVs as foreign through a similar missing-self mechanism. In this case, determining the crystal structure of IncU may reveal some structural similarities to such a human protein. In lieu of a crystal structure, the structural predictions detailed in this dissertation may be relevant to generate hypotheses of IncU function. Our finding that predicted IncU structures share homology with human GBP1 informs a hypothesis wherein *C. trachomatis* disguises inclusions as already 'marked' by cell-autonomous immune machinery in order to prevent recognition by the actual pathway.

Informing vaccine design

In the United States, over 100 million people are infected with *C. trachomatis* every year, and from 2015 to 2019 the annual number of chlamydia cases increased by 19%[2]. This concerning trend continues despite national screening recommendations and the availability of effective antibiotics to treat *C. trachomatis* infection[1]. We desperately need a vaccine protective against urogenital *C. trachomatis* infection. To date, there has been only a single phase-I clinical trial evaluating the safety and immunogenicity of a *C. trachomatis* subunit vaccine in humans[126]. The conclusions of this phase 1 trial revealed that the candidate vaccine was safe, and slightly improved antibody titers and IFNγ production by peripheral blood mononuclear cells were observed in individuals immunized with a CAF01 adjuvant compared to aluminum hydroxide[126]. While this trial represents a promising step in the right direction, the dearth of clinical trials evaluating

urogenital *Chlamydia* vaccines is a major concern. Given the time-intensive nature of these trials, at present we are likely more than a decade away from an approved vaccine against urogenital *Chlamydia*. Without a vaccine, the outlook for chlamydia control in the United States and abroad is bleak.

A recent preclinical study in the mouse model showed that immunization of mice with ultraviolet (UV)-inactivated *C. trachomatis* conjugated to novel charge-switching synthetic adjuvant particles (cSAP) elicited protective memory immunity in mice[105]. This protection was characterized by circulating effector CD4+ T cell recruitment to mucosal tissues of the female genital tract, which seeded this site with *C. trachomatis* specific tissue resident CD4+ T cell populations[105]. This protection agrees with previous findings that *C. trachomatis*-specific CD4+ T cells that arise following primary infection confer robust protection against *Chlamydia* challenge in the mouse model[49]. The most critical aspect of the observed protection against *C. trachomatis* by CD4+ T-cells is through their secretion of IFNγ, as IFNγ$^{-/-}$ mice fail to effectively control *C. trachomatis* infection[49]. Interestingly, a similarly critical aspect of *C. trachomatis* control in mice is a functional cell-autonomous immune response, as IRGM-deficient mice also fail to control *C. trachomatis* infection[49]. These published data in the mouse model support that CD4+ T cells are critical to confer sterilizing immunity against *C. trachomatis*, and that this protection is due in large part to IFNγ secretion by T-cells and likely their activation of cell-autonomous immunity in infected cells *in vivo*. Therefore, studies performed in mice suggesting a protective role of IFNγ should be interpreted with caution, as protective effects from cell-autonomous immune responses are not expected to translate to humans given that *C. trachomatis* readily is resistant to this pathway in its native host.

In 2011, a preclinical study was performed to evaluate the efficacy of a live-attenuated vaccine to prevent infection of nonhuman primates with ocular serovars of *C. trachomatis*[119]. The authors compared the infectivity of the A2497 ocular strain of *C. trachomatis* and a plasmid deficient strain of A2497 (A2497 P^-). The A2497 P^- strain displayed a drastic reduction in infectivity compared to the plasmid encoding strain[119]. Half of the 6 monkeys immunized with the A2497 P^- strain were completely protected against challenge with the parent strain. The other 3 animals in this group were infected but they shed less *C. trachomatis* than unimmunized animals throughout the 13-week observation period. The *C. trachomatis* plasmid has since been suggested to be unimportant to virulence in NHP[97], bringing into question the cause of attenuation in animals infected with the plasmid deficient strain. We analyzed the published genome of the A2497 parent and found that it encodes a frameshift mutation within its *incU* open reading frame. It is possible that the serial passage to select for the plasmid-deficient strain led to additional mutations within *incU*, which is a well-documented phenomenon[89]. We speculate that the frameshift within the A2497 population presented a low mutational threshold that could be overcome *in vivo* to restore the *incU* open reading frame in this strain. Additional *incU* mutations may have accumulated in the plasmid-deficient strain during its *in vitro* derivation, which could have increased the threshold of compensatory mutations needed to restore the open reading frame *in vivo*. If samples from this trachoma vaccine study are still accessible, it would be prudent to sequence the inocula used and organisms isolated from infected animals, to monitor the presence of *incU* mutants that our data suggest cause attenuated infection in the NHP model.

The clearest example of immunological protection against *C. trachomatis* in humans is from studies showing that women who spontaneously resolve *Chlamydia* infection are partially protected from reinfection[40]. This observation supports the notion that a *C. trachomatis* strain that fails to establish a productive infection may represent an opportunity to investigate a live-attenuated vaccination strategy. In theory, this approach could allow a potentially protective natural immune response to run its course in immunized patients without leading to advanced disease. A unique outcome of this dissertation is the identification of a CtΔ*incU* mutant strain that appeared to cause attenuated infection in the nonhuman primate model. The poor infectivity of *incU* mutants agrees with previous findings that *incU* ORFs from human clinical samples are intact—in contrast to the observed propensity of *incU* to accumulate frameshift mutations *in vitro*[88,89]. A critical future direction stemming from our work will be to confirm whether infection by CtΔ*incU* is attenuated in NHP through direct experiments, and to assess whether natural clearance of this mutant strain affords protection from rechallenge with wildtype *C. trachomatis*.

Final Thoughts

During the shared evolutionary history of *C. trachomatis* and its natural human host, it has had to evolve mechanisms to overcome detection and clearance by host innate immune pathways in order to survive in its intracellular niche. One example of this is the observation that *C. trachomatis* resists IFNγ-stimulated cell-autonomous immunity in human cells but fails to do so in mouse cells[59,62]. We have identified a novel virulence factor, IncU, that facilitates *C. trachomatis* evasion of human cell-autonomous immunity. Additionally, we show that NHP employ a human-like cell-autonomous immune response

that *C. trachomatis* functionally evades via IncU. Our findings suggest that *incU* mutants fail to replicate in the nonhuman primate model of *Chlamydia*. Follow up studies should be prioritized to confirm this finding and evaluate whether *C. trachomatis incU* mutants are viable candidates for a live-attenuated vaccine to combat the increasing rates of chlamydia across the globe.

References

1. Centers for Disease Control and Prevention. Chlamydial infection among Adolescents and Adults. (2021).
2. Centers for Disease Control and Prevention. Sexually Transmitted Disease Surveillance 2019. (2021).
3. Stamm, W. E. *Chlamydia trachomatis* Infections: Progress and Problems. *J. Infect. Dis.* **179**, S380–S383 (1999).
4. Price, M. J. *et al.* Risk of pelvic inflammatory disease following *Chlamydia trachomatis* infection: analysis of prospective studies. *Am. J. Epidemiol.* **178**, 484–92 (2013).
5. Lesiak-Markowicz, I., Schötta, A. M., Stockinger, H., Stanek, G. & Markowicz, M. *Chlamydia trachomatis* serovars in urogenital and ocular samples collected 2014–2017 from Austrian patients. *Sci. Rep.* **9**, 2017–2020 (2019).
6. Ahmad, B. & Patel, B. C. Trachoma. *Aust. J. Optom.* **53**, 381–387 (2021).
7. O'Connell, C. M. & Ferone, M. E. *Chlamydia trachomatis* GenitalInfections. *Microb. Cell* **3**, 390 (2016).
8. Dukers-Muijrers, N. H. *et al.* Oropharyngeal *Chlamydia trachomatis* in women; spontaneous clearance and cure after treatment (FemCure). *Sex Transm Infect* **97**, 147–151 (2021).
9. Ceovic, R. & Gulin, S. J. Lymphogranuloma venereum: diagnostic and treatment challenges. *Infect. Drug Resist.* **8**, 39 (2015).
10. Stoner, B. P. & Cohen, S. E. Lymphogranuloma Venereum 2015: Clinical

Presentation, Diagnosis, and Treatment. *Clin. Infect. Dis.* **61**, S865–S873 (2015).

11. Datta, B., Njau, F., Thalmann, J., Haller, H. & Wagner, A. D. Differential infection outcome of *Chlamydia trachomatis* in human blood monocytes and monocyte-derived dendritic cells. *BMC Microbiol.* **14**, 209 (2014).
12. Faris, R. *et al. Chlamydia trachomatis* Serovars Drive Differential Production of Proinflammatory Cytokines and Chemokines Depending on the Type of Cell Infected. *Front. Cell. Infect. Microbiol.* **9**, 1–14 (2019).
13. Moore, E. R. & Ouellette, S. P. Reconceptualizing the chlamydial inclusion as a pathogen-specified parasitic organelle: An expanded role for Inc proteins. *Front. Cell. Infect. Microbiol.* **4**, 157 (2014).
14. Hybiske, K. & Stephens, R. S. Mechanisms of host cell exit by the intracellular bacterium Chlamydia. *Proc. Natl. Acad. Sci. U. S. A.* **104**, 11430 (2007).
15. Coburn, B., Sekirov, I. & Finlay, B. B. Type III Secretion Systems and Disease. *Clin. Microbiol. Rev.* **20**, 535 (2007).
16. Elwell, C., Mirrashidi, K. & Engel, J. Chlamydia cell biology and pathogenesis. *Nat. Rev. Microbiol. 2016 146* **14**, 385–400 (2016).
17. Saka, H. A. *et al.* Quantitative proteomics reveals metabolic and pathogenic properties of *Chlamydia trachomatis* developmental forms. *Mol. Microbiol.* **82**, 1185 (2011).
18. Jewett, T. J., Miller, N. J., Dooley, C. A. & Hackstadt, T. The Conserved Tarp Actin Binding Domain Is Important for Chlamydial Invasion. *PLoS Pathog.* **6**, 1–11 (2010).
19. Lutter, E. I., Martens, C. & Hackstadt, T. Evolution and conservation of predicted

inclusion membrane proteins in chlamydiae. *Comp. Funct. Genomics* **2012**, (2012).

20. Dehoux, P., Flores, R., Dauga, C., Zhong, G. & Subtil, A. Multi-genome identification and characterization of chlamydiae-specific type III secretion substrates: the Inc proteins. *BMC Genomics* **12**, 109 (2011).
21. Bannantine, J. P., Griffiths, R. S., Viratyosin, W., Brown, W. J. & Rockey, D. D. A secondary structure motif predictive of protein localization to the chlamydial inclusion membrane. *Cell. Microbiol.* **2**, 35–47 (2000).
22. Gauliard, E., Ouellette, S. P., Rueden, K. J. & Ladant, D. Characterization of interactions between inclusion membrane proteins from *Chlamydia trachomatis*. *Front. Cell. Infect. Microbiol.* **5**, (2015).
23. Hybiske, K. Expanding the Molecular Toolkit for Chlamydia. *Cell Host Microbe* **18**, 11–13 (2015).
24. Agaisse, H. & Derré, I. Expression of the Effector Protein IncD in *Chlamydia trachomatis* Mediates Recruitment of the Lipid Transfer Protein CERT and the Endoplasmic Reticulum-Resident Protein VAPB to the Inclusion Membrane. *Infect. Immun.* **82**, 2037–47 (2014).
25. Nguyen, P. H., Lutter, E. I. & Hackstadt, T. *Chlamydia trachomatis* inclusion membrane protein MrcA interacts with the inositol 1,4,5-trisphosphate receptor type 3 (ITPR3) to regulate extrusion formation. *PLoS Pathog.* **14**, (2018).
26. Lutter, E. I., Barger, A. C., Nair, V. & Hackstadt, T. *Chlamydia trachomatis* inclusion membrane protein CT228 recruits elements of the myosin phosphatase pathway to regulate release mechanisms. *Cell Rep.* **3**, 1921 (2013).

27. Mital, J., Lutter, E. I., Barger, A. C., Dooley, C. A. & Hackstadt, T. *Chlamydia trachomatis* inclusion membrane protein CT850 interacts with the dynein light chain DYNLT1 (Tctex1). *Biochem. Biophys. Res. Commun.* **462**, 165 (2015).

28. Stanhope, R., Flora, E., Bayne, C. & Derré, I. IncV, a FFAT motif-containing Chlamydia protein, tethers the endoplasmic reticulum to the pathogen-containing vacuole. *Proc. Natl. Acad. Sci. U. S. A.* **114**, 12039–12044 (2017).

29. Clercq, E. De, Kalmar, I. & Vanrompay, D. Animal Models for Studying Female Genital Tract Infection with *Chlamydia trachomatis*. *Infect. Immun.* **81**, 3060 (2013).

30. Read, T. D. *et al.* Genome sequences of *Chlamydia trachomatis* MoPn and Chlamydia pneumoniae AR39. *Nucleic Acids Res.* **28**, 1397 (2000).

31. Maza, L. M. de la, Pal, S., Khamesipour, A. & Peterson, E. M. Intravaginal inoculation of mice with the *Chlamydia trachomatis* mouse pneumonitis biovar results in infertility. *Infect. Immun.* **62**, 2094 (1994).

32. Helble, J. D., Reinhold-Larsson, N. V. & Starnbach, M. N. Early Colonization of the Upper Genital Tract by Chlamydia muridarum Is Associated with Enhanced Inflammation Later in Infection. *Infect. Immun.* **87**, (2019).

33. Morrison, R. P., Feilzer, K. & Tumas, D. B. Gene Knockout Mice Establish a Primary Protective Role for Major Histocompatibility Complex Class II-Restricted Responses in *Chlamydia trachomatis* Genital Tract Infection. *Infect. Immun.* **63**, 4661–4668 (1995).

34. Stary, G. *et al.* A mucosal vaccine against *Chlamydia trachomatis* generates two waves of protective memory T cells. *Science (80-.).* **348**, (2015).

35. Pal, S., Peterson, E. M. & De La Maza, L. M. Factors influencing the induction of infertility in a mouse model of *Chlamydia trachomatis* ascending genital tract infection. *J. Med. Microbiol* **47**, 599–605 (1998).

36. Bekpen, C. *et al.* Death and Resurrection of the Human IRGM Gene. *PLoS Genet.* **5**, (2009).

37. Nigg, C. An unidentified virus which produces pneumonia and systemic infection in mice. *Science* **95**, 49–50 (1942).

38. Wolner-Hanssen, P., Patton, D. & Holmes, K. Protective immunity in pig-tailed macaques after cervical infection with *Chlamydia trachomatis*. *Sex. Transm. Dis.* **18**, 21–25 (1991).

39. Carvalho, C., Gaspar, A., Knight, A. & Vicente, L. Ethical and Scientific Pitfalls Concerning Laboratory Research with Non-Human Primates, and Possible Solutions. *Anim. an Open Access J. from MDPI* **9**, (2019).

40. Geisler, W. M., Lensing, S. Y., Press, C. G. & Hook, E. W. Spontaneous Resolution of Genital *Chlamydia trachomatis* Infection in Women and Protection from Reinfection. *J. Infect. Dis.* **207**, 1850 (2013).

41. Geisler, W. *et al.* The natural history of untreated *Chlamydia trachomatis* infection in the interval between screening and returning for treatment. *Sex. Transm. Dis.* **35**, 119–123 (2008).

42. Redgrove, K. A. & McLaughlin, E. A. The Role of the Immune Response in *Chlamydia trachomatis* Infection of the Male Genital Tract: A Double-Edged Sword. *Front. Immunol.* **0**, 534 (2014).

43. Su, H., Feilzer, K., Caldwell, H. D. & Morrison, R. P. *Chlamydia trachomatis*

Genital Tract Infection of Antibody-Deficient Gene Knockout Mice. *Infect. Immun.* **65**, 1993–1999 (1997).

44. Morrison, S. G. & Morrison, R. P. Resolution of Secondary *Chlamydia trachomatis* Genital Tract Infection in Immune Mice with Depletion of Both CD4+ and CD8+ T cells. *Infect. Immun.* **69**, 2643 (2001).
45. Li, L.-X. & McSorley, S. J. A re-evaluation of the role of B cells in protective immunity to Chlamydia infection. *Immunol. Lett.* **164**, 88 (2015).
46. León, B., Ballesteros-Tato, A., Misra, R. S., Wojciechowski, W. & Lund, F. E. Unraveling Effector Functions of B Cells During Infection: The Hidden World Beyond Antibody Production. *Infect. Disord. Drug Targets* **12**, 213 (2012).
47. Wojciechowski, W. *et al.* Regulation of type 2 immunity to H. polygyrus by effector B cells: Requirement for cytokine-producing B cells. *Immunity* **30**, 421–433 (2009).
48. Barr, T. A., Brown, S., Mastroeni, P. & Gray, D. TLR and B Cell Receptor Signals to B Cells Differentially Program Primary and Memory Th1 Responses to Salmonella enterica. *J. Immunol.* **185**, 2783–2789 (2010).
49. Gondek, D. C., Olive, A. J., Stary, G. & Starnbach, M. N. CD4 + T Cells Are Necessary and Sufficient To Confer Protection against *Chlamydia trachomatis* Infection in the Murine Upper Genital Tract . *J. Immunol.* **189**, 2441–2449 (2012).
50. Morrison, S. G., Su, H., Caldwell, H. D. & Morrison, R. P. Immunity to Murine *Chlamydia trachomatis* Genital Tract Reinfection Involves B Cells and CD4+ T Cells but Not CD8+ T Cells. *Infect. Immun.* **68**, 6979 (2000).
51. Schust, D. J. *et al. Chlamydia trachomatis* Immune Evasion via Downregulation of

MHC Class I Surface Expression Involves Direct and Indirect Mechanisms. *Infect. Dis. Obstet. Gynecol.* **2011**, (2011).

52. Helble, J. D., Gonzalez, R. J., Andrian, U. H. von & Starnbach, M. N. Gamma Interferon Is Required for Chlamydia Clearance but Is Dispensable for T Cell Homing to the Genital Tract. *MBio* **11**, (2020).

53. Gondek, D. C., Roan, N. R. & Starnbach, M. N. T cell responses in the absence of IFN-gamma exacerbate uterine infection with *Chlamydia trachomatis*. *J. Immunol.* **183**, 1313–1319 (2009).

54. Johansson, M., Schön, K., Ward, M. & Lycke, N. Studies in knockout mice reveal that anti-chlamydial protection requires TH1 cells producing IFN-gamma: is this true for humans? *Scand. J. Immunol.* **46**, 546–552 (1997).

55. Johansson, M., Schön, K., Ward, M. & Lycke, N. Genital tract infection with *Chlamydia trachomatis* fails to induce protective immunity in gamma interferon receptor-deficient mice despite a strong local immunoglobulin A response. *Infect. Immun.* **65**, 1032–1044 (1997).

56. Mercado, M., Du, W., Malaviarachchi, P. A., Gann, J. I. & Li, L.-X. Innate IFN-γ Is Essential for Systemic Chlamydia muridarum Control in Mice, While CD4 T Cell-Dependent IFN-γ Production Is Highly Redundant in the Female Reproductive Tract. *Infect. Immun.* **89**, (2021).

57. Bakshi, R. K. *et al.* An Adaptive *Chlamydia trachomatis*-Specific IFN-γ-Producing CD4 + T Cell Response Is Associated With Protection Against Chlamydia Reinfection in Women. *Front. Immunol* **9**, (2018).

58. Beatty, W. L., Belanger, T. A., Desai, A. A., Morrison, R. P. & Byrne, G. I.

Tryptophan depletion as a mechanism of gamma interferon-mediated chlamydial persistence. *Infect. Immun.* **62**, 3705–3711 (1994).

59. Haldar, A. K. *et al. Chlamydia trachomatis* Is Resistant to Inclusion Ubiquitination and Associated Host Defense in Gamma Interferon-Primed Human Epithelial Cells. *MBio* **7**, e01417-16 (2016).

60. Van Voorhis, W. C., Barrett, L. K., Cosgrove Sweeney, Y. T., Kuo, C. & Patton, D. L. Repeated *Chlamydia trachomatis* Infection of Macaca nemestrina Fallopian Tubes Produces a Th1-Like Cytokine Response Associated with Fibrosis and Scarring. *Infect. Immun.* **65**, 2175–2182 (1997).

61. Grayston, J. T. & Wang, S. The Potential for Vaccine against Infection of the Genital Tract with *Chlamydia trachomatis*. *Sex. Transm. Dis.* **5**, 73–77 (1978).

62. Haldar, A. K. *et al.* Ubiquitin systems mark pathogen-containing vacuoles as targets for host defense by guanylate binding proteins. *Proc. Natl. Acad. Sci. U. S. A.* **112**, E5628–E5637 (2015).

63. Al-Zeer, M. A., Al-Younes, H. M., Braun, P. R., Zerrahn, J. & Meyer, T. F. IFN-γ-Inducible Irga6 Mediates Host Resistance against *Chlamydia trachomatis* via Autophagy. *PLoS One* **4**, (2009).

64. Brinkworth, J. F. & Alvarado, A. S. Cell-autonomous immunity and the pathogen-mediated evolution of humans: Or how our prokaryotic and single-celled origins affect the human evolutionary story. *Q. Rev. Biol.* **95**, 215–246 (2020).

65. Lee, Y. *et al.* p62 Plays a Specific Role in Interferon-γ-Induced Presentation of a Toxoplasma Vacuolar Antigen. *Cell Rep.* **13**, 223–233 (2015).

66. Finethy, R. & Coers, J. Sensing the enemy, containing the threat: Cell-

autonomous immunity to *Chlamydia trachomatis*. *FEMS Microbiology Reviews* vol. 40 875–893 (2016).

67. Allen, L.-A. H., Hilbi, H., Enninga, J. & Mellouk, N. Cytosolic Access of Intracellular Bacterial Pathogens: The Shigella Paradigm. *Front. Cell. Infect. Microbiol.* **6**, 35 (2016).

68. Pizarro-Cerdá, J., Kühbacher, A. & Cossart, P. Entry of Listeria monocytogenes in Mammalian Epithelial Cells: An Updated View. *Cold Spring Harb. Perspect. Med.* **2**, (2012).

69. Coers, J. Sweet host revenge: galectins and GBPs join forces at broken membranes. *Cell. Microbiol.* **19**, (2017).

70. Thurston, T. L. M., Wandel, M. P., Von Muhlinen, N., Foeglein, Á. & Randow, F. Galectin 8 targets damaged vesicles for autophagy to defend cells against bacterial invasion. *Nature* **482**, 414–418 (2012).

71. Feeley, E. M. *et al.* Galectin-3 directs antimicrobial guanylate binding proteins to vacuoles furnished with bacterial secretion systems. *Proc. Natl. Acad. Sci. U. S. A.* **114**, E1698–E1706 (2017).

72. Deretic, V. Autophagy in Immunity and Cell-Autonomous Defense Against Intracellular Microbes. *Immunol. Rev.* **240**, 92 (2011).

73. Hunn, J. P. *et al.* Regulatory interactions between IRG resistance GTPases in the cellular response to Toxoplasma gondii. *EMBO J.* **27**, 2495–2509 (2008).

74. Haldar, A. K. *et al.* IRG and GBP Host Resistance Factors Target Aberrant, “Non-self” Vacuoles Characterized by the Missing of “Self” IRGM Proteins. *PLoS Pathog.* **9**, (2013).

75. Tretina, K., Park, E.-S., Maminska, A. & MacMicking, J. D. Interferon-induced guanylate-binding proteins: Guardians of host defense in health and disease. *J. Exp. Med.* **216**, 482 (2019).

76. Xavier, A., Al-Zeer, M. A., Meyer, T. F., Daumke Correspondence, O. & Daumke, O. hGBP1 Coordinates Chlamydia Restriction and Inflammasome Activation through Sequential GTP Hydrolysis ll hGBP1 Coordinates Chlamydia Restriction and Inflammasome Activation through Sequential GTP Hydrolysis. *CellReports* **31**, 107667 (2020).

77. Kravets, E. *et al.* The GTPase Activity of Murine Guanylate-binding Protein 2 (mGBP2) Controls the Intracellular Localization and Recruitment to the Parasitophorous Vacuole of Toxoplasma gondii. *J. Biol. Chem.* **287**, 27452 (2012).

78. Kim, B.-H. *et al.* A Family of IFN-γ–Inducible 65-kD GTPases Protects Against Bacterial Infection. *Science (80-.).* **332**, 717–721 (2011).

79. Wang, Y. *et al.* Development of a Transformation System for *Chlamydia trachomatis*: Restoration of Glycogen Biosynthesis by Acquisition of a Plasmid Shuttle Vector. *PLOS Pathog.* **7**, e1002258 (2011).

80. Wang, Y. *et al.* Development of Transposon Mutagenesis for Chlamydia muridarum. *J. Bacteriol.* **201**, (2019).

81. Stephens, R. S. *et al.* Genome sequence of an obligate intracellular pathogen of humans: *Chlamydia trachomatis*. *Science (80-.).* **282**, 754–759 (1998).

82. Suchland, R. J. *et al.* Chromosomal recombination targets in chlamydia interspecies lateral gene transfer. *J. Bacteriol.* **201**, 1–15 (2019).

83. Gomes, J. P. *et al.* Evolution of *Chlamydia trachomatis* diversity occurs by widespread interstrain recombination involving hotspots. *Genome Res.* **17**, 50 (2007).

84. Suchland, C. J. *et al.* Chromosomal recombination targets in Chlamydia interspecies lateral gene transfer. *J. Bacteriol.* **201**, 1–15 (2019).

85. Jeffrey, B. M., Suchland, R. J., Eriksen, S. G., Sandoz, K. M. & Rockey, D. D. Genomic and phenotypic characterization of in vitro-generated *Chlamydia trachomatis* recombinants. *BMC Microbiol.* **13**, (2013).

86. Haldar, A. K. *et al. Chlamydia trachomatis* is resistant to inclusion ubiquitination and associated host defense in gamma interferon-primed human epithelial cells. *MBio* **7**, (2016).

87. Weber, M. M., Bauler, L. D., Lam, J. & Hackstadt, T. Expression and localization of predicted inclusion membrane proteins in *Chlamydia trachomatis*. *Infect. Immun.* **83**, 4710–4718 (2015).

88. Sturdevant, G. L. *et al.* Frameshift mutations in a single novel virulence factor alter the in vivo pathogenicity of *Chlamydia trachomatis* for the female murine genital tract. *Infect. Immun.* **78**, 3660–3668 (2010).

89. Bonner, C. *et al. Chlamydia trachomatis* virulence factor CT135 is stable in vivo but highly polymorphic in vitro. *FEMS Pathog. Dis.* **73**, 43 (2015).

90. Nguyen, B. D. & Valdivia, R. H. Forward Genetic Approaches in *Chlamydia trachomatis*. *J. Vis. Exp.* **80**, 50636 (2013).

91. J, L., AA, A. & DD, R. Growth and development of tetracycline-resistant Chlamydia suis. *Antimicrob. Agents Chemother.* **45**, 2198–2203 (2001).

92. Bolger, A. M., Lohse, M. & Usadel, B. Trimmomatic: a flexible trimmer for Illumina sequence data. *Bioinformatics* **30**, 2114–2120 (2014).

93. Langmead, B. & Salzberg, S. L. Fast gapped-read alignment with Bowtie 2. *Nat. Methods 2012 94* **9**, 357–359 (2012).

94. Grabherr, M. G. *et al.* Full-length transcriptome assembly from RNA-Seq data without a reference genome. *Nat. Biotechnol. 2011 297* **29**, 644–652 (2011).

95. Touchon, M. & Rocha, E. P. C. From GC skews to wavelets: A gentle guide to the analysis of compositional asymmetries in genomic data. *Biochimie* **90**, 648–659 (2008).

96. Sturdevant, G. L. *et al.* Infectivity of urogenital *Chlamydia trachomatis* plasmid-deficient, CT135-null, and double-deficient strains in female mice. *Pathog. Dis.* **71**, 90–92 (2014).

97. Patton, D. L. *et al.* The *Chlamydia trachomatis* plasmid and CT135 virulence factors are not essential for genital tract infection or pathology in female pig-tailed macaques. *Infect. Immun.* **86**, (2018).

98. Filipe Almeida, F. *et al.* Polymorphisms in Inc Proteins and Differential Expression of inc Genes among *Chlamydia trachomatis* Strains Correlate with Invasiveness and Tropism of Lymphogranuloma Venereum Isolates. *J. Bacteriol.* **194**, 6574 (2012).

99. Yang, C. *et al.* Chlamydia evasion of neutrophil host defense results in NLRP3 dependent myeloid-mediated sterile inflammation through the purinergic P2X7 receptor. *Nat. Commun.* **12**, (2021).

100. Al-Zeer, M. A., Al-Younes, H. M., Lauster, D., Lubad, M. A. & Meyer, T. F.

Autophagy restricts *Chlamydia trachomatis* growth in human macrophages via IFNG-inducible guanylate binding proteins. *Autophagy* **9**, 50–62 (2013).

101. Carpenter, E. P., Beis, K., Cameron, A. D. & Iwata, S. Overcoming the challenges of membrane protein crystallography. *Curr. Opin. Struct. Biol.* **18**, 581 (2008).
102. Borges, V. *et al. Chlamydia trachomatis* In Vivo to In Vitro Transition Reveals Mechanisms of Phase Variation and Down-Regulation of Virulence Factors. *PLoS One* **10**, (2015).
103. Miyairi, I., Ramsey, K. H. & Patton, D. L. Duration of Untreated Chlamydial Genital Infection and Factors Associated with Clearance: Review of Animal Studies. *J. Infect. Dis.* **201**, S96–S103 (2010).
104. Haus, T. *et al.* Genome typing of nonhuman primate models: implications for biomedical research. *Trends Genet.* **30**, 482–487 (2014).
105. Stary, G. *et al.* A mucosal vaccine against *Chlamydia trachomatis* generates two waves of protective memory T cells. *Science* **348**, aaa8205 (2015).
106. Al-Zeer, M. A., Al-Younes, H. M., Braun, P. R., Zerrahn, J. & Meyer, T. F. IFN-γ-Inducible Irga6 Mediates Host Resistance against *Chlamydia trachomatis* via Autophagy. *PLoS One* **4**, 4588 (2009).
107. Fehlner-Gardiner, C. *et al.* Molecular basis defining human *Chlamydia trachomatis* tissue tropism: a possible role for tryptophan synthase. *J. Biol. Chem.* **277**, 26893–26903 (2002).
108. Roshick, C., Wood, H., Caldwell, H. D. & McClarty, G. Comparison of Gamma Interferon-Mediated Antichlamydial Defense Mechanisms in Human and Mouse Cells. *Infect. Immun.* **74**, 225 (2006).

109. Morrissey, I. *et al.* Serial passage of Chlamydia spp. in sub-inhibitory fluoroquinolone concentrations. *J. Antimicrob. Chemother.* **49**, 757–761 (2002).

110. Suchland, R. J., Sandoz, K. M., Jeffrey, B. M., Stamm, W. E. & Rockey, D. D. Horizontal Transfer of Tetracycline Resistance among Chlamydia spp. In Vitro. *Antimicrob. Agents Chemother.* **53**, 4604 (2009).

111. Su, H. & Caldwell, H. D. CD4 T Cells Play a Significant Role in Adoptive Immunity to *Chlamydia trachomatis* Infection of the Mouse Genital Tract. *Infect. Immun.* **63**, 3302–3308 (1995).

112. Dickinson, M. S. *et al.* Proximity-dependent proteomics of the *Chlamydia trachomatis* inclusion membrane reveals functional interactions with endoplasmic reticulum exit sites. *PLoS Pathog.* **15**, (2019).

113. Bar, D. Z. *et al.* Biotinylation by antibody recognition - a method for proximity labeling. *Nat. Methods* **15**, 127–133 (2018).

114. Caldwell, H. D., Kromhout, J., Schachter, J. & Proctor, F. L. Purification and Partial Characterization of the Major Outer Membrane Protein of *Chlamydia trachomatis*. *Infect. Immun.* **31**, 1161–1176 (1981).

115. Kokes, M. & Valdivia, R. H. Differential Translocation of Host Cellular Materials into the *Chlamydia trachomatis* Inclusion Lumen during Chemical Fixation. *PLoS One* **10**, e0139153 (2015).

116. Breuer, K. *et al.* InnateDB: systems biology of innate immunity and beyond-recent updates and continuing curation. *Nucleic Acids Res.* **41**, D1228-33 (2013).

117. Aeberhard, L. *et al.* The Proteome of the Isolated *Chlamydia trachomatis* Containing Vacuole Reveals a Complex Trafficking Platform Enriched for

Retromer Components. *PLoS Pathog.* **11**, e1004883 (2015).

118. Raghavan, M., Wijeyesakere, S. J., Peters, L. R. & Del Cid, N. Calreticulin in the immune system: ins and outs. *Trends Immunol.* **34**, 13 (2013).
119. Kari, L. *et al.* A live-attenuated chlamydial vaccine protects against trachoma in nonhuman primates. *J. Exp. Med.* **208**, 2217–2223 (2011).
120. Romine, M. F. *et al.* Elucidation of roles for vitamin B 12 in regulation of folate, ubiquinone, and methionine metabolism. *Proc. Natl. Acad. Sci. U. S. A.* **114**, E1205–E1214 (2017).
121. Anderson, L. N. *et al.* Live Cell Discovery of Microbial Vitamin Transport and Enzyme-Cofactor Interactions. *ACS Chem. Biol.* **11**, 345–354 (2016).
122. Li, P. *et al.* Ubiquitination and degradation of GBPs by a Shigella effector to suppress host defence. *Nature* **551**, 378–383 (2017).
123. Olive, A. J., Smith, C. M., Baer, C. E., Coers, J. & Sassetti, C. M. [Preprint] Mycobacterium tuberculosis evasion of Guanylate Binding Protein-mediated host defense in mice requires the ESX1 secretion system. *bioRxiv* (2020) doi:10.1101/2020.07.27.223362.
124. Mirrashidi, K. M. *et al.* Global mapping of the inc-human interactome reveals that retromer restricts chlamydia infection. *Cell Host Microbe* **18**, 109–121 (2015).
125. Praefcke, G. J. K. Regulation of innate immune functions by guanylate-binding proteins. *Int. J. Med. Microbiol.* **308**, 237–245 (2018).
126. Abraham, S. *et al.* Safety and immunogenicity of the chlamydia vaccine candidate CTH522 adjuvanted with CAF01 liposomes or aluminium hydroxide: a first-in-human, randomised, double-blind, placebo-controlled, phase 1 trial. *Lancet.*

Infect. Dis. **19**, 1091–1100 (2019).